

Sp. Coll.
LB
2369.2
.B528
1998

To the **CASE STUDY COMPARISONS OF STANDARD AND ENERGY
EFFICIENT POLYPHASE INDUCTION MOTORS SUBJECTED TO
UNBALANCED PHASE VOLTAGES**

Study Comparisons of Standard and Energy Efficient Polyphase Induction Motors Subjected to UNBALANCED PHASE VOLTAGES examined the final copy of this thesis and recommend that it be accepted in partial fulfillment of the requirements for the degree of Master of Science with a major in Electrical Engineering.

[Redacted Signature]

Dr. Ahmed Hassan Eltom, Chairperson

We have read this thesis and recommend its acceptance:

A Thesis

[Redacted Signature]

Presented for the

Master of Science Degree

The University of Tennessee at Chattanooga

[Redacted Signature]

Accepted for the Graduate Council

Brian L. Bidwell

[Redacted Signature]

November 1998 / Graduate Studies

DEDICATION

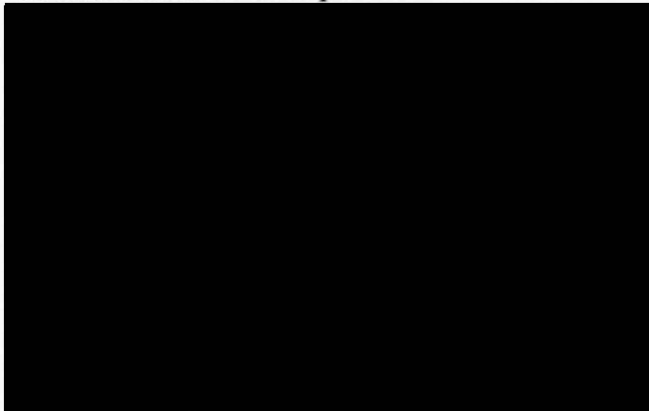
To my parents,

To the Graduate Council:


I am submitting a thesis written by Brian L. Bidwell entitled "Case Study Comparisons of Standard and Energy Efficient Polyphase Induction Motors Subjected to Unbalanced Phase Voltages." I have examined the final copy of this thesis and recommend that it be accepted in partial fulfillment of the requirements for the degree of Master of Science with a major in Electrical Engineering.


Dr. Ahmed Hassan Eltom, Chairperson

We have read this thesis and
recommend its acceptance:



Accepted for the Graduate Council


Dean of Graduate Studies

ACKNOWLEDGMENT

To my parents, I would like to express his thanks and appreciation to Dr. Elton for his unlimited help and guidance throughout this work. Also, I would like to express thanks to the committee members for their review and suggestions of this thesis: Dr. Thomason, Dr. Parten and Dr. Keilany.

used to study the efficiency, power factor and magnitude of these
between the proposed phase voltage (500V) and the

The main purpose of this study is to study the effect of the
phase voltage on the efficiency by increasing a high impedance load in the motor
circuit. In this study, a motor is used to illustrate the effect of phase
voltage on the efficiency by varying the phase voltage at the motor
terminals. The efficiency variation of a motor impedance with frequency is
characterized using a model that is based on Maxwell's equations. This
model has been verified in previous laboratory

In all cases considered, increasing phase voltage substantially reduced
the efficiency of the standard efficiency motors to drive loads equal to their
rated full load output power. When unbalanced phase voltage
conditions exist, the percentage increase in motor losses are higher for the
100, 150 and 200 hp standard efficiency motors and are higher for the 250

ACKNOWLEDGMENT

The author would like to express his thanks and appreciation to Dr. Eltom for his unlimited help and guidance throughout this work. Also, I would like to express thanks to the committee members for their review and suggestions of this thesis: Dr. Thomason, Dr. Parten and Dr. Keilany.

used to study the efficiencies, power losses and economics of motor behavior when unbalanced phase voltage system conditions exist.

Previous polyphase induction motor studies simulated unbalanced phase voltage conditions by assuming a high impedance fault at the motor terminals. In this study, a method is used to simulate unbalanced phase voltage conditions by varying the phase voltage at one of the motor terminals. The nonlinear variation of motor impedance with frequency is characterized using a model that is based on Maxwell's equations. This model has been verified in previous laboratory tests.

In all cases considered, increasing phase voltage unbalance caused the efficiencies of the standard efficiency motors to drop more rapidly than those of the energy efficient motors. When unbalanced phase voltage conditions exist, the percentage increase in rotor losses are higher for the 100, 150 and 200 hp standard efficiency motors and are higher for the 25,

This study investigates the behaviors and economics of standard and energy efficient polyphase induction motors under unbalanced phase voltage conditions of up to 5 percent. Motors sizes of 25, 50, 100, 150, 200, 250 and 300 hp are used in this investigation. Computer simulations are used to study the efficiencies, power losses and economics of motor behavior when unbalanced phase voltage system conditions exist.

Previous polyphase induction motor studies simulated unbalanced phase voltage conditions by assuming a high impedance fault at the motor terminals. In this study, a method is used to simulate unbalanced phase voltage conditions by varying the phase voltage at one of the motor terminals. The nonlinear variation of motor impedance with frequency is characterized using a model that is based on Maxwell's equations. This model has been verified in previous laboratory tests.

In all cases considered, increasing phase voltage unbalance caused the efficiencies of the standard efficiency motors to drop more rapidly than those of the energy efficient motors. When unbalanced phase voltage conditions exist, the percentage increase in rotor losses are higher for the 100, 150 and 200 hp standard efficiency motors and are higher for the 25,

50, 250 and 300 hp energy efficiency motors. Economic evaluations reveal that additional financial savings will occur if energy efficient motors are used in place of standard efficiency motors as unbalanced phase voltage conditions intensify. The payback time required to overcome the higher initial purchase costs of energy efficient motors are more quickly recovered when unbalanced phase voltage system conditions exist.

It is noted that slight reductions in full load rotor speed and increases in current occur when the motors are subjected to unbalanced phase voltages while constantly maintaining rated output torque. Each unbalanced phase voltage level corresponds to a unique rotor speed that is close to the full load operating speed when phase voltages are balanced.

APPENDIX F: Skin Effect.....	16
APPENDIX G: Electrical Model.....	20
APPENDIX H: Skin Effect Impedance Model of the Induction Motor.....	24
APPENDIX I: Motor Torque.....	27
J. Economics.....	28
3. METHODS OF INVESTIGATION.....	32
A. Skin Effect.....	33
B. Unbalanced Voltages.....	35

CHAPTER	Loss Calculations	PAGE
1.	INTRODUCTION.....	41
	A. The Unresolved Problems.....	42
	B. Research Objectives.....	3
2.	REVIEW OF LITERATURE.....	5
	A. Efficiency.....	6
	B. Motor Losses.....	8
	C. Motor Sizing.....	10
	D. Motor Rewinding.....	11
	E. Unbalanced Voltages.....	13
	F. Skin Effect.....	16
	G. Electrical Model.....	20
	H. Skin Effect Impedance Model of the Induction Motor.....	24
	I. Motor Torque.....	27
	J. Economics.....	28
3.	METHODS OF INVESTIGATION.....	32
	A. Skin Effect.....	33
	B. Unbalanced Voltages.....	35

C. Motor Operating Conditions.....	37
TABLE D. Loss Calculations.....	PAGE 40
B.1 E. Economic Methods.....	41
4.2 RESULTS AND DISCUSSIONS.....	44
B.3 A. Rotor Losses.....	44
B.4 B. Efficiencies.....	45
B.5 C. Economics.....	46
B.6 D. Graphs.....	47
5.7 CONCLUSION.....	104
WORKS CITED.....	107
APPENDICES.....	112
APPENDIX A. PROGRAM FLOW CHART AND LISTING.....	113
APPENDIX B. MOTOR DATA.....	124
APPENDIX C. EXAMPLE SKIN EFFECT CALCULATION.....	139
APPENDIX D. STARTING CURRENTS FOR 25 HP STM AND EEM VS. ROTOR SPEED IN PER UNIT.....	140

LIST OF TABLES

TABLE		PAGE
B.1	25 hp EEM and STM parameters.....	125
B.2	50 hp EEM and STM parameters.....	127
B.3	100 hp EEM and STM parameters.....	129
B.4	150 hp EEM and STM parameters.....	131
B.5	200 hp EEM and STM parameters.....	133
B.6	250 hp EEM and STM parameters.....	135
B.7	300 hp EEM and STM parameters.....	137
	Unbalance.....	49
4.2	Percent Decrease in Efficiencies for 25 hp STM and EEM vs. Percent Voltage Unbalance.....	50
4.3	Rotor Losses for 25 hp STM and EEM vs. Percent Voltage Unbalance.....	51
4.4	Percent Increase in Rotor Losses for 25 hp STM and EEM vs. Percent Voltage Unbalance.....	52
4.5	Yearly Savings for 25 hp by Using EEM over STM vs. Percent Voltage Unbalance.....	53

LIST OF FIGURES

FIGURE	PAGE
2.1	The Cross Section of a Deep Rotor Bar..... 19
2.2	Rotor Bar Equivalent Circuit..... 21
2.3	Positive Sequence of the Skin Effect Impedance Model..... 25
2.4	Negative Sequence of the Skin Effect Impedance Model..... 25
3.1	Steady State Region of Motor Torques with Corresponding Percent Voltage Unbalance vs. Slip or Speed in Per Unit..... 39
4.1	Efficiencies for 25 hp STM and EEM vs. Percent Voltage Unbalance..... 49
4.2	Percent Decrease in Efficiencies for 25 hp STM and EEM vs. Percent Voltage Unbalance..... 50
4.3	Rotor Losses for 25 hp STM and EEM vs. Percent Voltage Unbalance..... 51
4.4	Percent Increase in Rotor Losses for 25 hp STM and EEM vs. Percent Voltage Unbalance..... 52
4.5	Yearly Savings for 25 hp by Using EEM over STM vs. Percent Voltage Unbalance..... 53

4.6	Percent Increase in Yearly Saving for 25 hp by Using EEM over STM vs. Percent Voltage Unbalance.....	54
4.7	Payback Time for 25 hp STM and EEM vs. Percent Voltage Unbalance.....	55
4.8	Efficiencies for 50 hp STM and EEM vs. Percent Voltage Unbalance.....	57
4.9	Percent Decrease in Efficiencies for 50 hp STM and EEM vs. Percent Voltage Unbalance.....	58
4.10	Rotor Losses for 50 hp STM and EEM vs. Percent Voltage Unbalance.....	59
4.11	Percent Increase in Rotor Losses for 50 hp STM and EEM vs. Percent Voltage Unbalance.....	60
4.12	Yearly Savings for 50 hp by Using EEM over STM vs. Percent Voltage Unbalance.....	61
4.13	Percent Increase in Yearly Saving for 50 hp by Using EEM over STM vs. Percent Voltage Unbalance.....	62
4.14	Payback Time for 50 hp STM and EEM vs. Percent Voltage Unbalance.....	63

4.15	Efficiencies for 100 hp STM and EEM vs. Percent Voltage Unbalance.....	65
4.16	Percent Decrease in Efficiencies for 100 hp STM and EEM vs. Percent Voltage Unbalance.....	66
4.17	Rotor Losses for 100 hp STM and EEM vs. Percent Voltage Unbalance.....	67
4.18	Percent Increase in Rotor Losses for 100 hp STM and EEM vs. Percent Voltage Unbalance.....	68
4.19	Yearly Savings for 100 hp by Using EEM over STM vs. Percent Voltage Unbalance.....	69
4.20	Percent Increase in Yearly Saving for 100 hp by Using EEM over STM vs. Percent Voltage Unbalance.....	70
4.21	Payback Time for 100 hp STM and EEM vs. Percent Voltage Unbalance.....	71
4.22	Efficiencies for 150 hp STM and EEM vs. Percent Voltage Unbalance.....	73
4.23	Percent Decrease in Efficiencies for 150 hp STM and EEM vs. Percent Voltage Unbalance.....	74

4.24	Yearly Savings for 200 hp by Using EEM over STM vs. Rotor Losses for 150 hp STM and EEM vs. Percent Voltage Unbalance.....	85
	Unbalance.....	75
4.25	Percent Increase in Yearly Saving for 200 hp by Using EEM over STM vs. Percent Voltage Unbalance.....	86
	vs. Percent Voltage Unbalance.....	76
4.26	Payback Time for 200 hp STM and EEM vs. Percent Voltage Unbalance.....	87
	Yearly Savings for 150 hp by Using EEM over STM vs. Percent Voltage Unbalance.....	77
4.27	Efficiencies for 250 hp STM and EEM vs. Percent Voltage Unbalance.....	89
	Percent Increase in Yearly Saving for 150 hp by Using EEM over STM vs. Percent Voltage Unbalance.....	78
4.28	Percent Decrease in Efficiencies for 250 hp STM and EEM vs. Percent Voltage Unbalance.....	90
	Payback Time for 150 hp STM and EEM vs. Percent Voltage Unbalance.....	79
4.29	Rotor Losses for 250 hp STM and EEM vs. Percent Voltage Unbalance.....	91
	Efficiencies for 200 hp STM and EEM vs. Percent Voltage Unbalance.....	81
4.30	Percent Increase in Rotor Losses for 250 hp STM and EEM vs. Percent Voltage Unbalance.....	92
	Percent Decrease in Efficiencies for 200 hp STM and EEM vs. Percent Voltage Unbalance.....	82
4.31	Yearly Savings for 250 hp by Using EEM over STM vs. Rotor Losses for 200 hp STM and EEM vs. Percent Voltage Unbalance.....	93
	Unbalance.....	83
4.32	Percent Increase in Yearly Saving for 250 hp by Using EEM over STM vs. Percent Voltage Unbalance.....	94
	vs. Percent Voltage Unbalance.....	84

4.33	Yearly Savings for 200 hp by Using EEM over STM vs. Percent Voltage Unbalance.....	85
4.34	Percent Increase in Yearly Saving for 200 hp by Using EEM over STM vs. Percent Voltage Unbalance.....	86
4.35	Payback Time for 200 hp STM and EEM vs. Percent Voltage Unbalance.....	87
4.36	Efficiencies for 250 hp STM and EEM vs. Percent Voltage Unbalance.....	89
4.37	Percent Decrease in Efficiencies for 250 hp STM and EEM vs. Percent Voltage Unbalance.....	90
4.38	Rotor Losses for 250 hp STM and EEM vs. Percent Voltage Unbalance.....	91
4.39	Percent Increase in Rotor Losses for 250 hp STM and EEM vs. Percent Voltage Unbalance.....	92
4.40	Yearly Savings for 250 hp by Using EEM over STM vs. Percent Voltage Unbalance.....	93
4.41	Percent Increase in Yearly Saving for 250 hp by Using EEM over STM vs. Percent Voltage Unbalance.....	94

4.42	Payback Time for 250 hp STM and EEM vs. Percent Voltage Unbalance.....	95
4.43	Efficiencies for 300 hp STM and EEM vs. Percent Voltage Unbalance.....	97
4.44	Percent Decrease in Efficiencies for 300 hp STM and EEM vs. Percent Voltage Unbalance.....	98
4.45	Rotor Losses for 300 hp STM and EEM vs. Percent Voltage Unbalance.....	99
4.46	Percent Increase in Rotor Losses for 300 hp STM and EEM vs. Percent Voltage Unbalance.....	100
4.47	Yearly Savings for 300 hp by Using EEM over STM vs. Percent Voltage Unbalance.....	101
4.48	Percent Increase in Yearly Saving for 300 hp by Using EEM over STM vs. Percent Voltage Unbalance.....	102
4.49	Payback Time for 300 hp STM and EEM vs. Percent Voltage Unbalance.....	103
D.1	Starting Currents for 25 hp STM and EEM vs. Rotor Speed in Per Unit.....	144

CHAPTER 1

INTRODUCTION

Long gone is the era of carefree energy use with little regard for efficiency. In a previous time, simply considering the purchase cost of a polyphase induction motor would have sufficed for economic analysis. The climate has greatly changed in regards to energy efficiency and conservation expectations. Social and political pressures have worked to fuel a resistance to nuclear power generation. Obtaining rights of way for new power lines to meet growing power demands have been met with resistance and difficulty in many localities. To relieve the stress on the power system, power companies now work with industrial customers to correct power factor problems caused by the typical inductive machine loads used in industry. Polyphase squirrel cage induction motors are the most commonly used motor type in industry. Accounting for over 76 percent of the power used in industry, motors have become a ripe area for efficiency improvements (16).

The importance of this investigation into the effects that unbalanced phase voltages have on the efficiencies, rotor losses and the economics of a standard and energy efficient motors is made especially germane by the

Energy Policy Act (EPACT) of 1992 that was enforced by the government in October 1997. The EPACT standards require that all general purpose, polyphase, single speed, squirrel-cage induction motors manufactured for sale in the United States that are rated from 1-200 hp meet minimum efficiency standards (23). The Motor Challenge Program is an industry and government initiative that uses market forces to promote a systems approach to design, purchase, installation, and management of electric motor driven systems. Program objectives, in addition to improving industrial energy efficiency, include enhancing manufacturing productivity and reducing energy-related greenhouse gas emissions (23).

The Unresolved Problems

Unbalanced phase voltages applied at the motor terminals have not been fully examined in an accurate way. Unbalanced phase voltages occur when at least one of the phase voltages change from the rated level. Previous studies have modeled unbalanced phase voltages by using a high impedance fault at one of the phase voltages. This method of simulating unbalanced phase voltages allowed motor currents to be shunted to the ground through the fault, greatly distorting results. This does not provide a correct model for the study of the effects unbalanced phase voltage

conditions have on polyphase induction motors when investigating efficiencies, rotor losses, and economics.

Conventional economic evaluations of motors are conducted under the assumption that phase voltages are balanced, ignoring the fact that standard and energy efficient motors in operation encounter some percentage of unbalanced phase voltage. The effects of unbalanced voltage on efficiencies, rotor losses, and economics have not been fully investigated for standard and energy efficient polyphase induction motors.

Research Objectives

In this investigation, unbalanced phase voltages are simulated by varying the phase voltages at the motor terminals. The rotor bar skin effect impedance model is employed in a computer program to analyze and contrast the behaviors of polyphase induction motors when subjected to unbalanced phase voltage conditions. This skin effect impedance model more accurately accounts for the nonlinear dependence of rotor bar impedance with speed and frequency (1, 5). Energy efficient (EEM) and standard efficiency (STM) motors in sizes of 25, 50, 100, 150, 200, 250 and 300 hp were used to study the effects unbalanced phase voltages have on efficiencies, rotor losses and the economics of the motors. The reason it is

important to study efficiencies, rotor losses, and economic effects for polyphase induction motors resulting from unbalanced phase voltage conditions is that conventional analysis has only assumed balanced phase voltage conditions. Comparing the performances of standard and energy efficient motors based on unbalanced phase voltages lends insight into the selection of motors when subject to these conditions.

Chapter 2 contains mention of some of the previous research conducted on polyphase induction motors. The skin effect impedance model of the rotor bar, unbalanced phase voltages, rotor losses, efficiencies, motor loading, motor rewinding, physical differences between EEM and STM motors, and economics are reviewed.

Chapter 3 covers the methods used in doing the research. Methods used to implement this investigation into polyphase motor behavior when subjected to unbalanced phase voltages are covered in this chapter.

Chapter 4 contains the results and discussions. In this section graphs are presented for all motors that contrast the efficiencies, rotor losses and economic evaluations of all motors as they are subjected to unbalanced phase voltage conditions. Comparisons are made and discussed.

The overall conclusions of this work are presented in Chapter 5.

REVIEW OF LITERATURE

Reviewing previous work in the field of polyphase induction motors provides a background by which new investigations can be conducted. The information contained in this section provides the framework for intelligently understanding the contrasts between energy efficient motors (EEM) and standard efficiency motors (STM) in later chapters of this study. Terms are defined and insights are gained by more deeply considering aspects of polyphase induction motors.

This current investigation into unbalanced phase voltage effects on polyphase induction motors hinges on the importance of using the nonlinear rotor bar skin effect impedance model developed by Ortmeyer (5) and confirmed by Eltom (1) in laboratory tests. This Ortmeyer and Eltom rotor bar skin effect impedance model has its roots in the work done in 1951 by Babb and Williams (12) to more accurately model rotor bar impedance. Zocholl (14) also attempted to model rotor bar impedance by using linear straight line approximations of impedance that depended on slip.

Formula used with direct methods:

$$\text{Efficiency} = \text{output power}/(\text{input power}) * 100. \quad (2.1)$$

Efficiency

Efficiency is a measure of the ability of an electric motor to convert electrical energy to mechanical energy (10). Kilowatts of electrical power are supplied to the motor at its electrical terminals and the horsepower of mechanical energy is taken out of the motor at the rotating shaft (6). Montgomery (16) states that the efficiency of a motor will remain relatively constant throughout the motor's life if the silicon steel, or properly decarbonized cold rolled steel, used in the motor is never subjected to temperatures higher than 150 degrees centigrade. Standard steel does age and the losses can increase. Low carbon steel that contains a residual carbon will experience an approximate increase of 30 percent in losses after three weeks at 150 degrees centigrade (16).

Two very broad categories for determining efficiency exist: direct measurement methods and segregated loss methods (10). In direct measurement methods, both the input power and output power to the motor are measured directly. In the segregated loss methods, one or both are not measured directly. General formulas for efficiency calculations are shown. Formula used with direct methods:

$$\text{Efficiency} = \text{output power}/(\text{input power}) * 100. \quad (2.1)$$

Formulas used with segregated loss methods:

$$\text{Efficiency} = [(\text{input power} - \text{losses}) / \text{input power}] * 100 \quad (2.2)$$

or

$$\text{Efficiency} = [\text{output power} / (\text{output power} + \text{losses})] * 100. \quad (2.3)$$

Common definitions of efficiency in use are the following (22):

1) Average or Nominal Efficiency -- the average full load efficiency value obtained through testing a sample population of the same motor model.

2) Guaranteed Minimum or Expected Minimum Efficiency -- all motors purchased or a stated percentage of the motors purchased are guaranteed to have efficiencies that equal or exceed this full load value.

3) Apparent Efficiency -- the product of motor power factor and minimum efficiency. Energy consumption can vary considerably with this definition since the power factor can be high while the efficiency is low.

4) Calculated Efficiency -- an average expected efficiency based upon a relationship between design parameters and test results.

NEMA (National Electrical Manufacturers Association) has created an efficiency labeling standard which recognizes the realities of motor to motor variations and testing accuracy. This provides motor buyers with an effective means of price and performance comparisons for motors of similar

ratings. The NEMA specified Nominal (same as full load) efficiency is identified on the motor nameplate. The actual motor efficiency, according to NEMA standards, may lie anywhere between the minimum guaranteed value and the maximum expected value (9). The actual efficiency of the motor must be above the minimum efficiency, which is based on a 20% loss difference that follows a Gaussian distribution (4).

Motor Losses

There are five areas that make up the losses in induction motors (4). The primary I^2R loss is the ohmic loss caused by current passing through the stator windings. Increasing the copper winding wire size that goes around the stator core is an effective means of reducing this loss. The second area of motor loss is the secondary I^2R loss in the rotor bars and end rings (16). These are the ohmic losses in the rotor bars. At first thought, it might appear possible to reduce the rotor losses by adding more material to the rotor bars. Unfortunately, it is not this simple. Because the motor's starting torque is proportional to its rotor resistance (4), the motor must meet some specified value of starting torque usually defined by NEMA. This limits the range through which secondary (rotor) resistances can be varied. Energy efficient motors typically have longer rotors contributing to the increased

overall length of an energy efficient motor. Longer rotors can contribute to improved efficiency and less rotor power loss while maintaining proper starting torque because better skin effect characteristics allow higher starting resistances and lower running resistances. The iron core stator loss is the third area of loss. Energy efficient motors have longer iron stator cores that reduce hysteresis and eddy current losses (4) and reduce magnetic flux densities (22). Energy efficient motors are longer than similarly sized standard efficiency motors, even though they both have the same frame type and mounting configuration. Thinner laminations also reduce the thickness of the iron core. Improved permeability electromagnetic silicon steel, as opposed to the standard carbon steel (9), works to reduce the magnetic flux densities in the energy efficient motor (22). This is why the most energy efficient motors will contain more iron and more copper than a standard motor of the same rating. Friction and windage losses are the fourth group of losses. The cooling fan inside the motor and the friction of the bearings are the major sources of friction and windage losses. These can be reduced by using smaller, more efficient fans and by using bearings of higher quality with less kinetic friction. Because energy efficient motors run cooler, they have fewer losses to dissipate resulting in the use of a smaller cooling fan.

The final and fifth source of loss, stray load loss, is the most elusive of all. Defined as the difference between total motor losses and the sum of the other four losses, these “residual” (9) losses are complex and difficult to control. They are reduced by careful design and manufacturing process control to optimize the air gap between stator and rotor (9). The positive improvements in loss control for the energy efficient motor can be summed up by the following characteristics (13): longer rotors, longer stator cores, more magnetic material, larger gauge wire in the windings, lower flux density, and a smaller air gap.

Motor Sizing

When a motor is overrated with a much higher rating than is needed to drive the load, the power factor drops significantly to between 65 and 100 percent of the full rated load and the efficiency drops significantly below about 50 percent of full the rated load. This is a great source of energy waste. Despite the fact that motors which are oversized for a particular use reduce efficiency and increase energy costs, industries use oversized motors for some of the following reasons (22):

- 1) To ensure against motor failures in absolutely critical processes;
- 2) Lack of knowledge of actual load;

- 3) To build in capability to accommodate future increases in production;
- 4) To guard against load fluctuations that may exceed the motor's rating;
- 5) Maintenance staff replace failed motors with next larger model;
- 6) To operate under adverse conditions such as phase voltage unbalance.

Motors that are oversized suffer from both efficiency and power factor reduction penalties. Rated efficiency will usually occur as long as the motor is operated between 65 to 100 percent of the full rated load (22). The Motor Challenge Program works to clear up the common misconceptions industry may hold that results in the practice of motor oversizing.

Motor Rewinding

Rewinding of the modern squirrel cage induction motor is typically defined as replacing the stator windings around the iron cores. Since the rotors are cast aluminum (16) or have rotor bars, there is seldom anything done to the rotor when the motor is rewound. In rare cases, the rotor may also be recast. Rewinding a standard motor to try and achieve a more energy efficient motor is subject to some controversy as to its effectiveness. The decision of replacing a burned out motor with a new energy efficient one, versus rewinding the old existing motor, is a difficult choice to make in many circumstances due to the uncertainty of the efficiency that can be

achieved by rewinding the existing motor. The efficiency of a failed motor before its failure occurs is often unknown and the efficiency after rewinding can also be unclear (4). Rewound motors can be less efficient than they were originally because of increases in eddy currents lower efficiency.

Because most losses occur in the stator windings, theoretically it should be possible to decrease these I^2R losses. Since the iron core size and material is not changed, the area for improvement when rewinding a motor is to improve the quality of the wire windings around the cores to decrease I^2R losses. Some manufacturers do not completely fill the slots in the stator core with wire when manufactured (4). These motors are prime candidates for a rewinding with slightly larger diameter copper wire to reduce the loss and increase the efficiency.

The quality of the motor rewinding shop is a determining factor in how much of an efficiency improvement can be made by rewinding the motor. Newer motors are more likely to have the latest rotor bar designs that maximize the beneficial skin effects. With increases in eddy current losses due to rewinding, the motor may not operate as efficiently as it originally did. In a typical rewind, the stator is heated to a temperature high enough to burn out its winding insulation (22). There is a trade off in

rewinding time versus a good job. High heat can be used to quickly soften the varnish for easy coil removal at the expense of damaging the motor's iron core. If the stator core is heated above 700 degree Fahrenheit, the insulation between the stator laminations will break down (4, 22). This will increase eddy current losses and lower the motor's operating efficiency. After the laminations are damaged, the insulation cannot be repaired nor the efficiency loss restored without restacking the iron with new laminates (22).

Unbalanced Voltages

Unbalanced phase voltages applied to polyphase induction motors cause efficiencies to decrease and power losses to increase. The rotor bar impedance and the current rise with increasing percent phase voltage unbalance and decreasing rotor speed. Therefore, the importance of unbalanced phase voltages must be emphasized. The analysis of a three phase circuit in which phase voltages and currents are balanced is relatively simple since the treatment of a single phase leads directly to the three phase solution (21). When a three phase system has unbalanced phase voltages the method of analysis is by symmetrical components and sequence networks. The method of symmetrical components was presented by Fortescue in a paper in 1918 (21). This method is now recognized as the

classic way of analyzing unbalanced voltage conditions in three phase (2.5)

machines and power systems.

Stated in a fundamental form, symmetrical component analysis means that an unbalanced group of n associated vectors, all of the same type, can be resolved into n sets of balanced vectors (21). The n vectors of each set are of equal length and symmetrically located with respect to each other (21). In a practical way, Clarke, Wagner, and Evans stated the equations for calculating the three sequence voltages (4, 21):

$$V_{a0} = (V_a + V_b + V_c)/3, \quad (2.4)$$

$$V_{a1} = (V_a + aV_b + a^2V_c)/3,$$

$$V_{a2} = (V_a + a^2V_b + aV_c)/3,$$

where a is the rotational operator,

$$a = \exp(j120).$$

Sequence networks are three circuit diagrams that illustrate the sequences.

V_{a0} , V_{b1} , and V_{c2} are the zero, positive and negative sequence voltages,

1) The negative sequence currents produce an increased total copper loss in respectively. V_a , V_b , and V_c are the phase voltages.

Unbalanced phase voltages can easily be discussed in terms of percent voltage unbalance (PVU). This is defined as (17, 19):

$$2) \text{ PVU} = \frac{\text{maximum voltage deviation from average voltage} * 100}{\text{average voltage}} \quad (2.5)$$

heating in the stator.
NEMA has specified a standard that says motors must be able to tolerate a 3) Core loss, which has an uneven spatial distribution, increases a negligible percent voltage unbalance (PVU) in phase voltages of plus or minus 5 amount for increases in negative sequence voltage of less than 15% or less percent of rated phase voltage (22). Operation under unusual service

Skin Effect

conditions may result in efficiency losses and the consumption of additional energy. Both standard and energy efficient motors can have their efficiencies and useful life reduced by a poorly maintained electrical system (22). The effect of voltage unbalance in a polyphase induction motor is the skin effect as "ac impedance". Exploiting the similarities with transmission line theory, Babb and Williams were able to find mathematical descriptions for the "ac impedances" of different types and geometries of rotor bars based on frequency. This counter-rotating flux produced by the voltage unbalance produces nearly a 120 Hz current in the rotor of an induction motor at low slip (20). Excessive heating of polyphase induction motors during unbalanced voltage conditions can be attributed to the following factors (18):

The goal of good induction motor design is to keep the rotor losses low by keeping the rotor resistances low at the full load speed to avoid poor efficiency. The torque developed by the motor is directly proportional to 1) The negative sequence currents produce an increased total copper loss in the rotor resistance and inversely proportional to the motor slip (6). Since both rotor and stator and a decrease in net shaft torque for a given positive the motor slip is equal to one at standstill, a large rotor resistance is needed sequence current.

to develop a high starting torque. This conflicting situation is easily solved in wound rotor induction motors when external rotor resistance is supplied

- 2) The unbalanced currents produce an unbalanced spatial distribution of heating in the stator.
- 3) Core loss, which has an uneven spatial distribution, increases a negligible amount for increases in negative sequence voltage of less than 15%.

Skin Effect

Skin effects have long been known in areas of electrical engineering. Original research was done in 1951 by Babb and Willams (12) on the skin effect in the rotor bars of induction motors. Babb and Willams referred to the skin effect as “ac impedance”. Exploiting the similarities with transmission line theory, Babb and Willams were able to find mathematical descriptions for the “ac impedances” of different types and geometries of rotor bars based on frequency.

The goal of good induction motor design is to keep the rotor losses low by keeping the rotor resistances low at the full load speed to avoid poor efficiency. The torque developed by the motor is directly proportional to the rotor resistance and inversely proportional to the motor slip (6). Since the motor slip is equal to one at standstill, a large rotor resistance is needed to develop a high starting torque. This conflicting situation is easily solved in wound rotor induction motors when external rotor resistance is supplied

via slip rings that can be varied to have maximum rotor resistance at starting and less at full load operating speed. For squirrel cage induction motors the rotor conductors are not accessible for any external control of resistance.

The details of how the skin effect actually works are very important. Therefore, in squirrel cage induction motors the skin effect in the rotor bars must be fully exploited for optimal motor performance and design.

Because of higher reliability, longer life, and lower cost, squirrel cage induction motors are considered the workhorses of all motors. In order to have suitable starting torque, deep bar, double cage, and triple cage induction motors have been designed to optimize the skin effect phenomena to achieve good starting torque and full load torque efficiency (8).

When the rotor is locked, the rotor frequency equals the stator frequency. As the motor reaches full load operating speed, the rotor frequency approaches 2-3 Hz. This is explained by equation 2.6 (11).

$$F_r = S * F_s, \quad (2.6)$$

$$S = (\omega_s - \omega_r) / \omega_s, \quad (2.7)$$

$$\omega_s = (120 * F_s) / P, \quad (2.8)$$

where,

F_r = rotor frequency Hz,

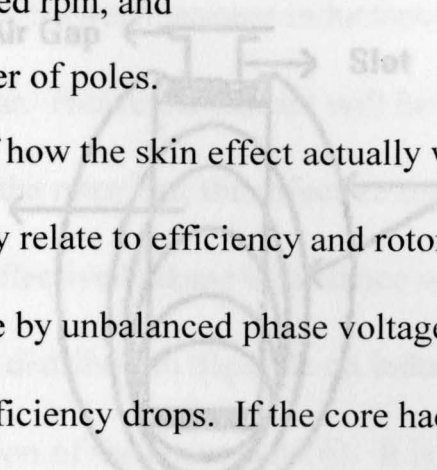
F_s = stator frequency Hz,

S = motor slip p.u.,

ω_s = synchronous speed rpm,

ω_r = rotor speed rpm, and

P = the number of poles.



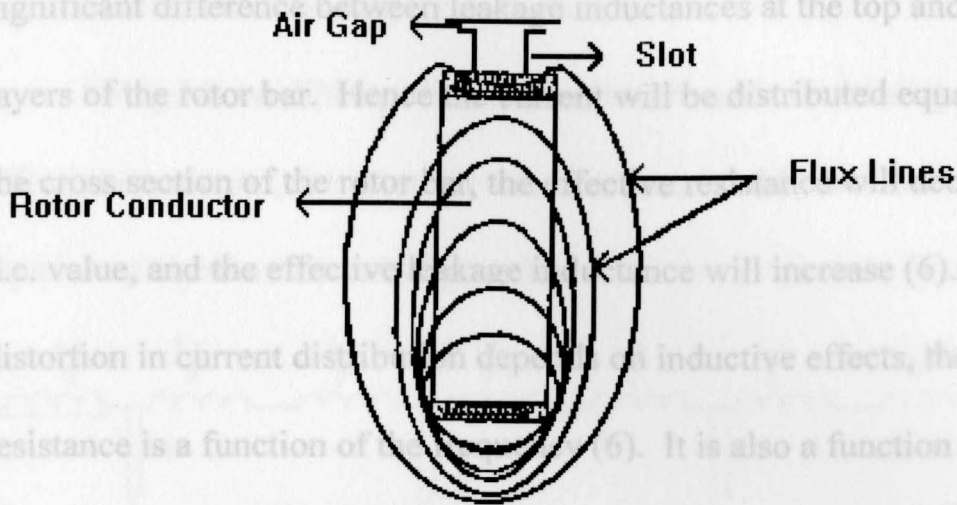
The details of how the skin effect actually works are very important because they directly relate to efficiency and rotor losses. When the rotor speed is reduced due by unbalanced phase voltages, rotor bar resistance is increased and the efficiency drops. If the core had infinite permeability, all the leakage flux lines, produced by the current flowing through the conductor, would close their paths the same way that the biggest flux line closes in figure 2.1 (6). However, most of the flux lines close their loops in a shorter path because the core has magnetic resistivity as shown in figure 2.1 (6). The distortion in the biggest flux line's path at the top of the slot is due to the air gap's high magnetic resistivity (6).

The leakage inductance is proportional to the number of leakage flux lines (6).

In addition, current in the upper layers will lead to the current in the lower ones (6). This phenomenon is called skin effect. The nonuniform current distribution results in an increase in the effective rotor bar resistance and a smaller decrease in its effective leakage inductance (3).

As the motor accelerates, the rotor frequency decreases, and hence the effect

of leakage flux lines weakens (6). Consequently, there will be no significant difference between leakage inductances at the top and bottom layers of the rotor bar. Hence, the current will be distributed equally over the cross section of the rotor bar. However, as the frequency increase to its d.c. value, and the effective leakage inductance will increase (6). Since the distortion in current distribution due to inductive effects, the effective resistance is a function of frequency (6). It is also a function of the depth of the bar and the permeability and resistivity of the bar material (3).



Electrical Model

Figure 2.1 The Cross Section of a Deep Rotor Bar

The use of the skin effect impedance model is important because it

As shown in figure 2.1 the bottom layers will be surrounded by more leakage flux lines than those at the top. Therefore, the inductance of the bottom layers would be much larger than those of the top layers. Most of the rotor current will be forced to flow through the layers that are closer to the air gap. In addition, current in the upper layers will lead to the current in the lower ones (6). This phenomenon is called skin effect. The nonuniform current distribution results in an increase in the effective rotor bar resistance and a smaller decrease in its effective leakage inductance (3). As the motor accelerates, the rotor frequency decreases, and hence the effect

of leakage flux lines weakens (6). Consequently, there will be no significant difference between leakage inductances at the top and bottom layers of the rotor bar. Hence the current will be distributed equally over the cross section of the rotor bar, the effective resistance will decrease to its d.c. value, and the effective leakage inductance will increase (6). Since the distortion in current distribution depends on inductive effects, the effective resistance is a function of the frequency (6). It is also a function of the depth of the bar and the permeability and resistivity of the bar material (3).

Electrical Model

The use of the skin effect impedance model is important because it more accurately relates the nonlinear impedance dependency to speed. The details of the practical use of this lumped parameter electrical circuit type model to represent the skin effect in the rotor bars was developed by Ortmeyer (5) and is used in the computer program to analyze the polyphase induction motors. It is general practice in electromagnetic theory that when computing the inductance of a circuit from Maxwell's equations that the inductance is separated into two groups: an external inductance and an internal inductance. The external inductance is a function of the geometry of the circuit and the materials involved, and is not a function of the currents

flowing in the conductor. The internal inductance, however, is a function of the current distribution in the conductor (5).

Using Maxwell's equations, Ohm's Law, and considering the skin effect phenomenon, the rotor bar can be represented by a series of N equivalent circuits shown in figure 2.2.

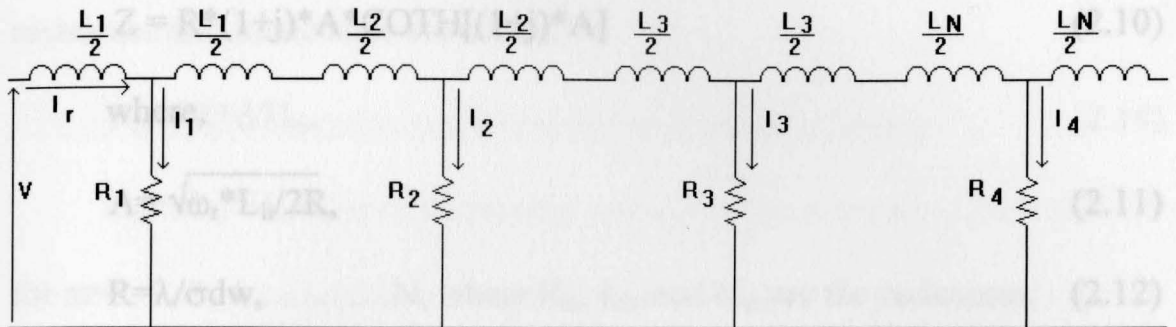


Figure 2.2 Rotor Bar Equivalent Circuit

The rotor current is the sum of the current in each segment,

$$I_r = \sum_{i=1}^n I_i. \quad (2.9)$$

This equivalent circuit of the squirrel cage induction motor is capable of predicting the current distribution in the bar. The physical basis and the reasonable assumptions of this model make it a more precise representation of the induction motor than previous models (5).

The parameters of this representation have been calculated in terms of the physical properties of the rotor bar. It is preferable to express

resistances and inductances of this rotor bar in terms of quantities that can be measured by electrical tests.

The rotor bar equivalent circuit of figure 2.2 is valid for both transient and steady state conditions as shown by Ortmeier (5). It was shown (5, 12) that the internal impedance of the rotor bar for a steady state condition is

$$Z = R(1+j)A \operatorname{COTH}[(1+j)A] \quad (2.10)$$

$$\text{where, } A = \sqrt{\omega_r L_{ii} / 2R} \quad (2.14)$$

$$A = \sqrt{\omega_r L_{ii} / 2R}, \quad (2.11)$$

$$R = \lambda / \sigma d w, \quad (2.12)$$

$$L_{ii} = \mu \lambda d / w, \quad (2.13)$$

and

ω_r = angular frequency, radians/sec,

λ = bar length,

d = bar depth,

w = bar width,

σ = conductivity coefficient,

μ = permeability of the core.

This impedance can be measured as a function of angular frequency ω_r and values of R and L_{ii} can be determined. R and L_{ii} can also be expressed in terms of rotor bar physical parameters, as indicated in equation 2.12 and 2.13.

Comparisons of these expressions with the rotor bar segment resistance and inductance show that:

$$R_m = R \cdot d / H_m, \tag{2.14}$$

$$L_m = L_{ii} \cdot H_m / d, \tag{2.15}$$

for $m=1, 2, 3, 4, \dots, N$, where R_m , L_m and H_m are the resistance, inductance, and depth of segment H , respectively (5). The parameters of the rotor bar representation of figure 2.2 can then be determined from the electrical properties of the rotor bar.

The accuracy of the rotor bar model with a specific number of bar segments represented can be determined by comparisons of the steady state solutions of that representation with the steady state solution given in equation 2.10.

The required parameters are R and L_{ii} from equations 2.12 and 2.13, the range of frequencies of interest, and the relative depth of each rotor bar segment. In reference (12) it is noted that convergence is faster if varying

depths are used with smaller segments near the top of the bar, where current will be concentrated at higher frequencies. The four segment approximation to the rotor bar is suggested by Ortmeyer (5) and uses the top 10 percent for the first segment, the next 20 percent for the second segment, 30 percent for the third segment, and 40 percent for the last segment. A similar division of segments is used throughout this study.

The Skin Effect Impedance Model of the Induction Motor

Ortmeyer developed a rotor bar model based on the rotor bar skin effect equivalent circuit that is capable of modeling the rotor bar current distribution and effective dynamic impedance but neglects the highly damped electrical transients (5). This skin effect impedance model is based on electrical machine theory. This theory is based on a set of assumptions applicable to all types of electrical machines (6). This model is applicable for use in some dynamic motor conditions as well (1,5). The positive and negative sequences of the steady state equivalent circuit of the skin effect impedance model of the induction motor are shown in figures 2.3 and 2.4, respectively.

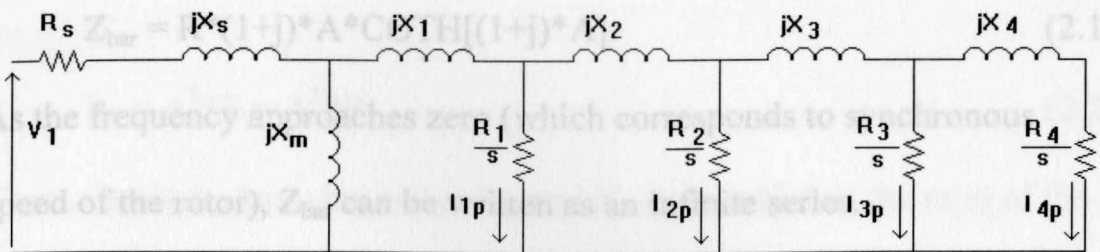


Figure 2.3 Positive sequence of the skin effect impedance model

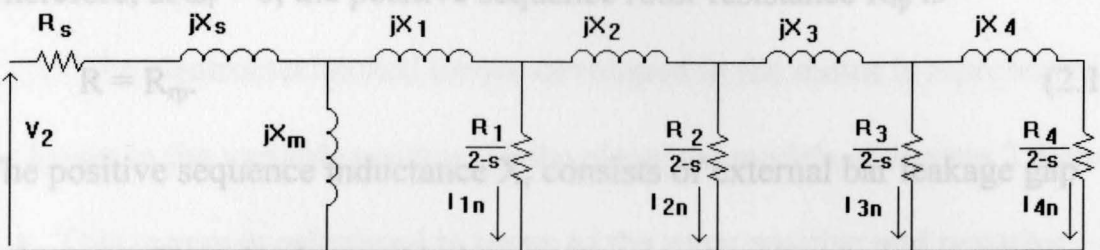


Figure 2.4 Negative sequence of the skin effect impedance model

A complete detail of this model is discussed by Ortmeier (5). This model accounts for the nonlinear relationship between rotor bar impedance and frequency. Eltom compared this model with laboratory fault tests on motors and his results established that the model is accurate and reliable for steady state conditions with quickly subsiding electrical transients (1).

The skin effect model of the induction motor requires more specific data than previous induction motor models. From equation 2.16 the internal rotor bar impedance will be:

$$Z_{\text{bar}} = R*(1+j)*A*\text{COTH}[(1+j)*A]. \quad (2.16)$$

As the frequency approaches zero (which corresponds to synchronous speed of the rotor), Z_{bar} can be written as an infinite series.

Since $A = \sqrt{\omega_r * L_{ii}/2R}$, the bar impedance is

$$Z_{\text{bar}} = R[1 + [(1+j)A]^2/3 - \dots] = R + j\omega_r L_{ii}/3. \quad (2.17)$$

Therefore, at $\omega_r = 0$, the positive sequence rotor resistance R_{rp} is

$$R = R_{rp}. \quad (2.18)$$

The positive sequence inductance X_r consists of external bar leakage gap inductance X_{gap} plus internal inductance at $\omega_r = 1$ p.u.

$$X_{\text{gap}} + L_{ii}/3 = X_r. \quad (2.19)$$

Finally, the values of X_{gap} and L_{ii} must be determined. These can be found

at $\omega_r = 2$ p.u. from either the rotor negative sequence resistance R_m or the

rotor negative sequence inductance L_m . At $\omega_r = 2$ p.u. the real part of

equation 2.17 equals the negative sequence rotor resistance.

$$\text{Re}(Z_{\text{bar}}) = RA \frac{[\text{Sinh}(2A) + 2\text{Sin}(2A)]}{\text{Cosh}(2A) - \text{Cos}(2A)} = R_m. \quad (2.20)$$

In equation 2.20, the quantity inside the brackets is approximately equal to

one, so

$$A = R_m/R = R_m/R_{rp}, \quad (2.21)$$

or

$$L_{ii} = A^2 * R = A^2 * R_{rp}. \quad (2.22)$$

Then, simply by knowing either R_{rp} and X_r , or A , which is the ratio of the rotor negative and positive sequence resistances, the positive and negative sequence skin effect models can be developed.

Motor Torque

The electromechanical torque developed in the motor is represented by losses in the variable resistors in the electrical models of figures 2.3 and 2.4. This torque is calculated in terms of the rotor positive and negative losses and the motor slip as shown in equation 2.23.

$$T_{em} = I_{r+}^2 [R_{rp}/s] - I_{r-}^2 [R_{rn}/(2-s)] \quad (2.23)$$

or

$$T_{em} = T_{ep} - T_{en} \quad (2.24)$$

where,

T_{em} is the electromechanical torque developed by the motor,

T_{ep} is the positive sequence torque,

T_{en} is the negative sequence torque,

I_{r+} and I_{r-} are the rotor positive and negative sequence currents, and

R_{rp} and R_{rn} are the rotor positive and negative sequence resistances.

Economics

The goal of motor purchasing is to seek to maximize efficiency while minimizing the purchase price. Economic evaluation of motors depends on efficiency.

The simple payback method is typically used for individual or smaller quantities of motors to compare energy efficient motors to standard efficiency motors. To determine the savings realized by using a high efficiency motor, the following calculation may be performed (9).

$$S = 0.746 * hp * L * C * N * [(100/E_B) - (100/E_A)] \quad (2.25)$$

where,

S = annual savings, \$/year, (2.27)

L = percentage of full operating load,

C = cost of electricity \$/KWH, and (2.28)

N = running time, hr/yr, of number of years of operation.

E_B = standard motor efficiency under actual load condition, and life

E_A = energy-efficient motor efficiency under actual load conditions.

After the annual saving is computed, the payback period in years can be found by considering the difference in purchase prices of the motors (7). (2.28)

$$PBP = CD/S \quad (2.26)$$

where, Comprehensive evaluation method takes into account the time value
 PBP = payback period, years, and
 CD = cost differences between two motors, dollars.

The Efficiency Evaluation Factor method is used by many companies that have large groups of motors that run the same number of hours per year at the same power costs (10). To expedite the comparison of these motors under similar conditions, an efficiency factor can be calculated based on the expected motor operating life in years, the power cost, and the hours per year of running time. This efficiency factor can be expressed in dollars per kilowatt.

$$EF(\$/kw) = C * N * n, \quad (2.27)$$

C = Average energy cost, dollars per kWh,

N = Running time, hrs. per year, and (2.30)

n = Period of evaluation of number of years of operation.

The evaluation factor can then be used to find the life cycle savings. Life cycle savings give the dollar savings in energy over the period the motors are being evaluated (7).

$$LCS = 0.746 * hp * EF[(100/E_B) - (100/E_A)]. \quad (2.28)$$

W = Apparent years of operation,

The comprehensive evaluation method takes into account the time value of money and the impact of inflation on power costs to determine the Present Worth Evaluation Factor (PWEF) (9).

The effective interest rate takes into account the power cost inflation rate and the internal rate of return on investment (9).

$$i = \{(1+R_2)/(1+R_1)-1\}, \quad (2.29)$$

i = effective rate of return (percent/100),

R_1 = expected annual rate of increase in power (percent/100),

R_2 = internal rate of return on investments (percent/100).

The apparent years of operation (W) are the years of operation considering the present worth (9). They are found by applying the effective interest rate to the uniform series present worth (9).

$$W = \{(1+i)^n - 1\} / \{i(1+i)^n\}, \quad (2.30)$$

n = number of years of operation of period of evaluation,

Present Worth Evaluation Factor (PWEF) (9),

$$PWEF (\$/KW) = C * N * W, \quad (2.31)$$

C = Average energy cost, \$/kWh,

N = Running time, hours per year,

W = Apparent years of operation,

Present Worth Life Cycle Savings (PWLCS) (9), and

$$PWLCS = 0.746 * hp * PWEF[100/E_B - 100/E_A]. \quad (2.32)$$

The Concise Saving Evaluation Method compares the motors to be evaluated to a perfect motor which would have an efficiency of 100 percent. The present worth cost of losses over the motor life cycle is then evaluated (9). The method is very attractive when many motor ratings and/or vendors are being evaluated (9).

$$PW \text{ Losses} = 0.746 * hp * PWEF[100/E - 1], \quad (2.33)$$

PW Losses = Present worth cost of motor losses,
E = Efficiency of motor being evaluated.

The present worth cost of motor losses is then added to the cost of each motor being evaluated and a decision is made on the basis of the most economical design (9).

The original data collected in the delta format to a wye format for simplicity and uniformity of analysis. The main tool that provided the investigative capabilities was the computer with the mathematical computing environment of Matlab. This chapter reviews the general methods and formulas used in the computer program to investigate the motors.

$$L = P_{avg} \times t \quad (2.34)$$

METHODS OF INVESTIGATION

Comparison studies were conducted between energy efficient (EEM) and standard efficiency (STM) polyphase induction motors using the information from 14 motor data sheets supplied by a manufacturer. Half of the motors were STM and half were EEM. Motors of 25, 50, 100, 150, 200, 250 and 300 hp sizes were used in this case study. The pertinent aspects of the original motor data sheets from the manufacturer are presented on concise motor data sheets supplied in Appendix B. The motor manufacturer conducted the original data gathering lab tests for some of the motors in a wye configuration and for some of the motors in a delta configuration. Standard delta to wye transformation formulas provided the means necessary to convert the original data collected in the delta format to a wye format for simplicity and uniformity of analysis. The main tool that provided the investigative capabilities was the computer with the mathematical computing environment of Matlab. This chapter reviews the general methods and formulas used in the computer program to investigate the motors.

$$L_{ll} = r_{mag}^2 / r_r \quad (3.2)$$

Skin Effect

The skin effect impedance model developed by Ortmeyer (5) and tested by Eltom (1) is used to model the rotor bar skin effects in this research. Previous research has confirmed that the electrical transients subside quickly enough to allow sufficient accuracy using the skin effect impedance model of the rotor bar (5). This skin effect impedance model has been carefully reviewed in the previous chapter from a more theoretically viewpoint. The methods of implementation of the skin effect impedance model used in this study are now explored here. The skin effect impedance models are shown in figures 2.2, 2.3 and 2.4.

Using the motor parameters r_s , x_s , x_m , r_r , $r_{r\text{ start}}$, x_r , and s_{fl} the skin effect electrical circuit model parameters can be calculated. From Zocholl's (14) equations of the linear approximation to the rotor bar skin effect, the following equation can be adapted for use here to find the negative rotor resistance value.

$$r_{\text{meg}} = (r_{\text{rstart}} - r_r) * (2 - s_{fl}) + r_r. \quad (3.1)$$

The internal inductance L_{ii} , that is a function of the current distribution in the rotor bar conductor, is calculated (5).

$$L_{ii} = r_{\text{meg}}^2 / r_r. \quad (3.2)$$

The rotor bar equivalent circuit parameters L_1 , L_2 , L_3 and L_4 that are shown in figure 2.2 can now be calculated.

$$L_1 = L_{ii} * 0.1, \quad (3.3)$$

$$L_2 = L_{ii} * 0.2,$$

$$L_3 = L_{ii} * 0.3,$$

$$L_4 = L_{ii} * 0.4.$$

The external inductance x_{gap} is a function of the geometry of the circuit and the materials involved and is not a function of the currents flowing in the rotor bar conductor (5).

$$x_{\text{gap}} = x_r - L_{ii} / 3. \quad (3.4)$$

The parameters of figures 2.3 and 2.4 showing the impedance models for the positive and negative sequences, respectively, can be found. Summing the inductances based on the methods of Babb and Willams (12) and others (1, 5) yields the following.

$$x_1 = x_{\text{gap}} + L_1 / 2, \quad (3.5)$$

$$x_2 = L_1 / 2 + L_2 / 2,$$

$$x_3 = L_2 / 2 + L_3 / 2,$$

$$x_4 = L_3 / 2 + L_4 / 2.$$

The constant resistance values that apply to figures 2.2, 2.3 and 2.4 are calculated.

$$R_1 = r_r / 0.1, \quad (3.6)$$

$$R_2 = r_r / 0.2, \quad (3.8)$$

$$R_3 = r_r / 0.3, \quad (3.9)$$

$$R_4 = r_r / 0.4. \quad (3.10)$$

These constant resistances are converted to variable resistances that vary with frequency when they are divided by the slip, as presented in figures 2.3 and 2.4, as R_n/s and $R_n/(2-s)$ for positive and negative sequences, respectively.

Unbalanced Voltages

The motors in this study were subjected to unbalanced voltage conditions where one of the three phase voltages drops. It is known that zero sequence voltages resulting from an unbalanced set of line voltages will not cause any zero sequence current in the motor windings so long as the motor neutral is not connected to ground or any other return path to the power supply (4). Since this is almost always the case, in the vast majority of motor installations, there is no need to consider the zero sequence

component in the analysis (4). Considering the positive and negative

$$PVU = \frac{\text{maximum deviation from average voltage}}{\text{average voltage}} * 100. \quad (3.13)$$

sequence voltages by using the phase voltages yields the following.

$$\text{Since } V_{\text{pos}} = (V_{\text{var}} + aV_b + a^2V_c)/3, \quad (3.7)$$

$$\text{the fol } V_{\text{neg}} = (V_{\text{var}} + a^2V_b + aV_c)/3, \quad (3.8)$$

$$a = \exp(j120), \quad (3.9)$$

$$a^2 = \exp(j240). \quad (3.10)$$

The PVU equation above was used to find V_{var} at integer values of PVU

Since the per unit system is used in the computer program, the phase voltage

from 0 to 5 percent. This allowed computation of the positive and negative

magnitudes are all 1 per unit. The angles of the phase voltages are the

sequence voltages for PVU's from 0 to 5 percent at integer values. This

standard 0, 240, 120 degrees for phases a (V_{var}), b, and c, respectively. To

was necessary to reduce the computation time of the computer since the

clarify, V_{var} is 1 per unit only when balanced phase voltage conditions exist.

positive and negative sequence voltages, V_{pos} and V_{neg} , are always the same

The phase angles stay the same at all times. V_{var} magnitude is lowered

for all motors in the case studies. Therefore, the values for V_{pos} and V_{neg}

below 1 per unit to simulate the phase voltage unbalanced conditions up to

were computed and entered into a look up table in the computer program to

5 PVU (percent voltage unbalance) throughout this investigation. This

cut down on the repetitive computation time by the computer.

leads to the following equations:

Motor Operating Conditions

$$V_{\text{pos}} = 1/3(V_{\text{var}} + 2), \quad (3.11)$$

This research simulates very realistic unbalanced phase voltage

$$V_{\text{neg}} = 1/3(V_{\text{var}} - 1). \quad (3.12)$$

operating conditions that actual motors are subjected to frequently during

The phase voltages used in the PVU equation are taken as magnitude values

operating conditions. Phase voltage unbalances are simulated in this study

only. The PVU calculations are carried out using the following equation.

by varying the phase voltage at the motor terminals. The possibility of

$$\text{PVU} = \frac{\text{maximum deviation from average voltage}}{\text{average voltage}} * 100. \quad (3.13)$$

Since under voltage methods are used, the PVU equation can be reduced to the following.

$$\text{PVU} = \frac{2 - 2V_{\text{var}}}{V_{\text{var}} + 2} * 100. \quad (3.14)$$

The PVU equation above was used to find V_{var} at integer values of PVU from 0 to 5 percent. This allowed computation of the positive and negative sequence voltages for PVU's from 0 to 5 percent at integer values. This torque level of the motor under balanced conditions. Each time that the PVU level increases, the electromagnetic torque curve of the motor moves down as shown in figure 3.1. Even though the electromagnetic torque curve of the motor moves down, the load torque is maintained at the 100 percent rated full load torque level. This maintenance of electromagnetic torque level comes at the expense of increasing current consumption by the motor as the PVU level increases.

Motor Operating Conditions

This research simulates very realistic unbalanced phase voltage operating conditions that actual motors are subjected to frequently during operating conditions. Phase voltage unbalances are simulated in this study by varying the phase voltage at the motor terminals. The possibility of

motor operation under unbalanced phase voltages is a more likely occurrence than a line to ground fault.

Calculated using the skin effect impedance motor models, figure 3.1 shows how the steady state region of interest is used in this study. The original full load balanced operating conditions are first calculated by the computer program. Then, as the voltage becomes unbalanced, the new slightly increased slips (decreased speeds) are found while continuing to maintain a constant electromagnetic torque which is set at the rated output torque level of the motor under balanced conditions. Each time that the PVU level increases, the electromagnetic torque curve of the motor moves down as shown in figure 3.1. Even though the electromagnetic torque curve of the motor moves down, the load torque is maintained at the 100 percent rated full load torque level. This maintenance of electromagnetic torque level comes at the expense of increasing current consumption by the motor as the PVU level increases.

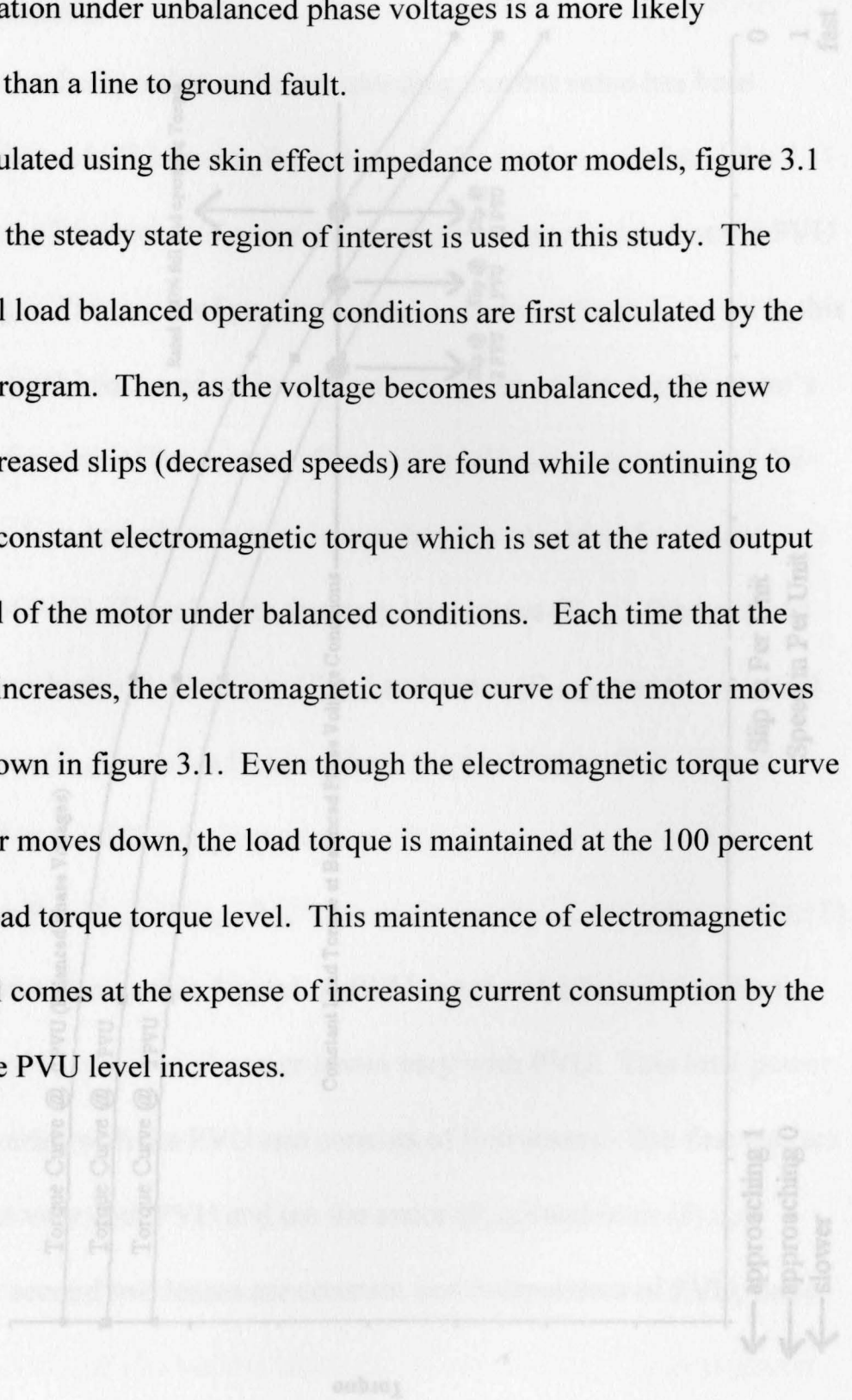
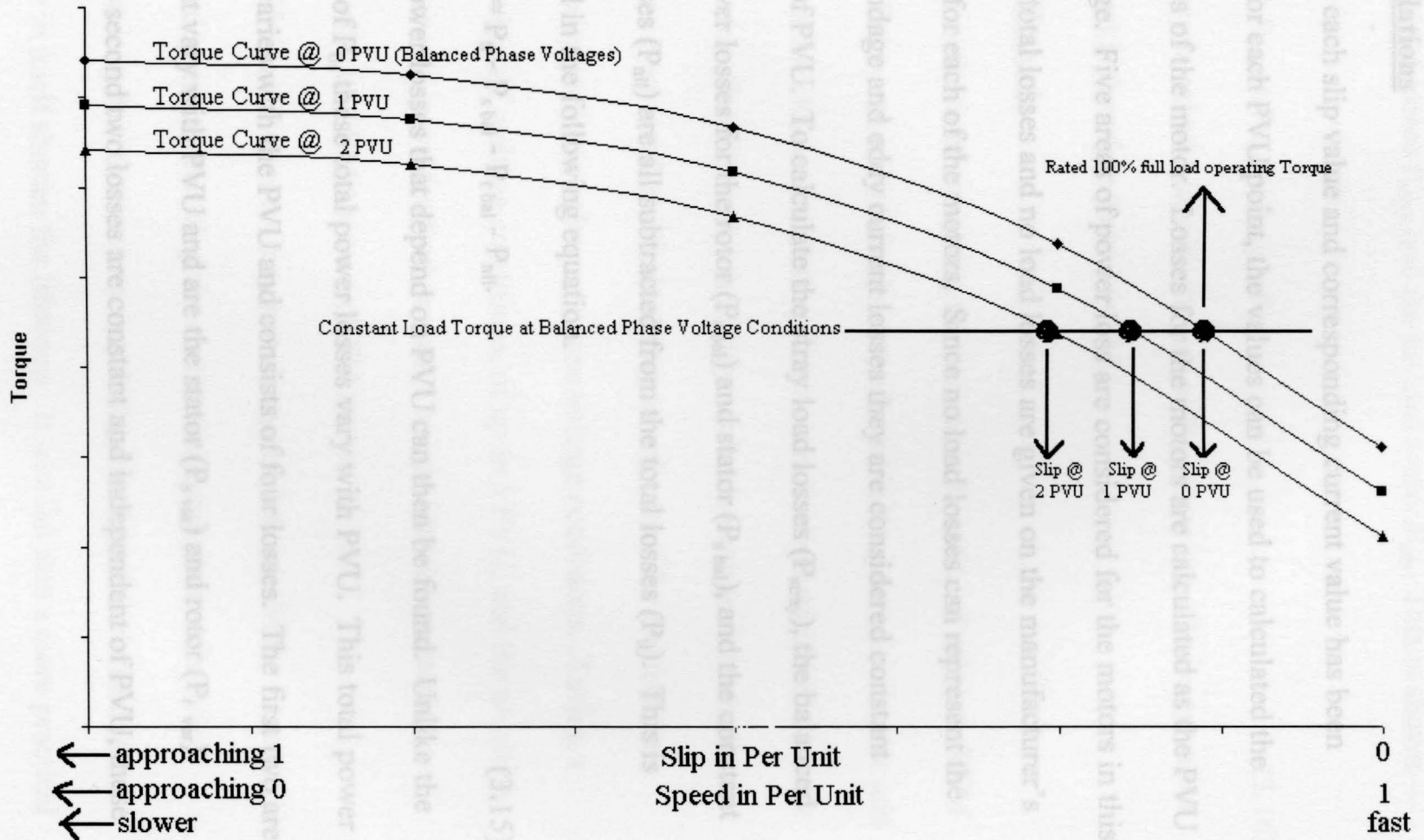


Figure 3.1: Steady State Region of Motor Torques with Corresponding Percent Voltage Unbalance Vs. Slip or Speed in Per Unit



Loss Calculations

After each slip value and corresponding current value has been calculated for each PVU point, the values can be used to calculate the power losses of the motor. Losses for the motors are calculated as the PVU levels change. Five areas of power loss are considered for the motors in this study. The total losses and no load losses are given on the manufacturer's data sheets for each of the motors. Since no load losses can represent the friction, windage and eddy current losses they are considered constant regardless of PVU. To calculate the stray load losses (P_{stray}), the balanced voltage power losses for the rotor ($P_{r \text{ bal}}$) and stator ($P_{s \text{ bal}}$), and the constant no load losses (P_{nll}) are all subtracted from the total losses (P_{tl}). This is summarized in the following equation.

$$P_{\text{stray}} = P_{\text{tl}} - P_{s \text{ bal}} - P_{r \text{ bal}} - P_{\text{nll}} \quad (3.15)$$

The total power losses that depend on PVU can then be found. Unlike the total losses of P_{tl} , these total power losses vary with PVU. This total power loss (P_{loss}) varies with the PVU and consists of four losses. The first two are the ones that vary with PVU and are the stator ($P_{s \text{ var}}$) and rotor ($P_{r \text{ var}}$) losses. The second two losses are constant and independent of PVU, these

are the stray load losses P_{stray} and the no load losses P_{nl} . This is shown below.

$$P_{\text{loss}} = P_{\text{s var}} + P_{\text{r var}} + P_{\text{stray}} + P_{\text{nl}}. \quad (3.16)$$

The efficiency is calculated with the use of P_{loss} since the efficiency varies with PVU and is therefore linked to PVU.

Economic Methods

Many methods of analyzing the economic benefits of using an EEM versus an STM motor are available as reviewed in the previous chapter and in other literature. Motor purchase prices were obtained with the help of a local distributor. Traditionally, the many available economic methods and formulas have been used in a limited way to only consider the motors' operation under perfectly balanced phase voltage conditions. Taking a pessimistic view of voltage conditions, of up to 5 PVU, and the resulting motor efficiencies, provides further useful insight into the economic benefits of using an EEM versus an STM motor.

The lifetime of a motor may not always be known. Many economic calculations depend on knowing the motors expected years of service. Ironically the very fact that motors may be operated on unbalanced phase voltage may in itself shorten the lifetimes. It was felt that a more practical

approach to economic analysis would be to consider the method of simple payback analysis along with the payback method in years.

$$S = 0.746 * hp * L * C * N * [(100/E_B) - (100/E_A)] \quad (3.17)$$

where,

S = annual savings, \$/year,

L = 100 percent full operating load,

C = cost of electricity at \$0.07/KWH,

N = running time, 8760 hr/yr,

E_B = standard motor efficiency under actual load condition,

E_A = energy-efficient motor efficiency under actual load conditions.

After the annual saving is computed the payback period in years can be found by considering the difference in purchase prices of the motors (7).

$$PBP = CD/S \quad (3.18)$$

where,

PBP = payback period, years,

CD = cost differences between two motors, dollars.

These economic methods were extended in this study to include the economics, based on efficiency, as the PVU increases. Using this method

provides useful results. This economic analysis is possible since the efficiencies of the motors have been made dependent on PVU.

The computer program was used to investigate and compare the behaviors of motors subjected to unbalanced phase voltage conditions. The graphs show the results of this labor. All values displayed on the graphs are in per unit and percentages.

Rotor Losses

Each STM and EEM motor pair followed a trend of higher rotor losses for the STM motors during both the balanced and unbalanced phase voltage conditions. All STM and EEM motors had rotor losses that increased with increasing PVU. EEM motors in the 25, 50, 250 and 300 hp groups had rotor losses that increased faster than the rotor losses for the corresponding STM motors. STM motors in the 100, 150 and 200 hp groups had rotor losses that increased faster than the rotor losses for the corresponding EEM motors. Possible explanations could be slight differences in rotor bar construction or composition. The highest rotor losses of 0.0163 and 0.0181 per unit at 0 and 5, respectively, occurred for the 25 hp STM motor. The lowest rotor losses of 0.007 and 0.008 per unit at 0 and 5 PVU, respectively, occurred for the 250 hp EEM motor. The

CHAPTER 4

RESULTS AND DISCUSSIONS

The computer program was used to investigate and compare the behaviors of motors subjected to unbalanced phase voltage conditions. The graphs show the results of this labor. All values displayed on the graphs are in per unit and percentages.

Rotor Losses

Each STM and EEM motor pair followed a trend of higher rotor losses for the STM motors during both the balanced and unbalanced phase voltage conditions. All STM and EEM motors had rotor losses that increased with increasing PVU. EEM motors in the 25, 50, 250 and 300 hp groups had rotor losses that increased faster than the rotor losses for the corresponding STM motors. STM motors in the 100, 150 and 200 hp groups had rotor losses that increased faster than the rotor losses for the corresponding EEM motors. Possible explanations could be slight differences in rotor bar construction or composition. The highest rotor losses of 0.0163 and 0.0181 per unit at 0 and 5, respectively, occurred for the 25 hp STM motor. The lowest rotor losses of 0.007 and 0.008 per unit at 0 and 5 PVU, respectively, occurred for the 250 hp EEM motor. The

largest differences in rotor losses, between an STM and EEM motor pair, were 0.0047 per unit at 0 and 5 PVU for the 25 hp motor pair. The smallest differences in rotor losses, between any STM and EEM motor pairs, occurred for both the 50 and 250 hp motor pairs at 0.0003 per unit. This occurred for the 250 hp motor pair at 0 and 5 PVU and for the 50 hp motor pair only at 5 PVU. The largest percentage increase in rotor loss was 18 percent at 5 PVU for the 100 hp STM motor. The smallest percentage increase in rotor loss was 10.9 percent at 5 PVU for the 200 hp EEM motor. The largest difference between percentage increases in rotor loss was 4.9 percent at 5 PVU for the 25 hp motor pair. The smallest difference between percentage increases in rotor loss was 0.07 percent at 5 PVU for the 50 hp motor pair.

Efficiencies

All efficiencies were lower for STM motors than for corresponding EEM motors and all efficiencies decreased with increasing PVU levels. The percentage decreases in the efficiencies of the STM motors were larger than the percentage decreases of the EEM motors. Smaller sized motors had larger decreases in efficiencies at 5 PVU. The largest decreases in efficiencies occurred for the 25 hp motor pair at 0.53 and 0.41 percent for

the STM and EEM motors, respectively. The smallest decreases in efficiencies at 5 PVU occurred for the 200 hp motor pair at 0.24 and 0.18 percent for the STM and EEM motors, respectively. The motor pair with the largest difference, between STM and EEM motor efficiencies, occurred for the 25 hp motor pair at a difference of 2.7 per unit. The motor pair with the smallest difference, between STM and EEM efficiencies, occurred for the 200 hp motor pair at a difference of 1.3 per unit. The largest percentage decrease difference in efficiencies, between an STM and EEM motor pair, was 0.12 percent at 5 PVU for the 25 hp motor pair. The smallest percentage decrease difference in efficiencies, between an STM and EEM motor pair, was 0.013 percent at 5 PVU for the 300 hp motor pair.

Economics

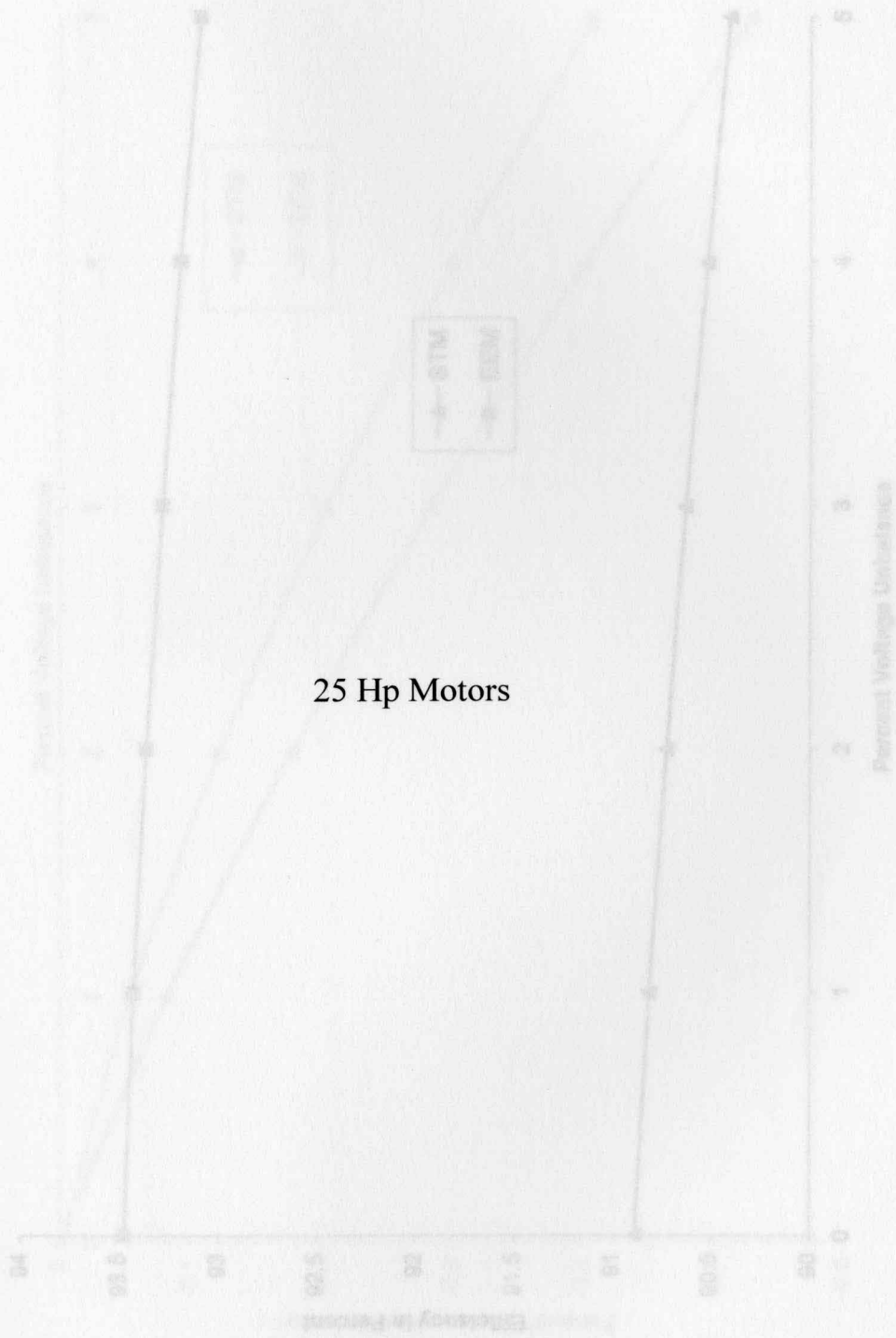
Clearly it would be highly unlikely that a motor would constantly be subjected to the worst voltage conditions possible. The percentage of time each PVU condition existed in any given locality would be an obscure matter to determine. Taking the most pessimistic view possible, of up to 5 PVU, clearly demonstrates the economic superiority of the EEM motors. The simple payback method clearly shows that the yearly savings can be quickly realized by using an EEM motor instead of an STM motor. The

highest yearly savings obtained were \$2251.60 and \$2271.40 at 0 and 5 PVU, respectively, for the 250 hp motor pair. The lowest yearly savings obtained were \$348.88 and \$365.78 at 0 and 5 PVU, respectively, for the 25 hp motor pair. The largest percentage increase in yearly savings was for the 25 hp motor pair at 4.8 percent and the smallest percentage increase in yearly savings was for the 250 hp motor pair at 0.88 percent. The shortest payback recovery times were 1.21 and 1.15 years at 0 and 5 PVU, respectively, for the 25 hp motor pair. The longest payback recovery times were 2.29 and 2.19 years at 0 and 5 PVU for the 200 hp motor pair.

Graphs

The graphs are grouped by motor sizes of 25, 50, 100, 150, 200, 250 and 300 hp. There are seven graphs for each motor size. These seven graphs are the efficiencies, percent decrease in efficiencies, rotor losses, percent increase in rotor losses, yearly savings, percent increase in yearly savings and payback times. Every quantity displayed on the graphs is plotted versus PVU.

Figure 4.1: Efficiencies for 25 hp STM and EEM vs. Percent Voltage Unbalance



25 Hp Motors

Figure 4.1: Efficiencies for 25 hp STM and EEM vs. Percent Voltage Unbalance

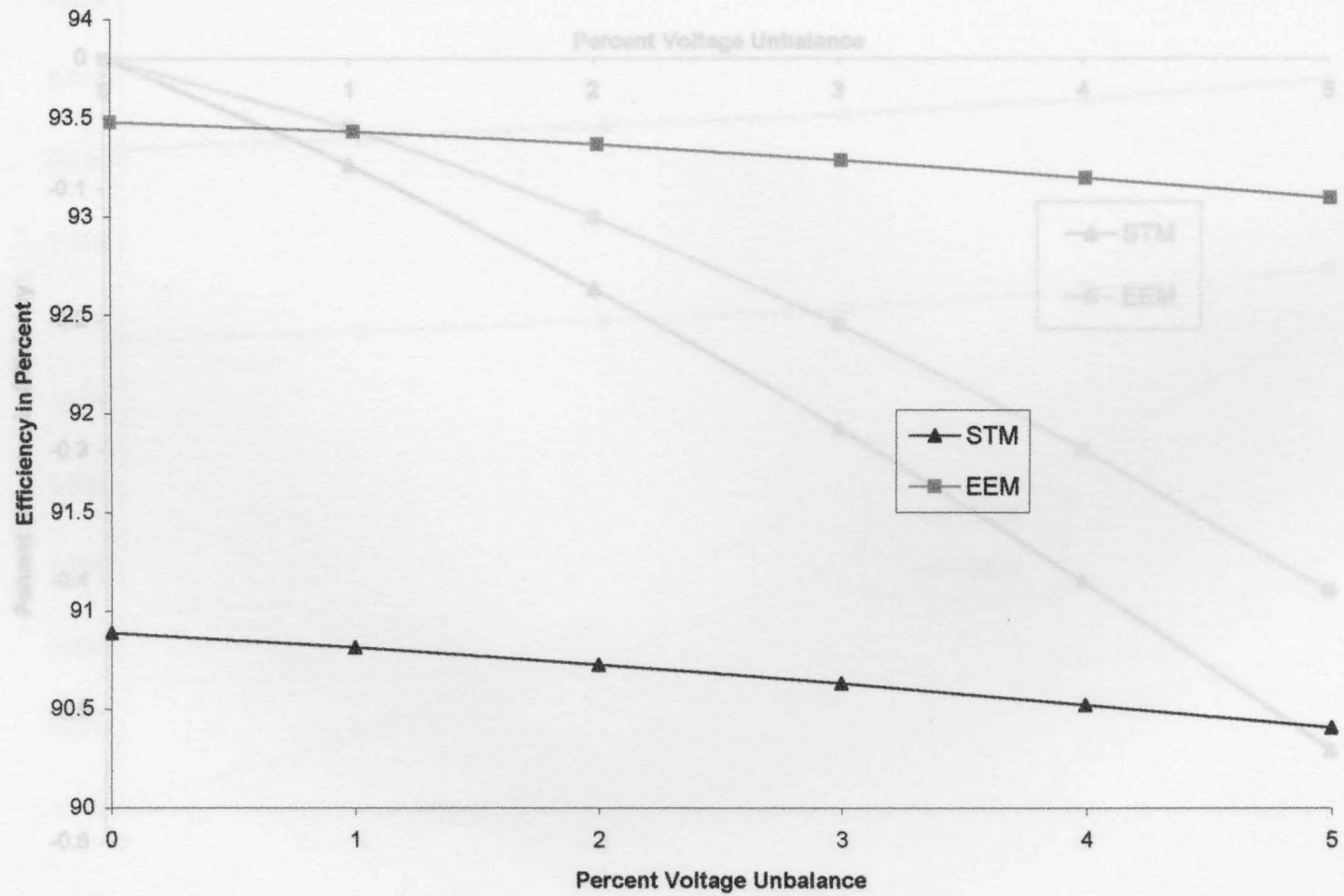


Figure 4.2: Percent Decrease in Efficiencies for 25 hp STM and EEM vs. Percent Voltage Unbalance

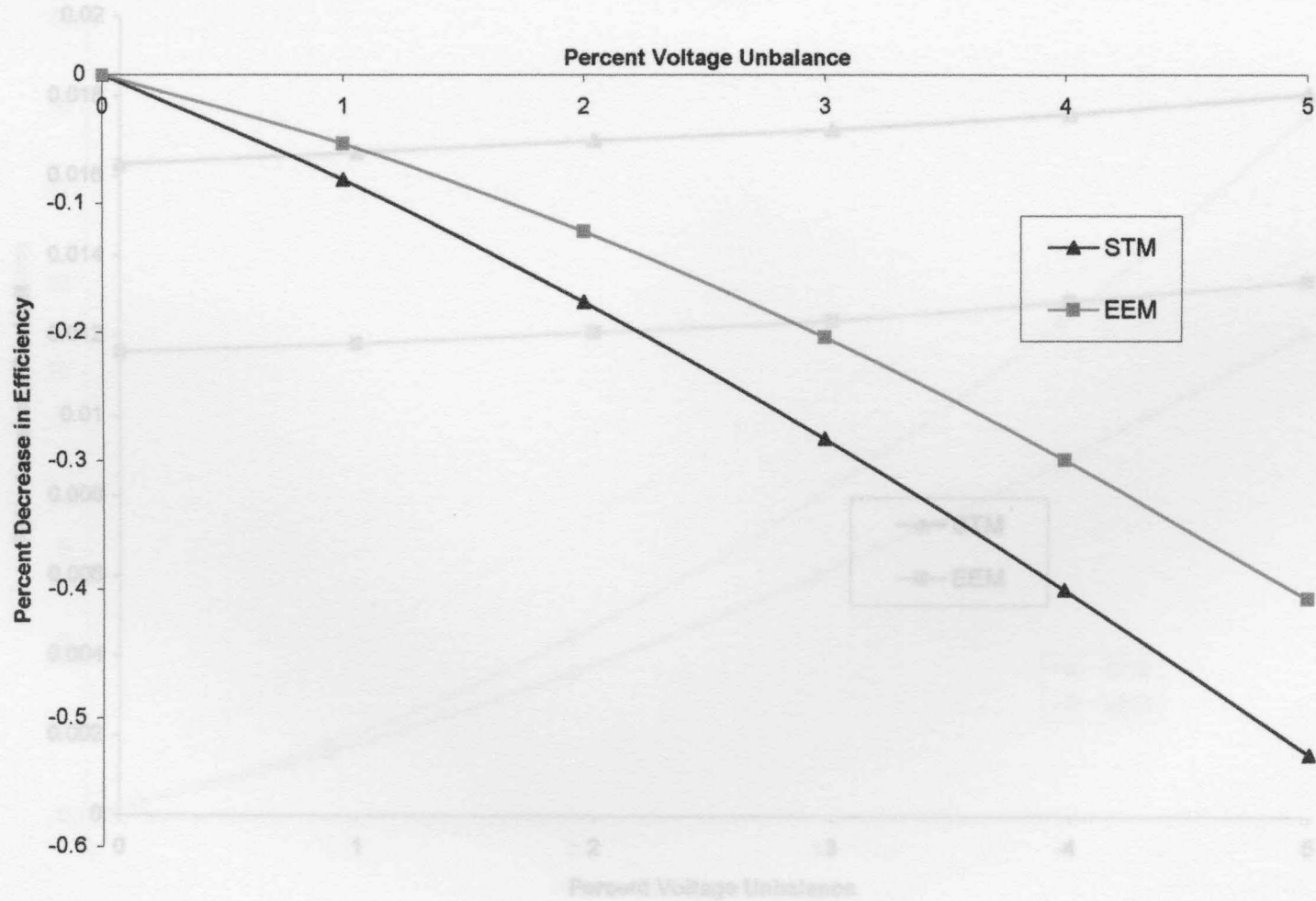


Figure 4.3: Rotor Losses for 25 hp STM and EEM vs. Percent Voltage Unbalance

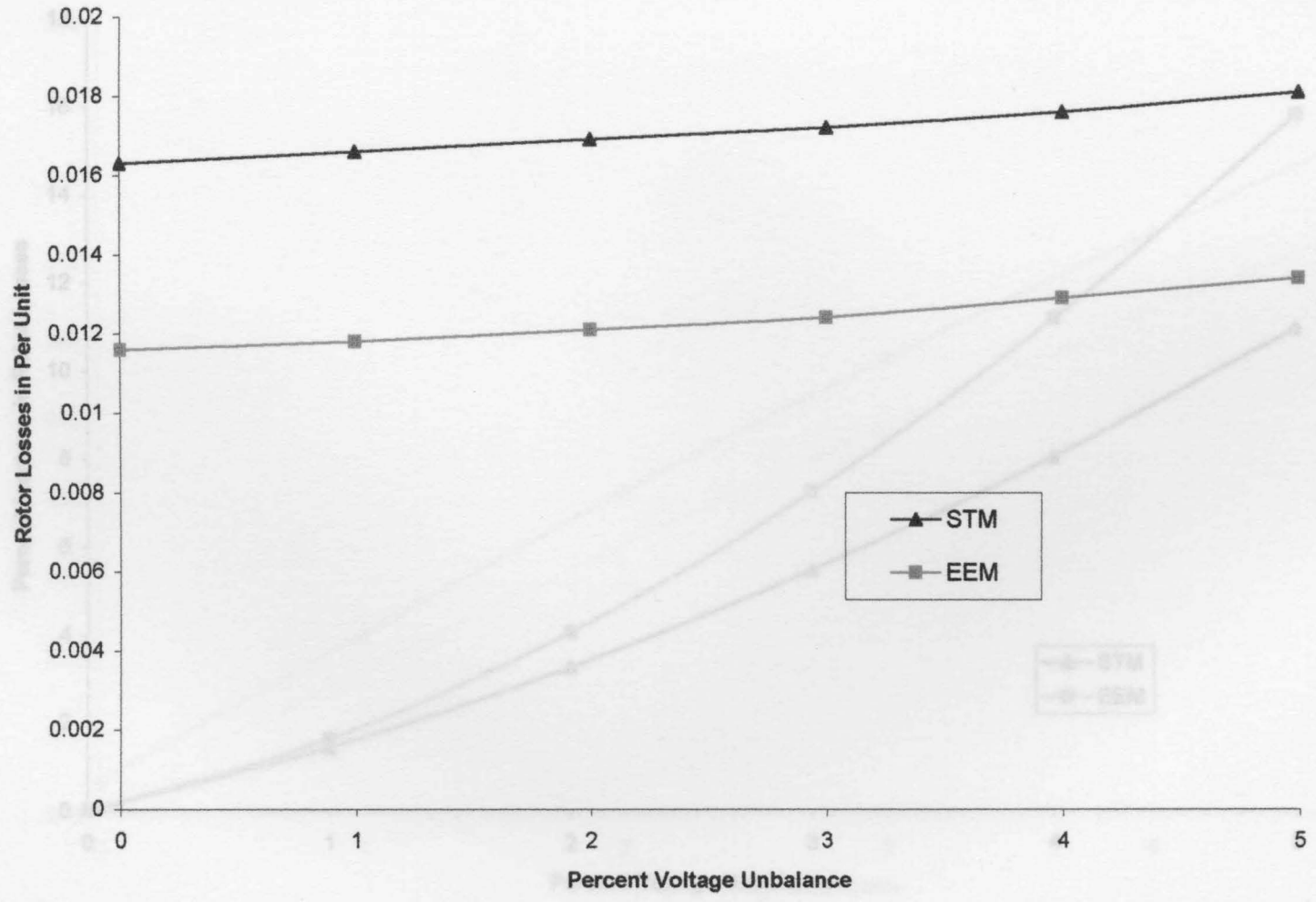


Figure 4.4: Percent Increase in Rotor Losses for 25 hp STM and EEM vs. Percent Voltage Unbalance

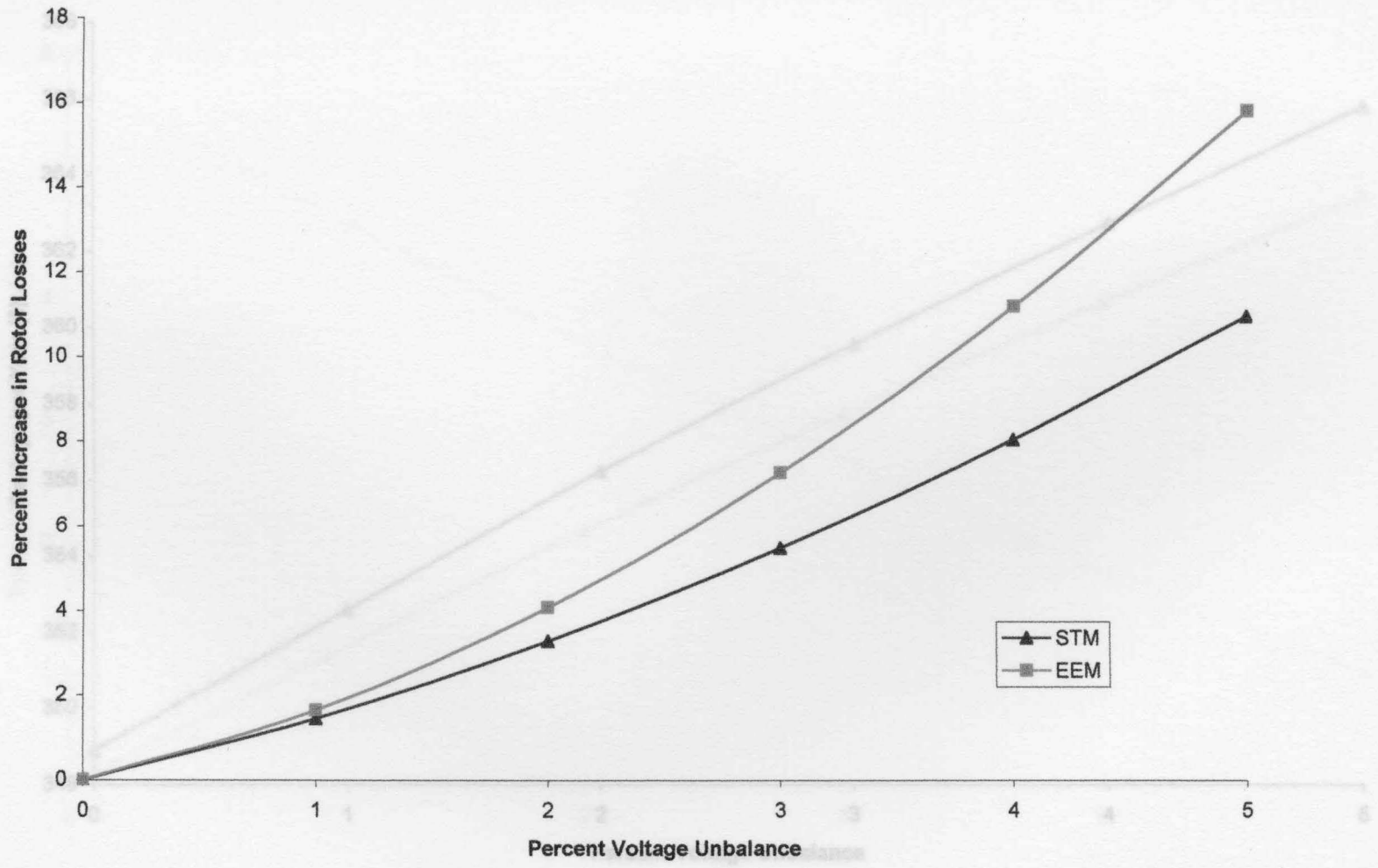


Figure 4.5: Yearly Savings for 25 hp by Using EEM over STM vs. Percent Voltage Unbalance

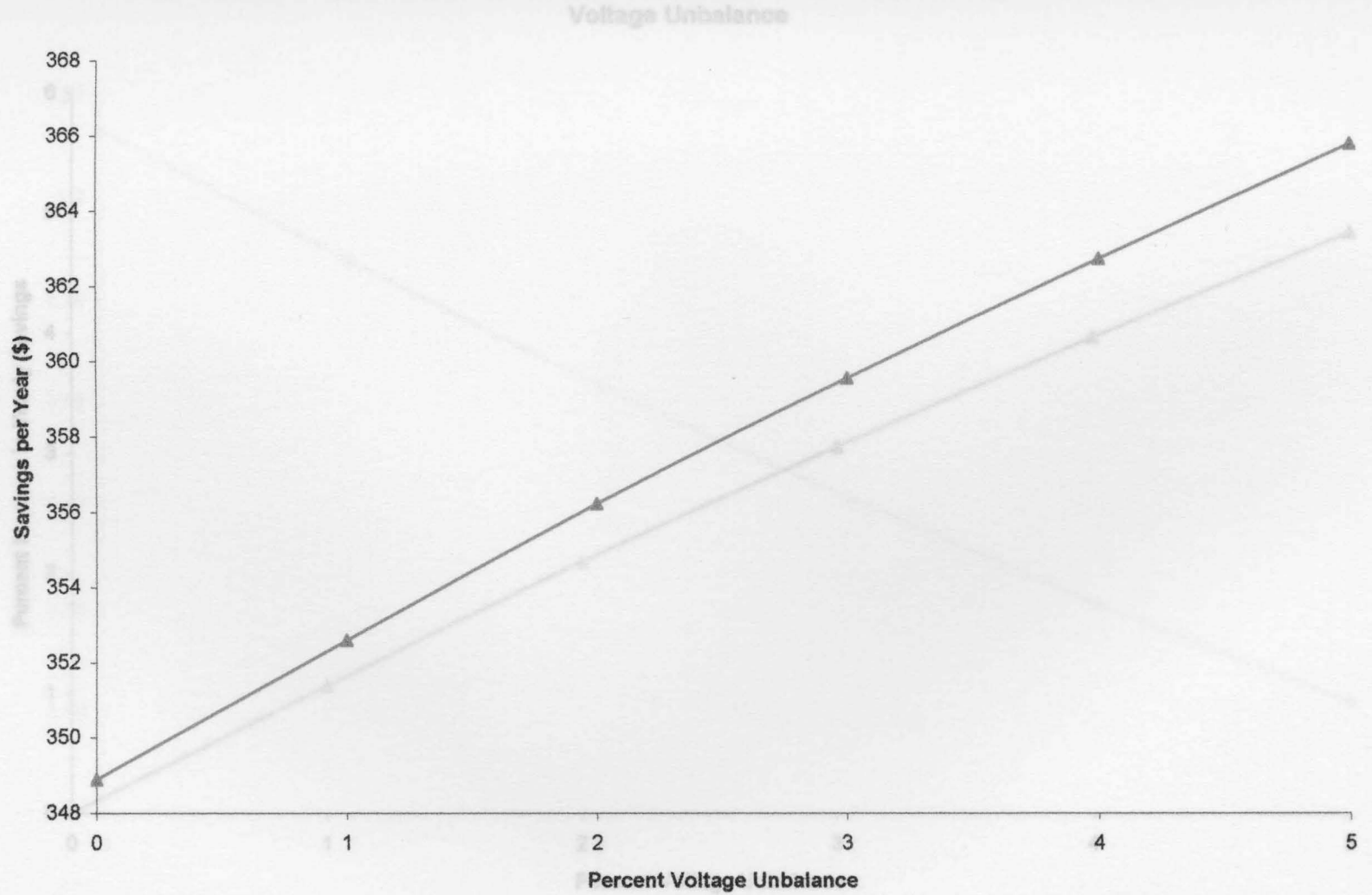


Figure 4.6: Percent Increase in Yearly Savings for 25 hp by Using EEM over STM vs. Percent Voltage Unbalance

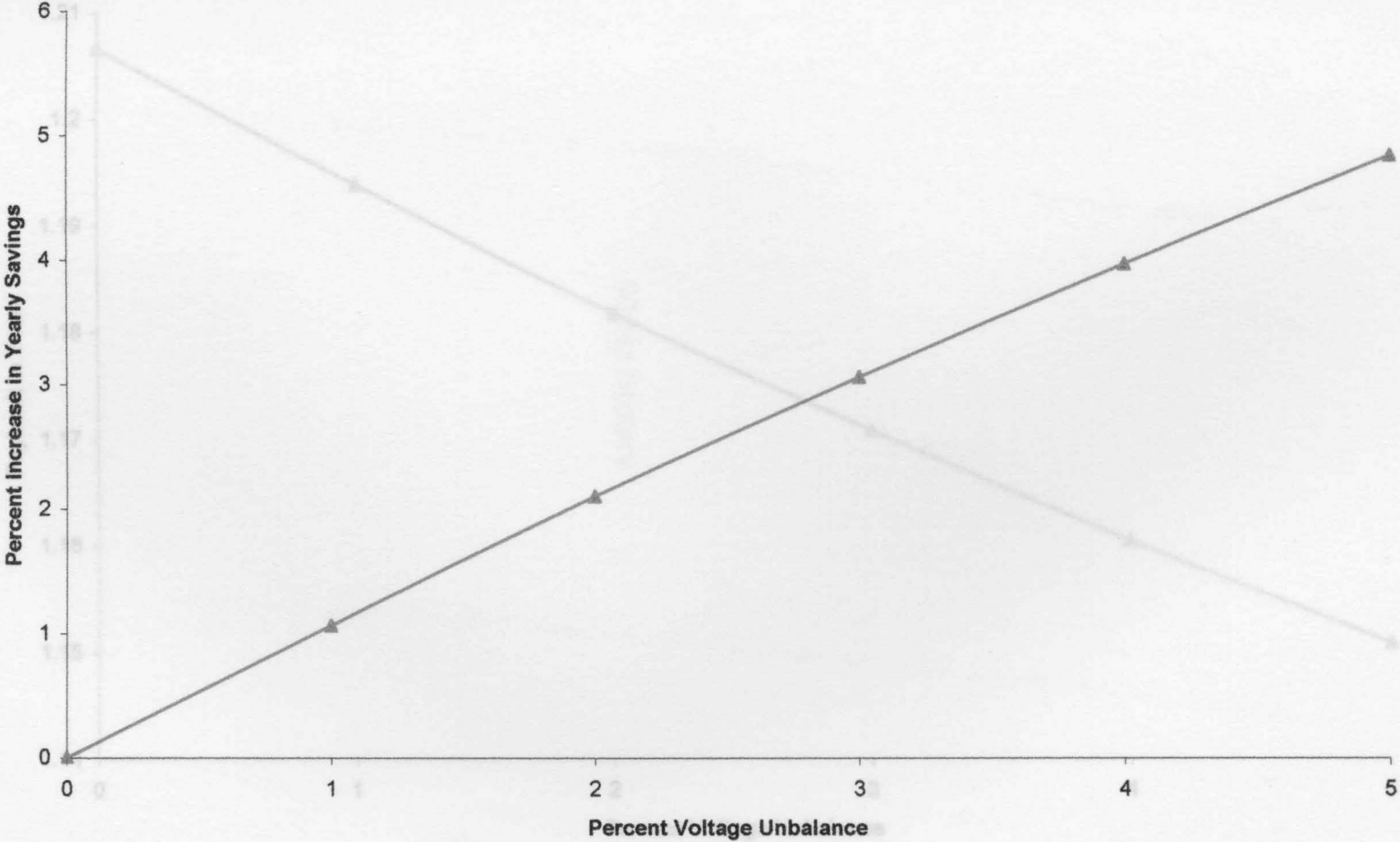


Figure 4.7: Payback Time for 25 hp STM and EEM vs. Percent Voltage Unbalance

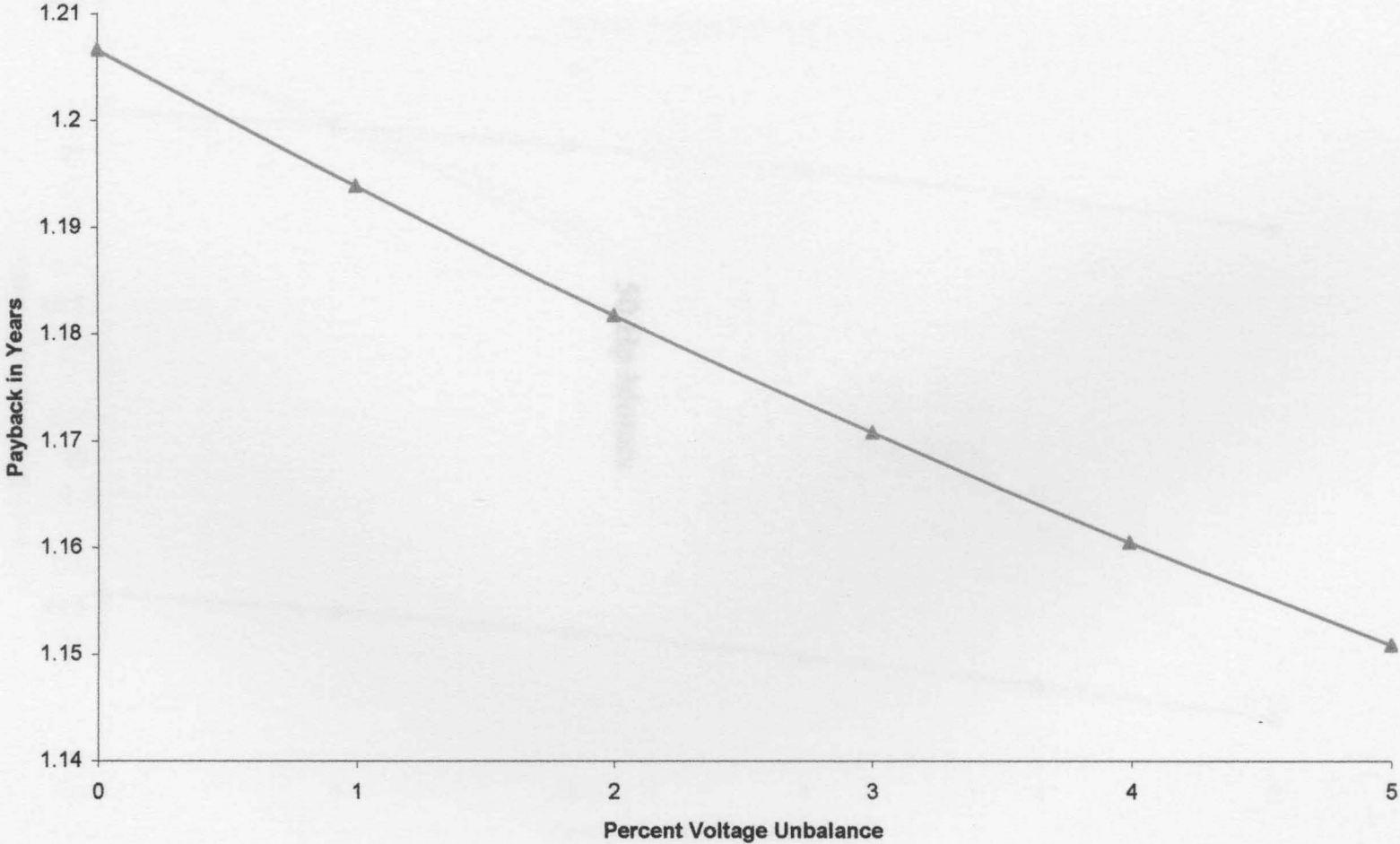
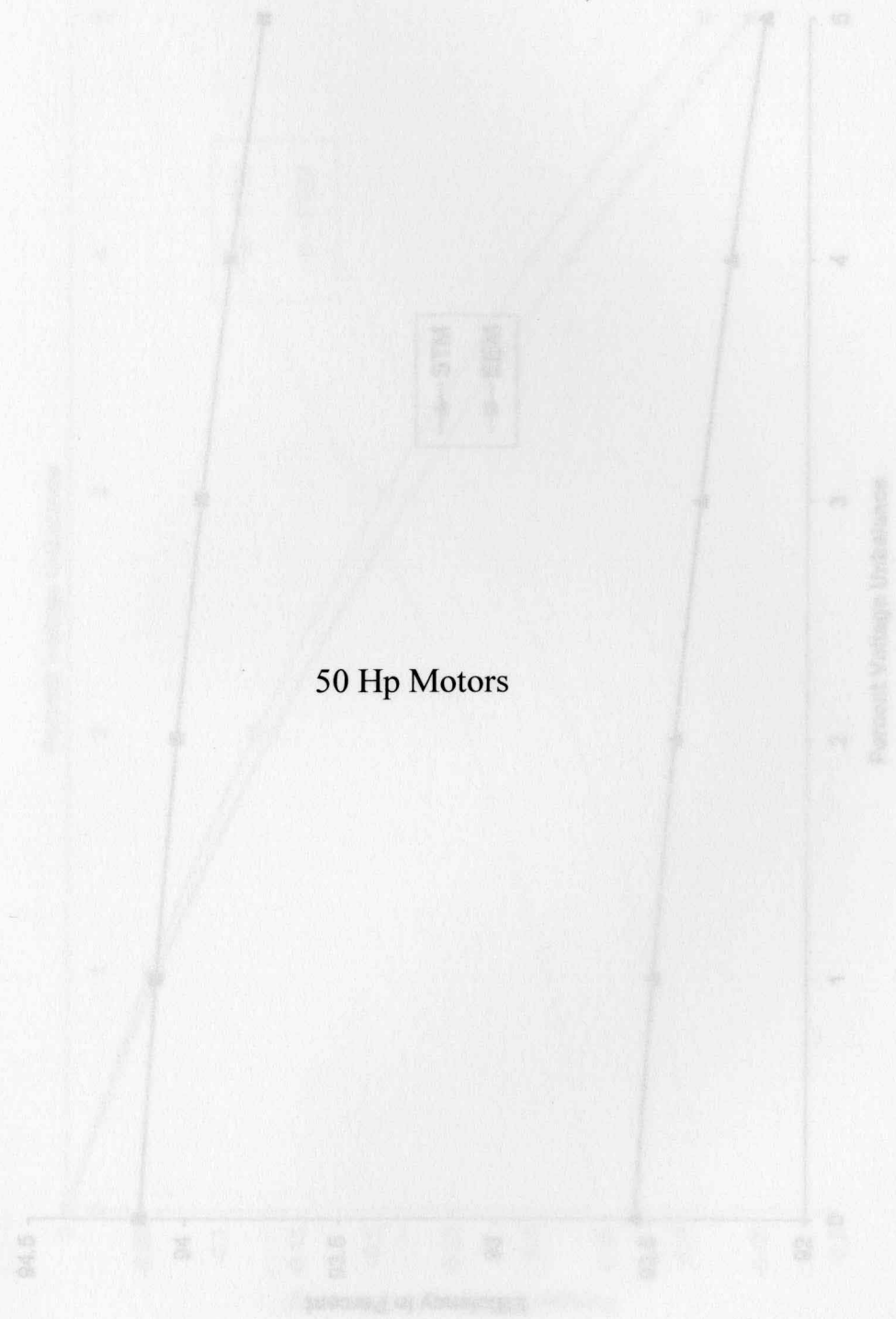


Figure 4.8: Efficiencies for 50 hp STM and EEM vs. Percent Voltage Unbalance



50 Hp Motors

Figure 4.8: Efficiencies for 50 hp STM and EEM vs. Percent Voltage Unbalance

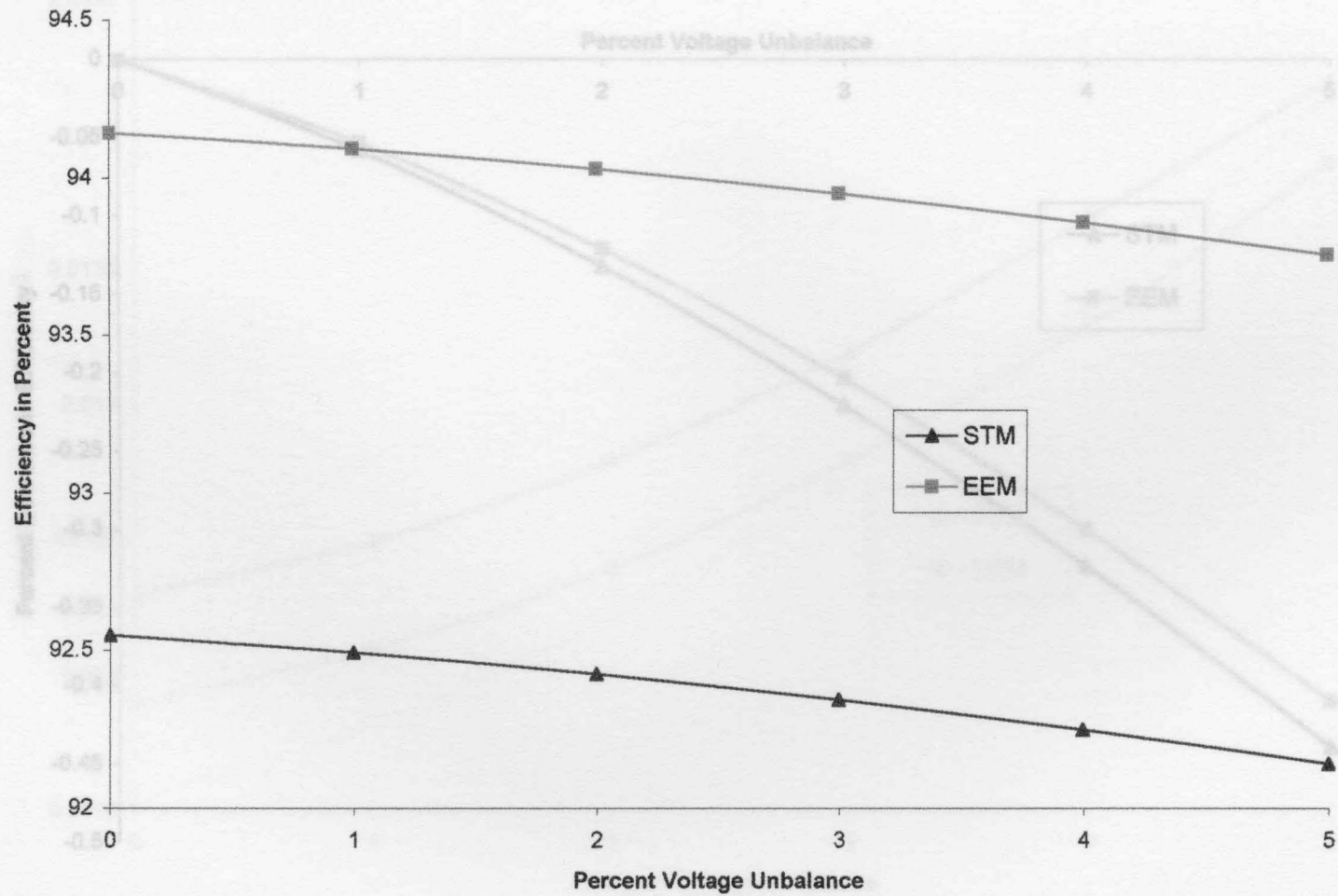


Figure 4.9: Percent Decrease in Efficiencies for 50 hp STM and EEM vs. Percent Voltage Unbalance

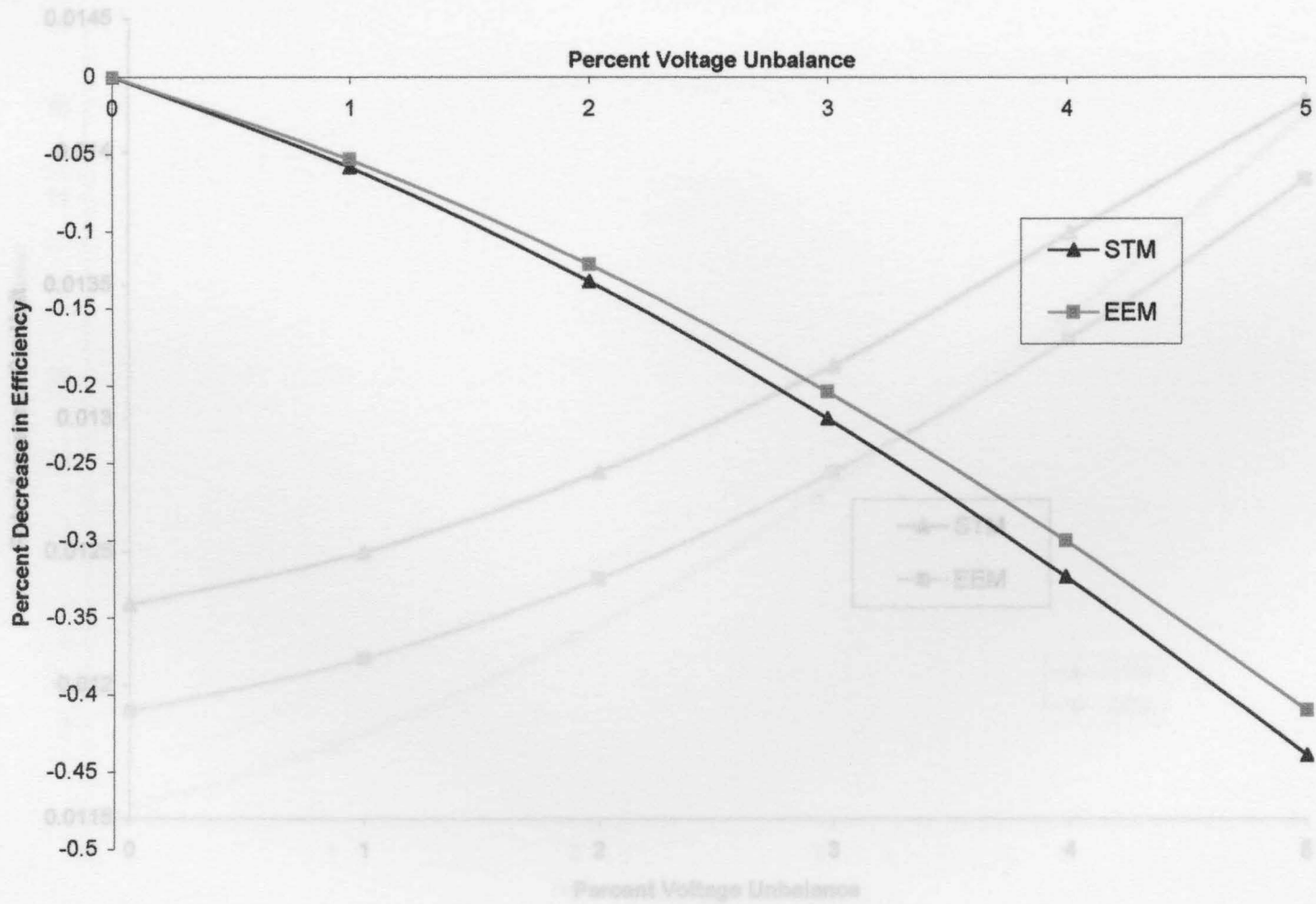


Figure 4.10: Rotor Losses for 50 hp STM and EEM vs. Percent Voltage Unbalance

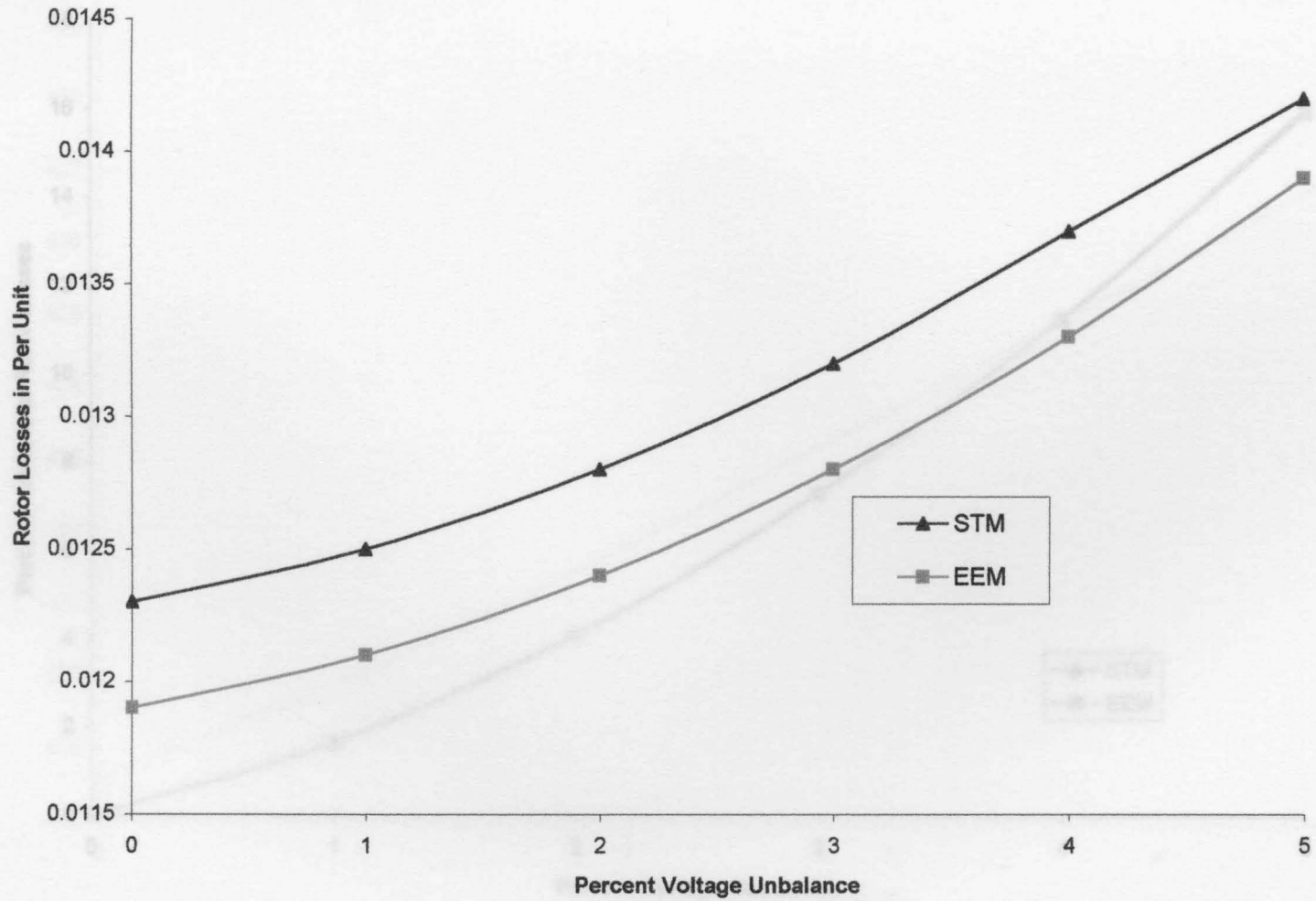


Figure 4.11: Percent Increase in Rotor Losses for 50 hp STM and EEM vs. Percent Voltage Unbalance

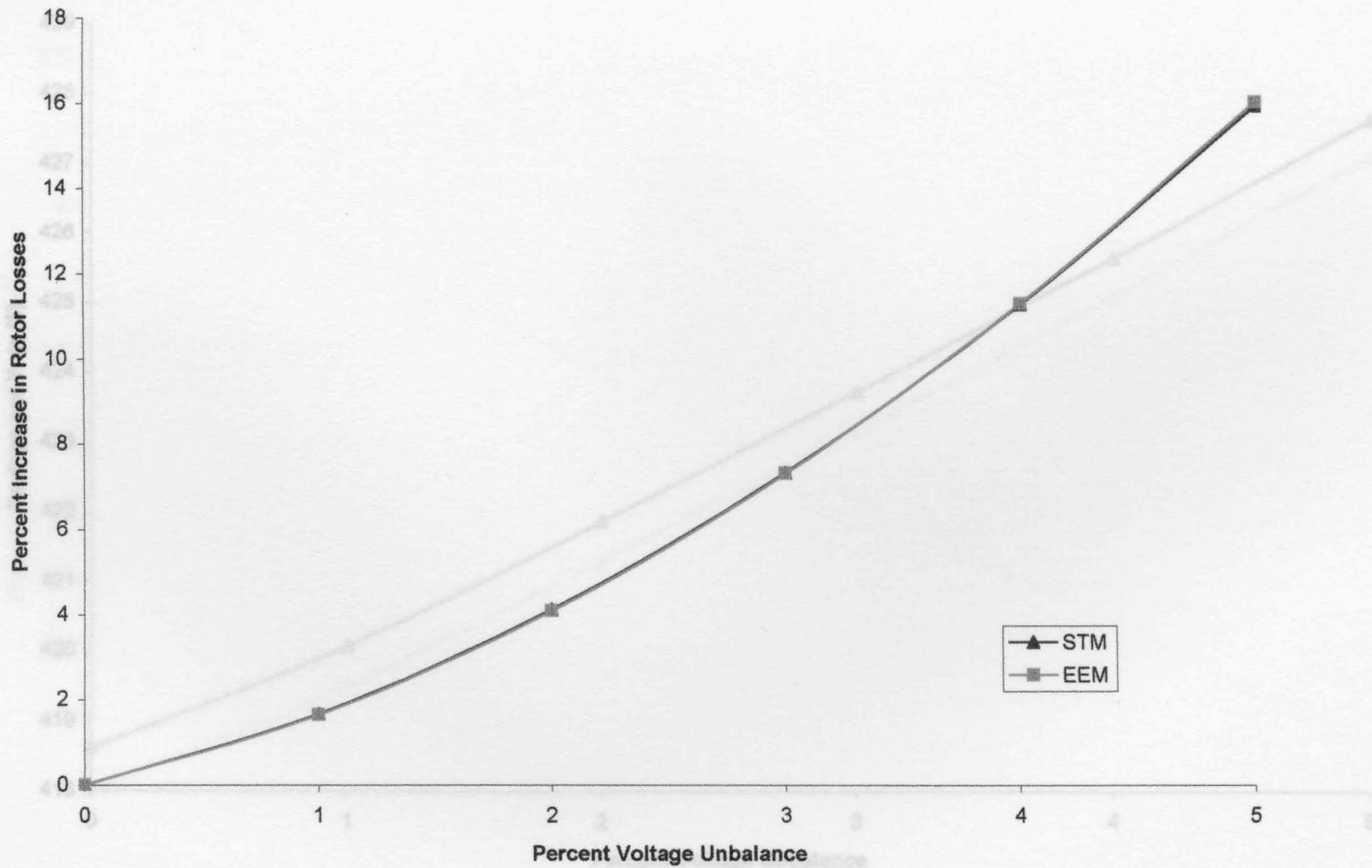


Figure 4.12: Yearly Savings for 50 hp by Using EEM over STM vs. Percent Voltage Unbalance

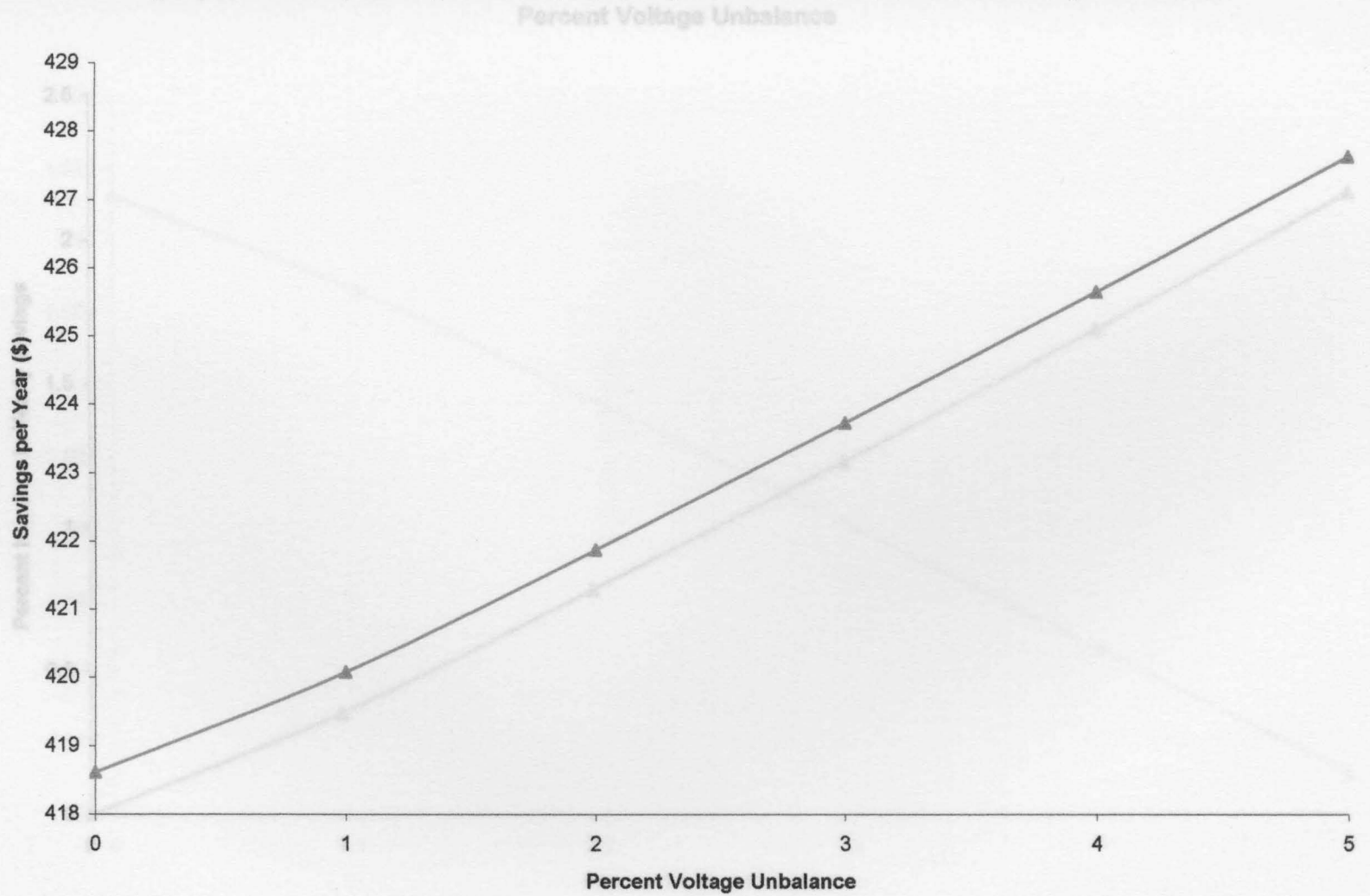


Figure 4.13: Percent Increase in Yearly Savings for 50 hp by Using EEM over STM vs. Percent Voltage Unbalance

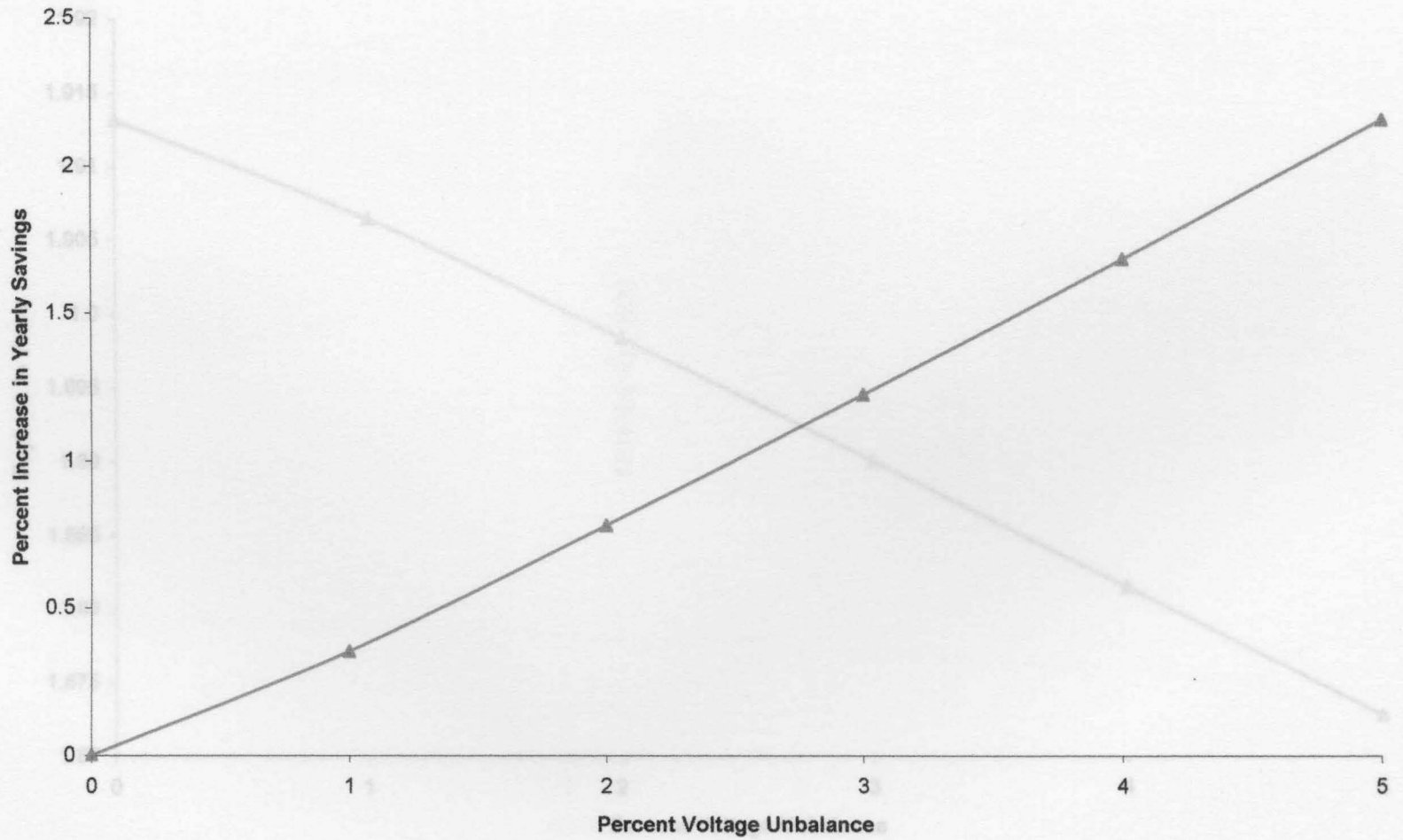


Figure 4.14: Payback Time for 50 hp STM and EEM vs. Percent Voltage Unbalance

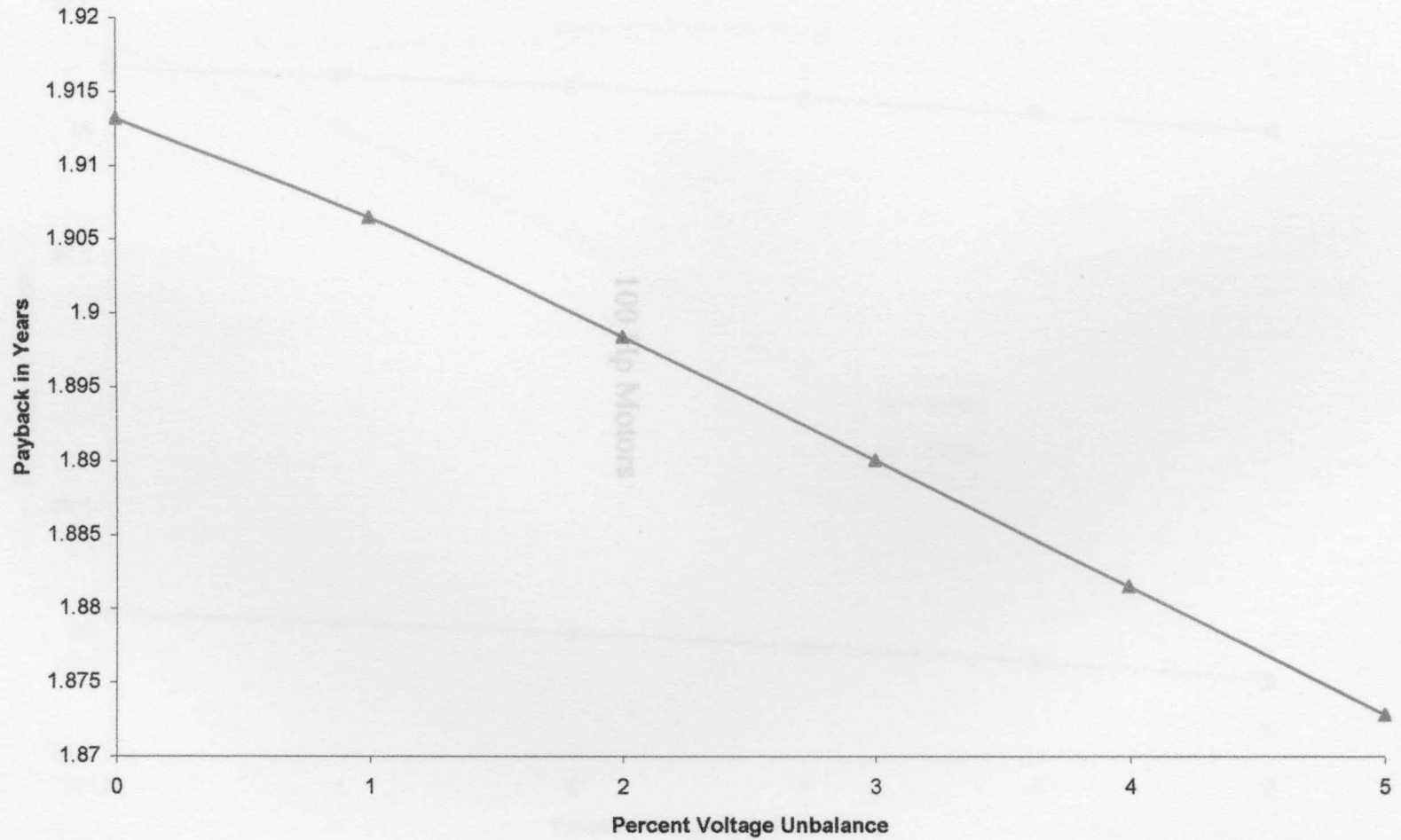
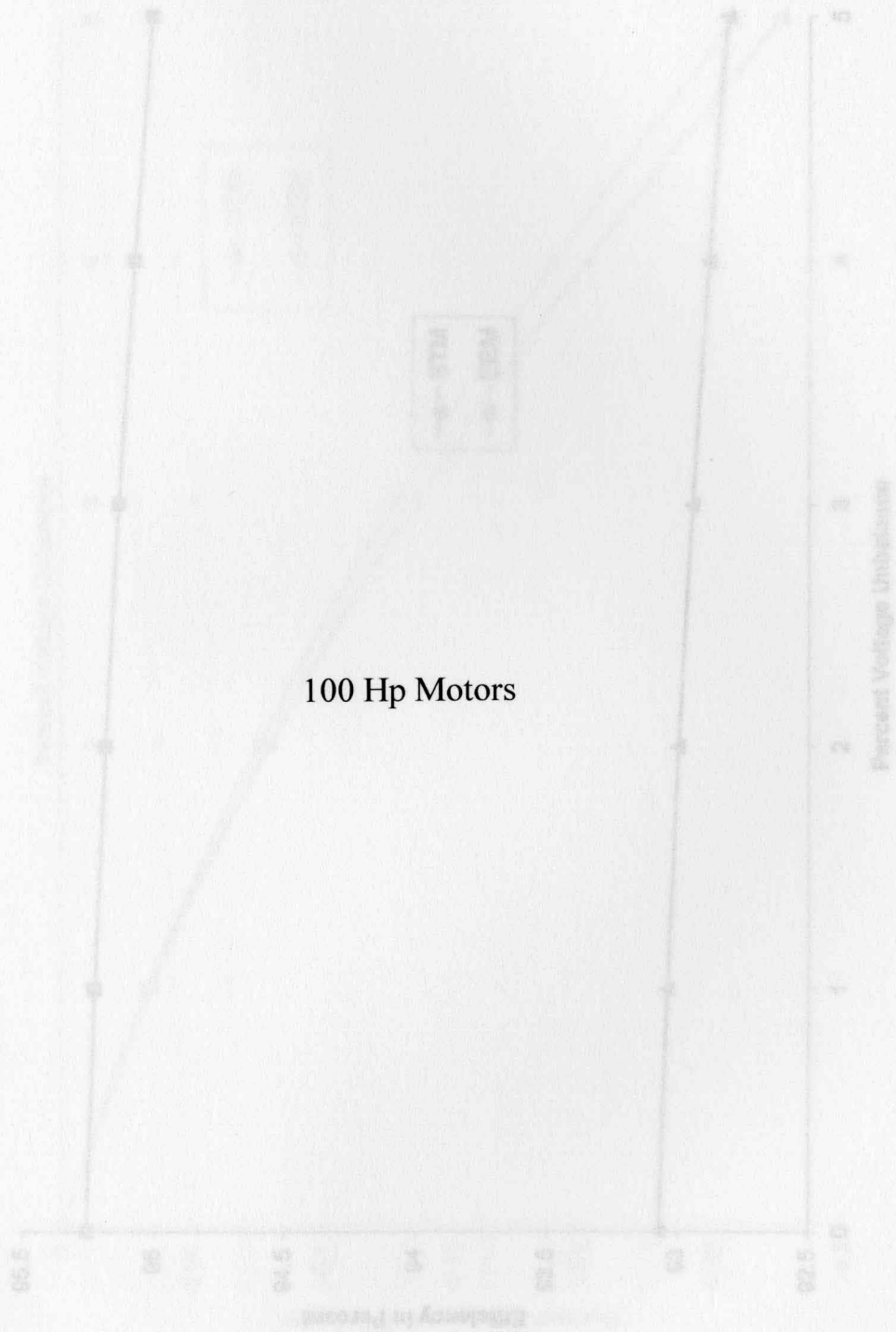


Figure 4.16: Efficiencies for 100 hp STM and EEM vs. Percent Voltage Unbalance



100 Hp Motors

Figure 4.15: Efficiencies for 100 hp STM and EEM vs. Percent Voltage Unbalance

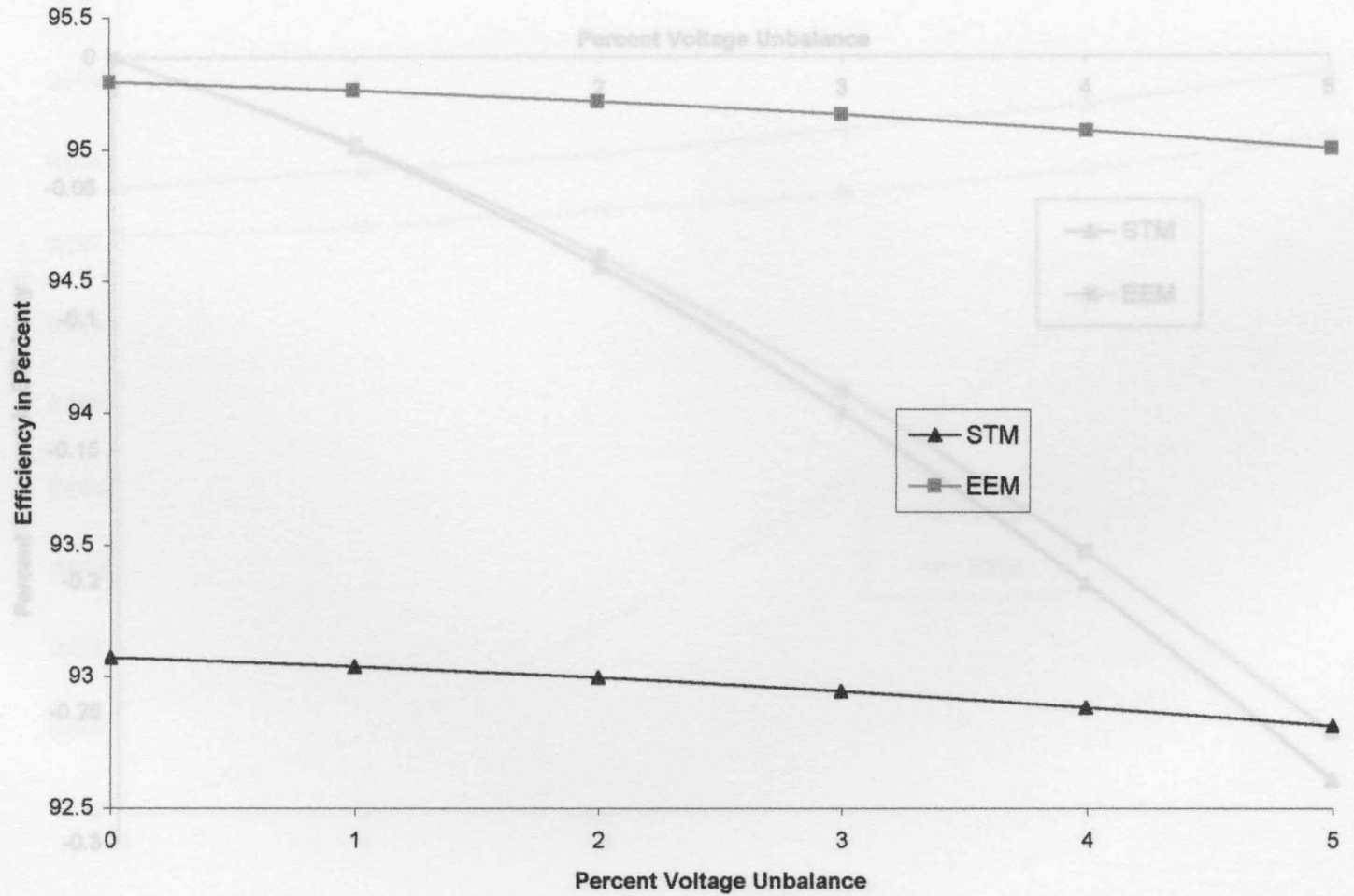


Figure 4.16: Percent Decrease in Efficiencies for 100 hp STM and EEM vs. Percent Voltage Unbalance

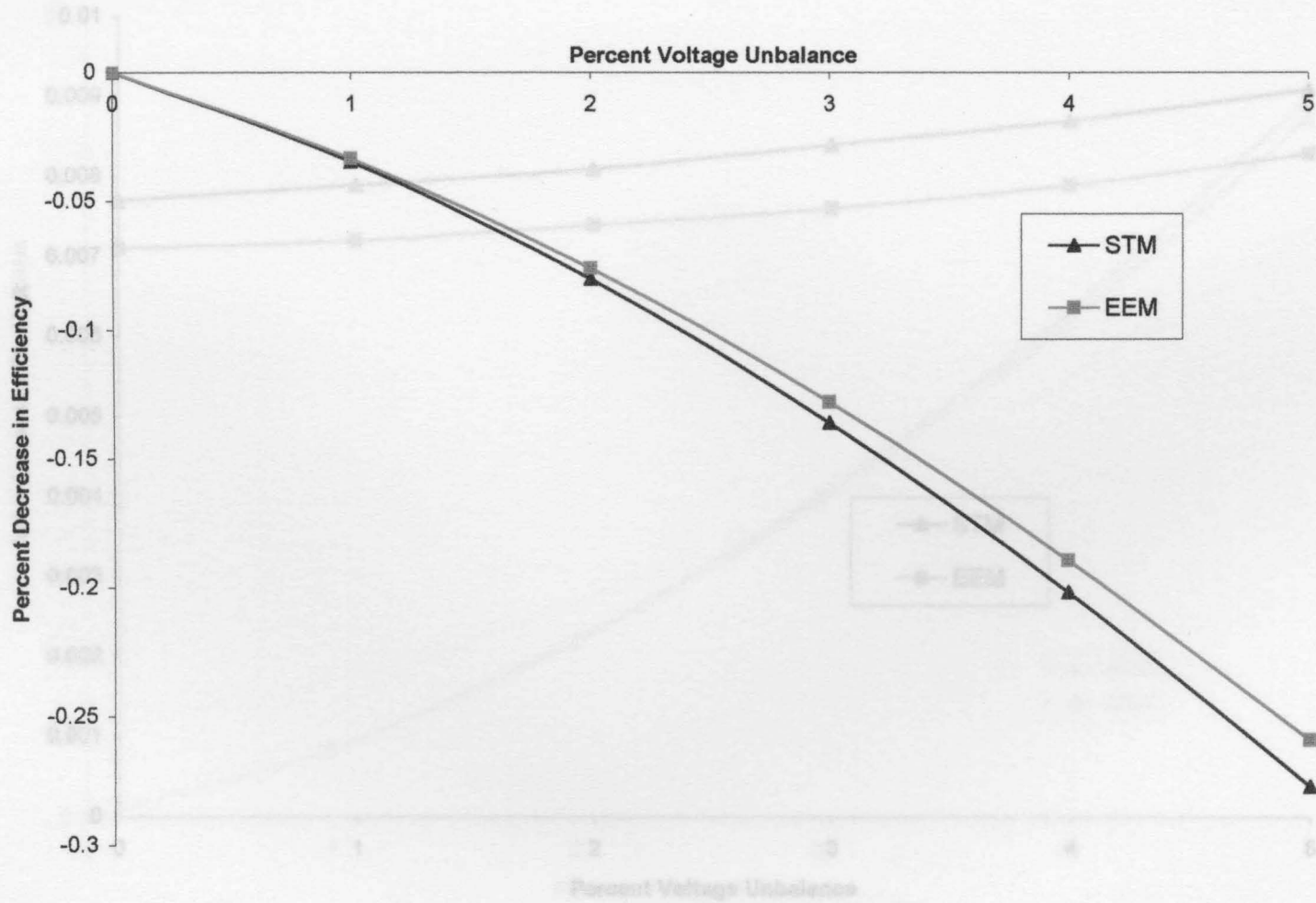


Figure 4.17: Rotor Losses for 100 hp STM and EEM vs. Percent Voltage Unbalance

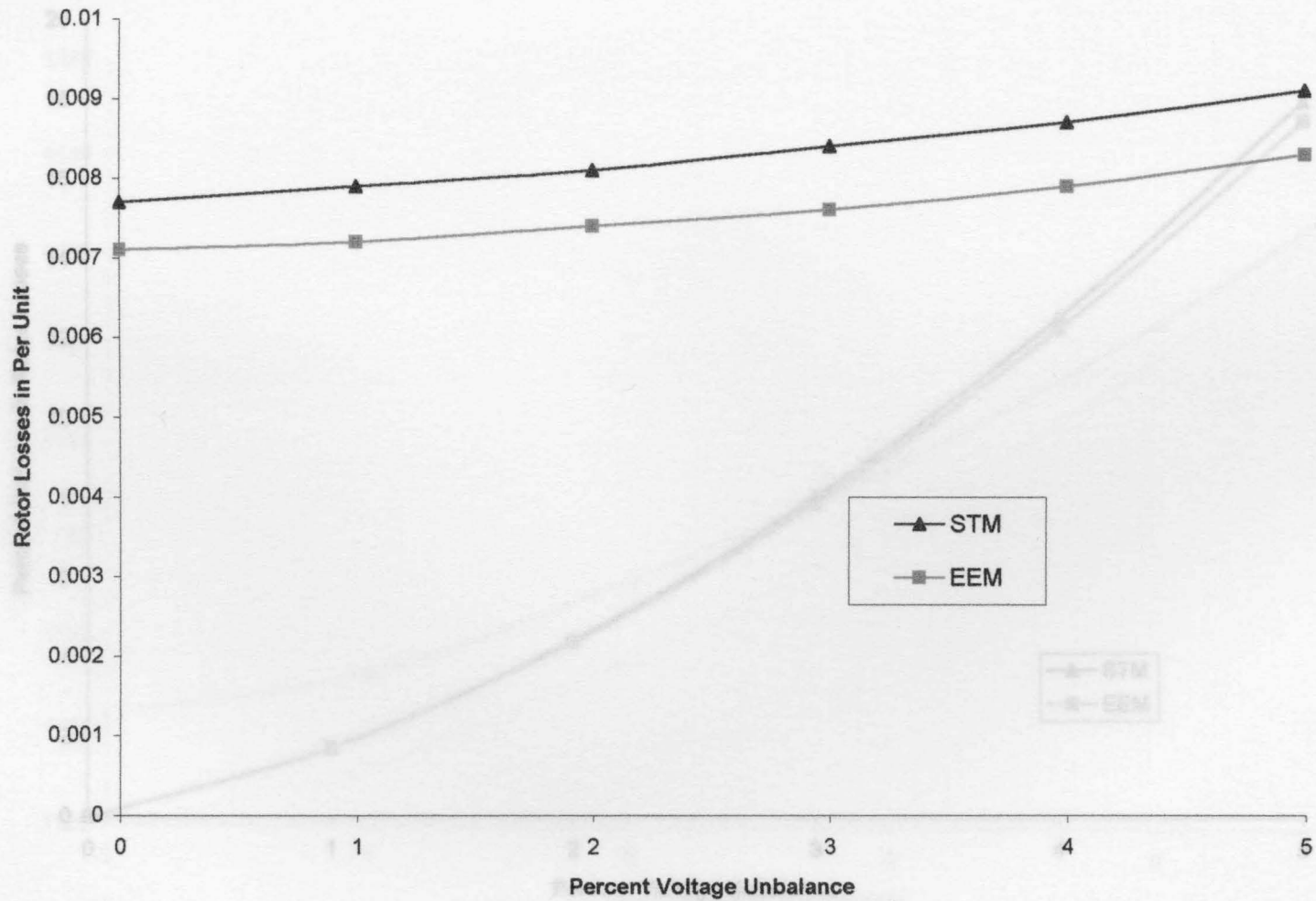


Figure 4.18: Percent Increase in Rotor Losses for 100 hp STM and EEM vs. Percent Voltage Unbalance

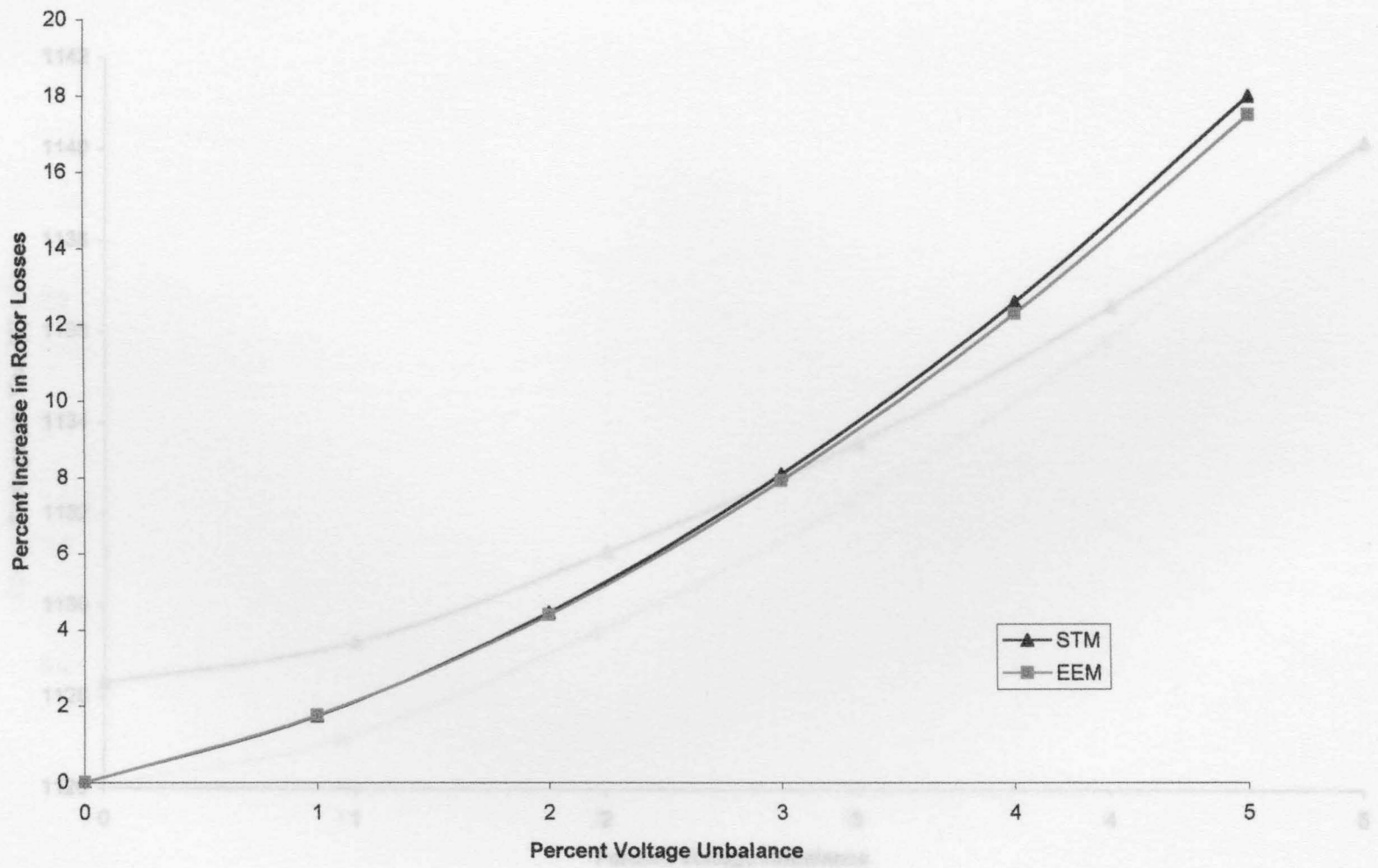


Figure 4.19: Yearly Savings for 100 hp by Using EEM over STM vs. Percent Voltage Unbalance

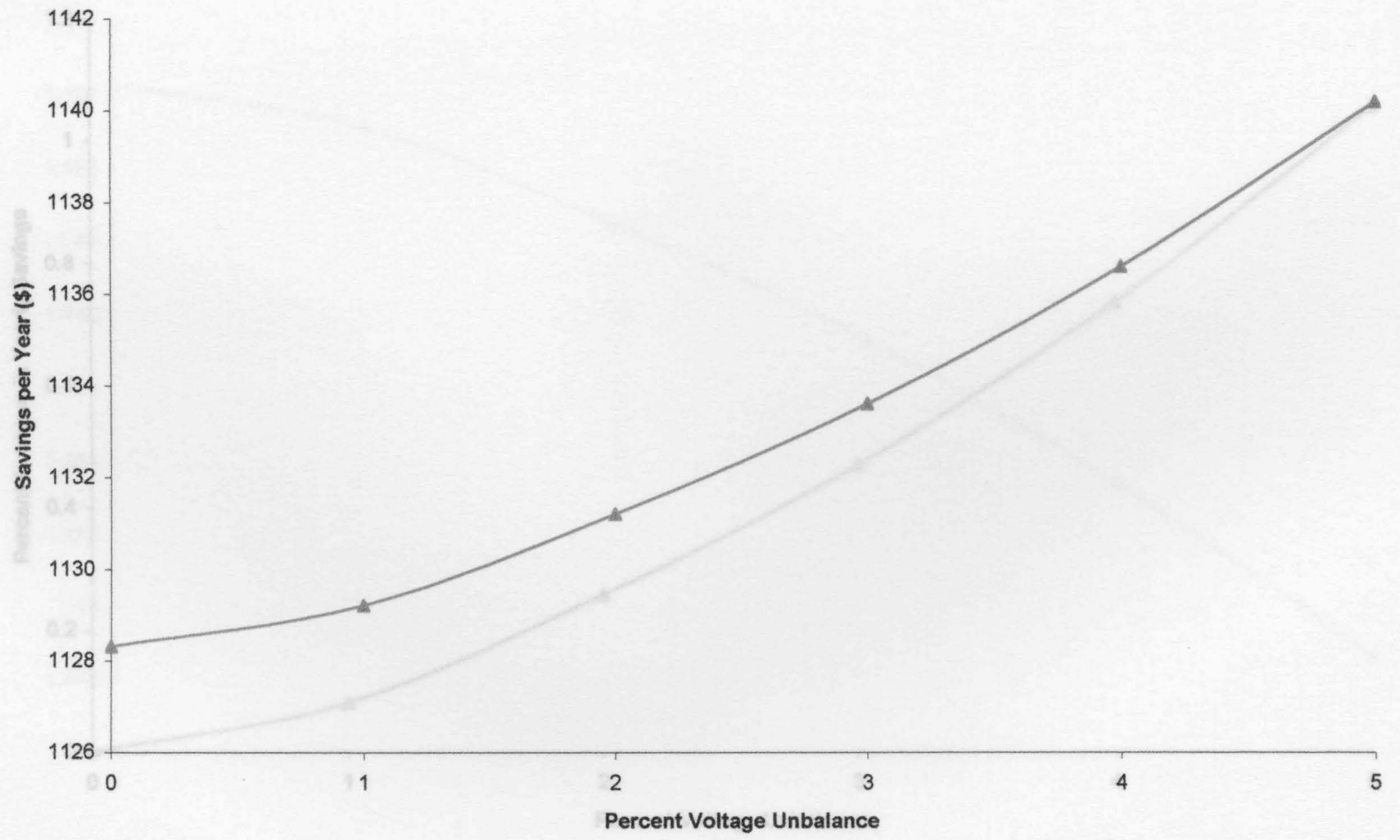


Figure 4.20: Percent Increase in Yearly Savings for 100 hp by Using EEM over STM vs. Percent Voltage Unbalance

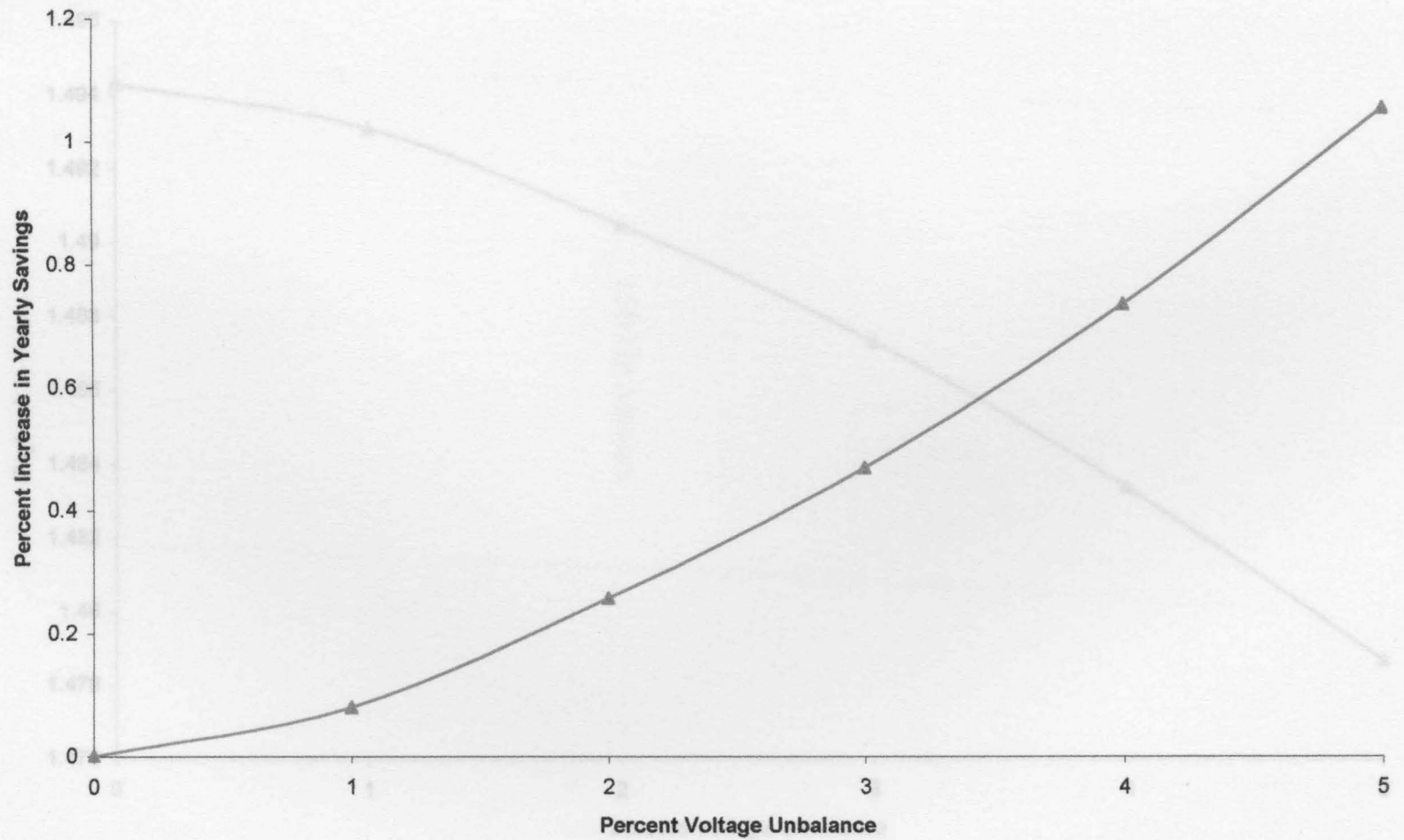


Figure 4.21: Payback Time for 100 hp STM and EEM vs. Percent Voltage Unbalance

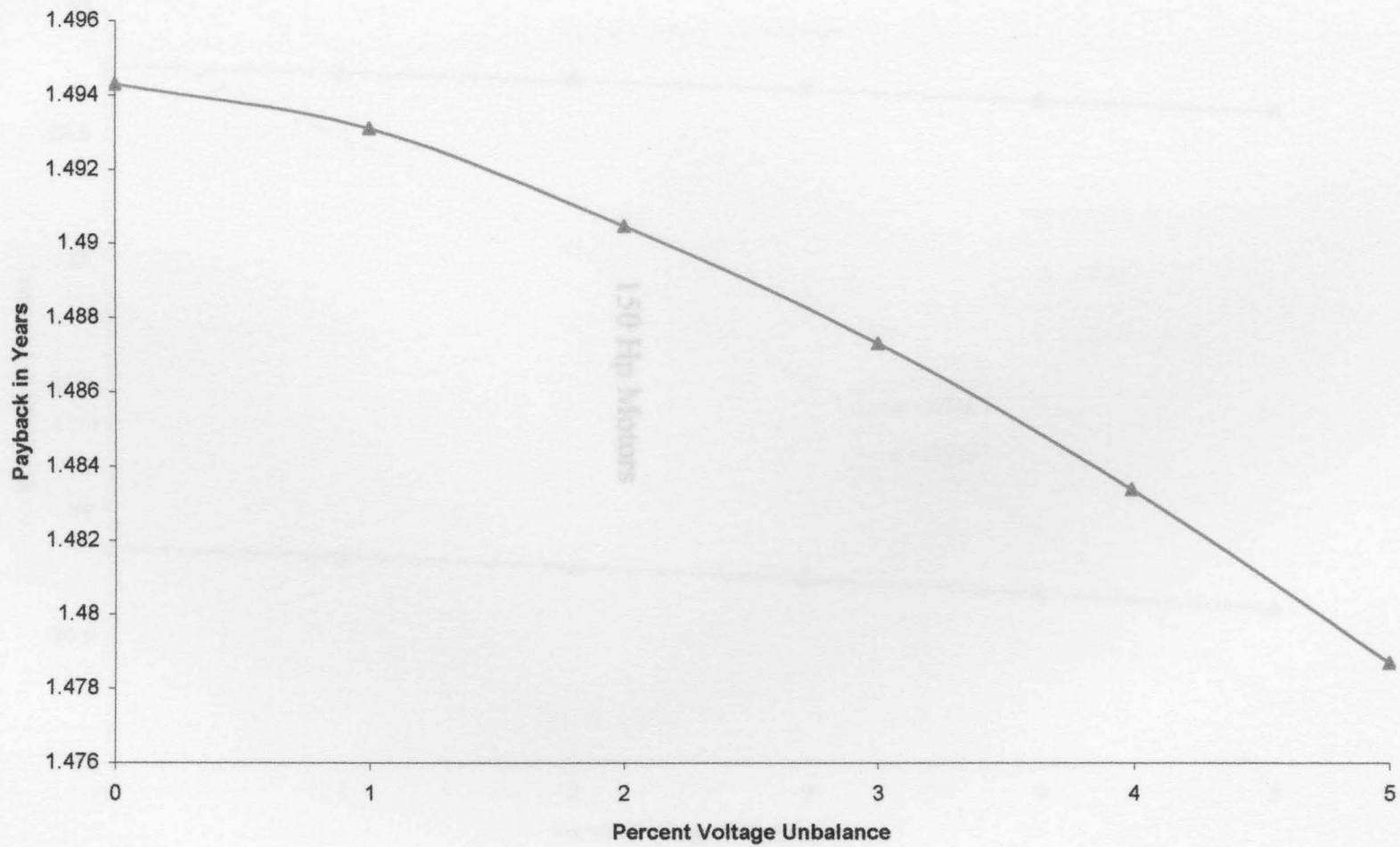
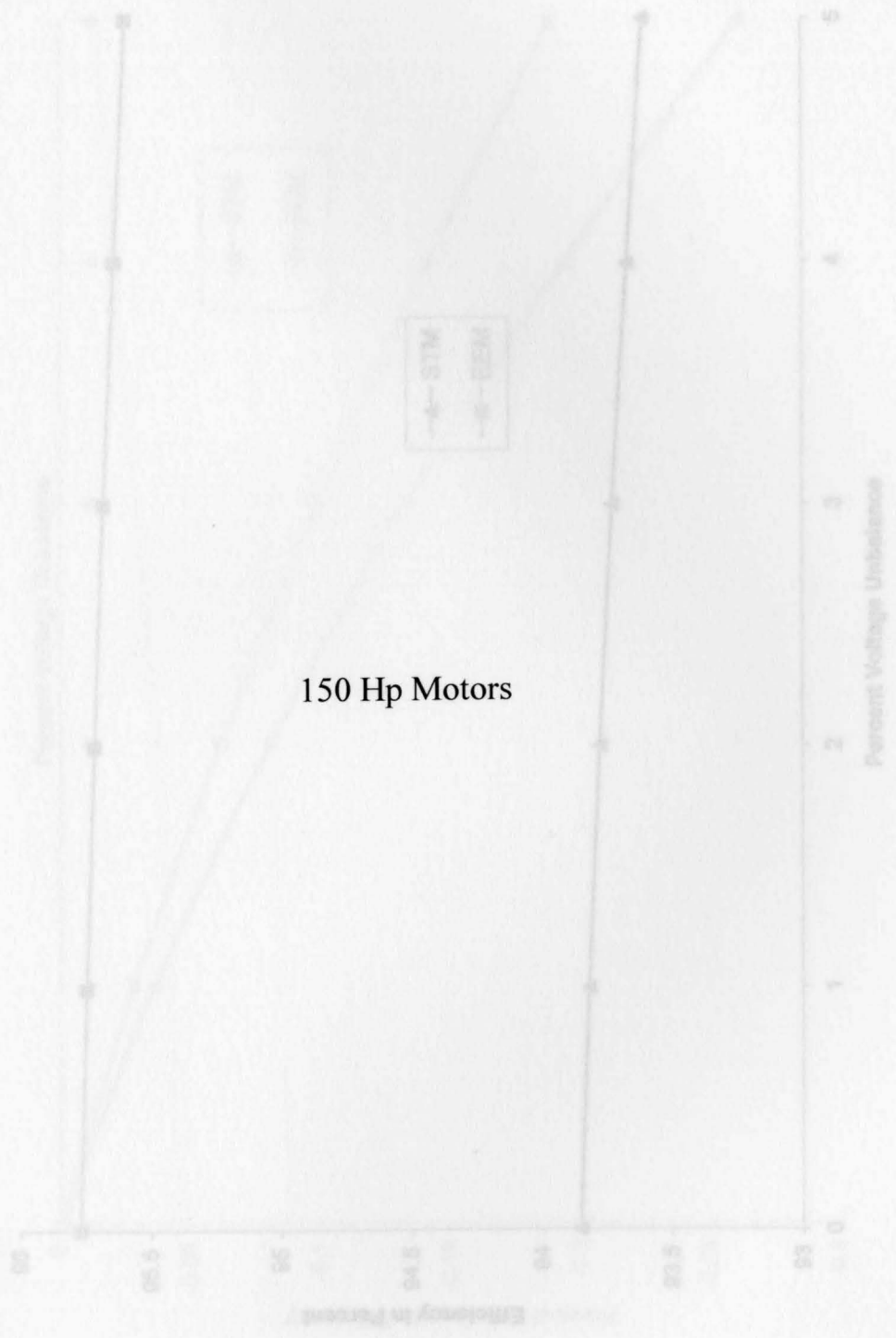


Figure 4.22: Efficiencies for 150 Hp STM and EEM vs. Percent Voltage Unbalance



150 Hp Motors

Figure 4.22: Efficiencies for 150 hp STM and EEM vs. Percent Voltage Unbalance

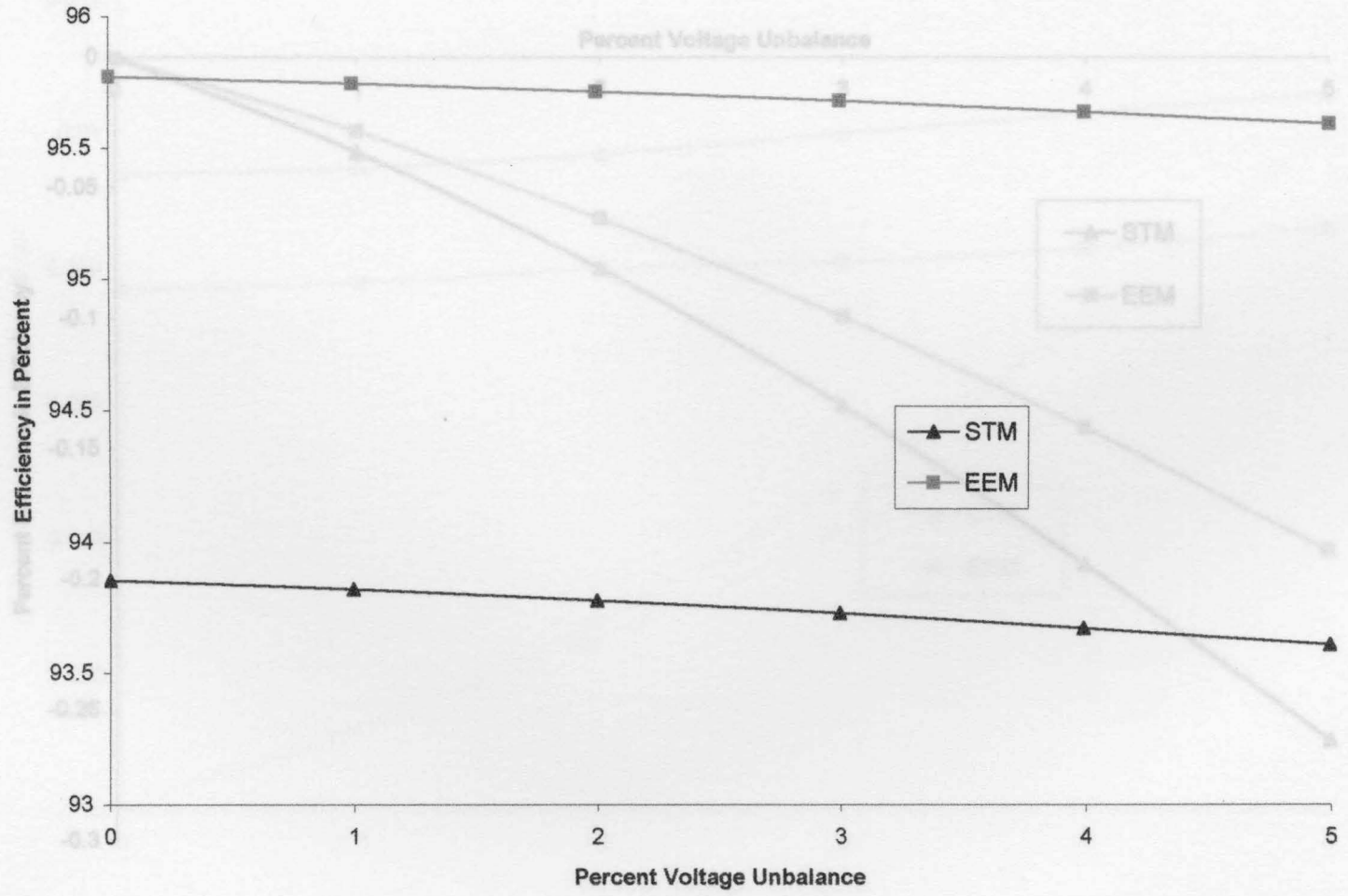


Figure 4.23: Percent Decrease in Efficiencies for 150 hp STM and EEM vs. Percent Voltage Unbalance

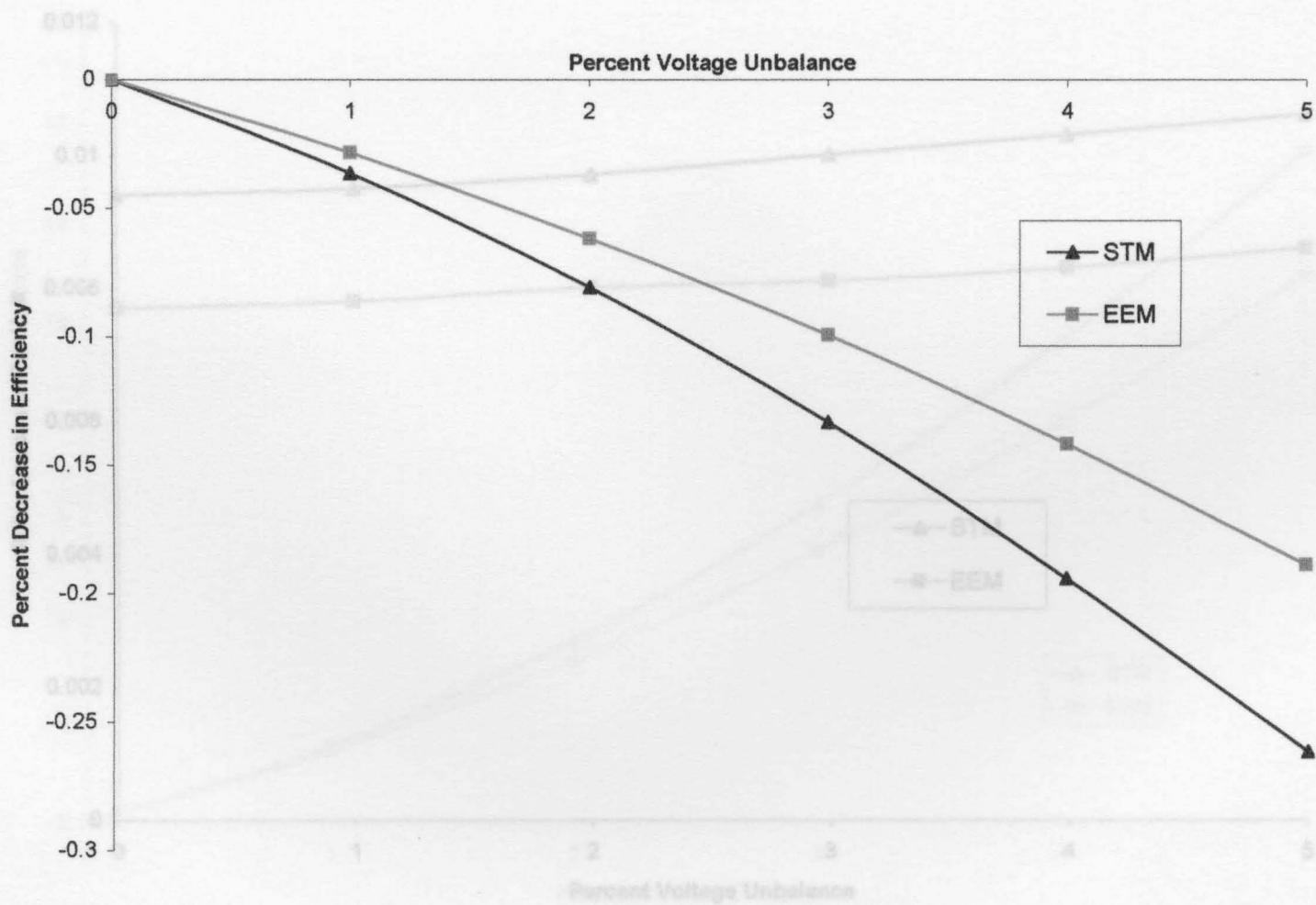
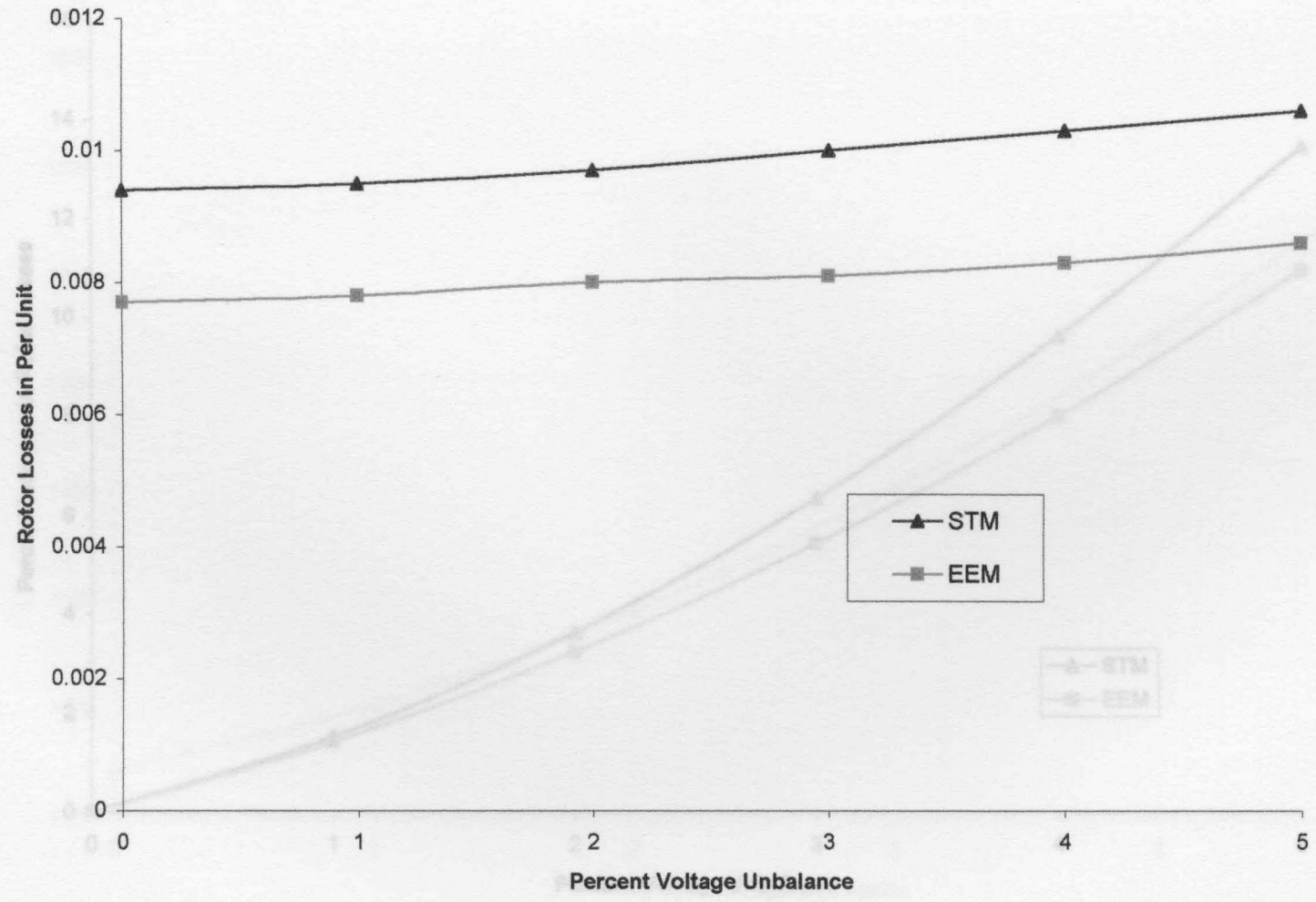


Figure 4.24: Rotor Losses for 150 hp STM and EEM vs. Percent Voltage Unbalance



75

Figure 4.25: Percent Increase in Rotor Losses for 150 hp STM and EEM vs. Percent Voltage Unbalance

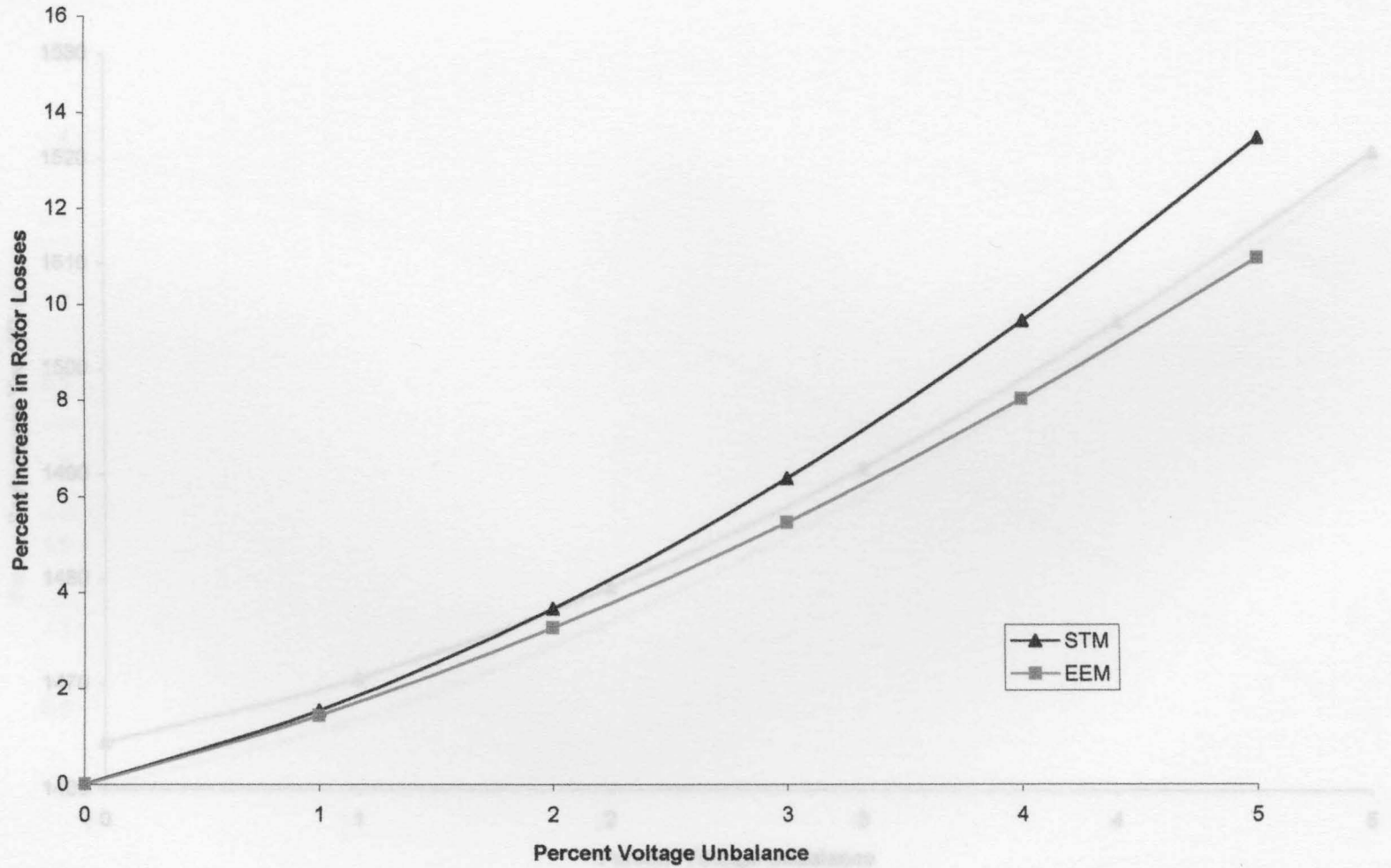


Figure 4.26: Yearly Savings for 150 hp by Using EEM over STM vs. Percent Voltage

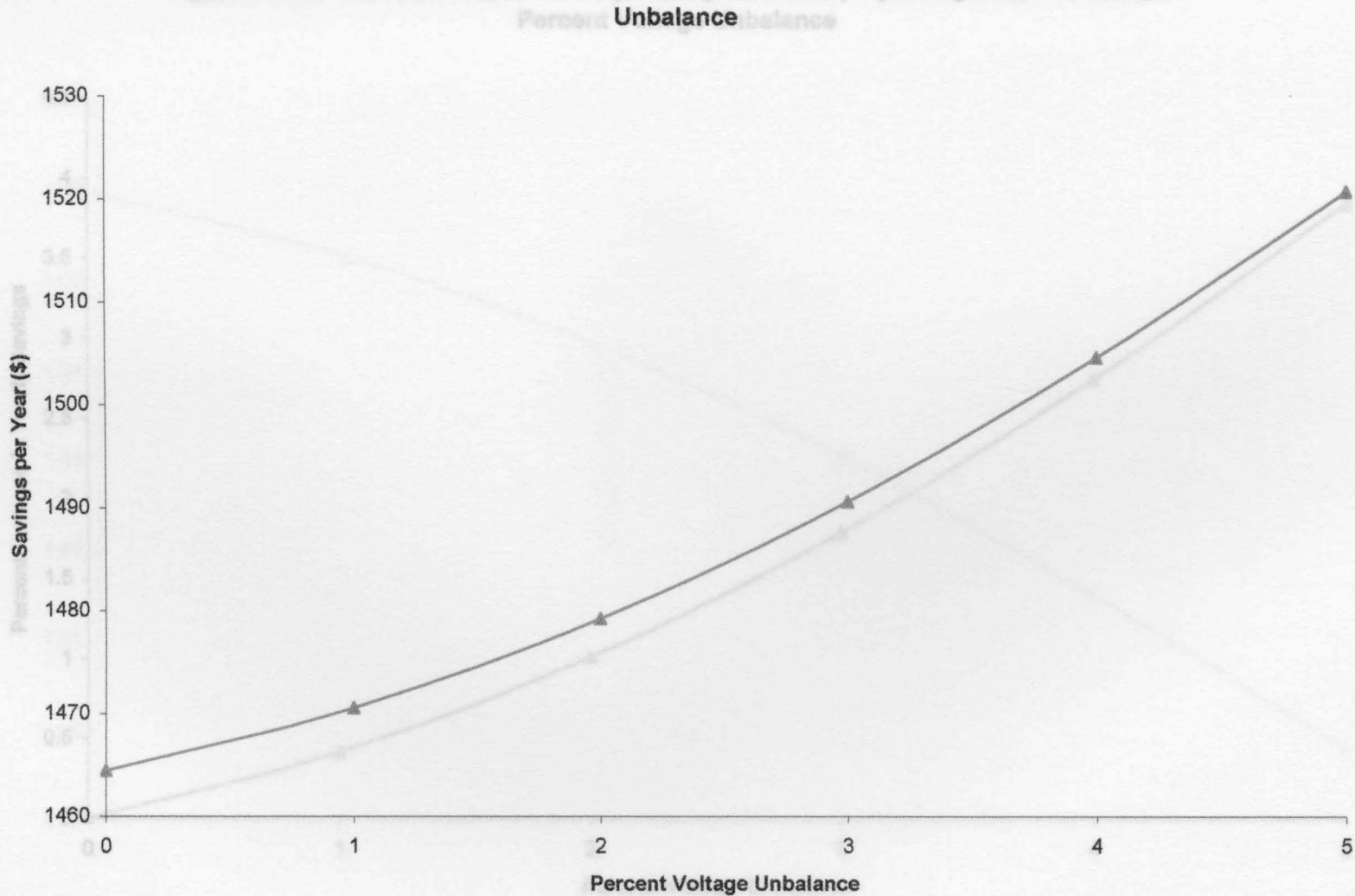


Figure 4.27: Percent Increase in Yearly Savings for 150 hp by Using EEM over STM vs. Percent Voltage Unbalance

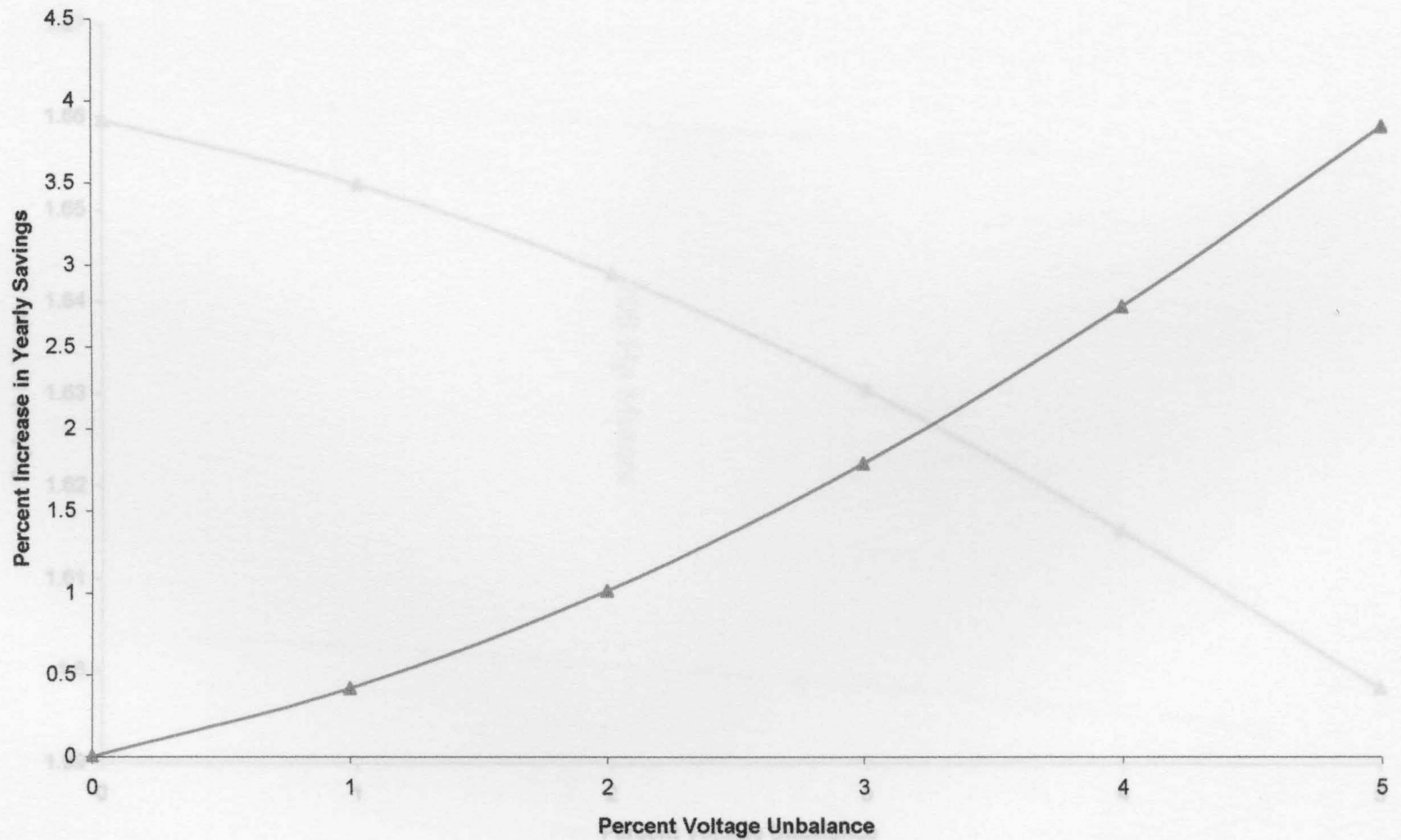


Figure 4.28: Payback Time for 150 hp STM and EEM vs. Percent Voltage Unbalance

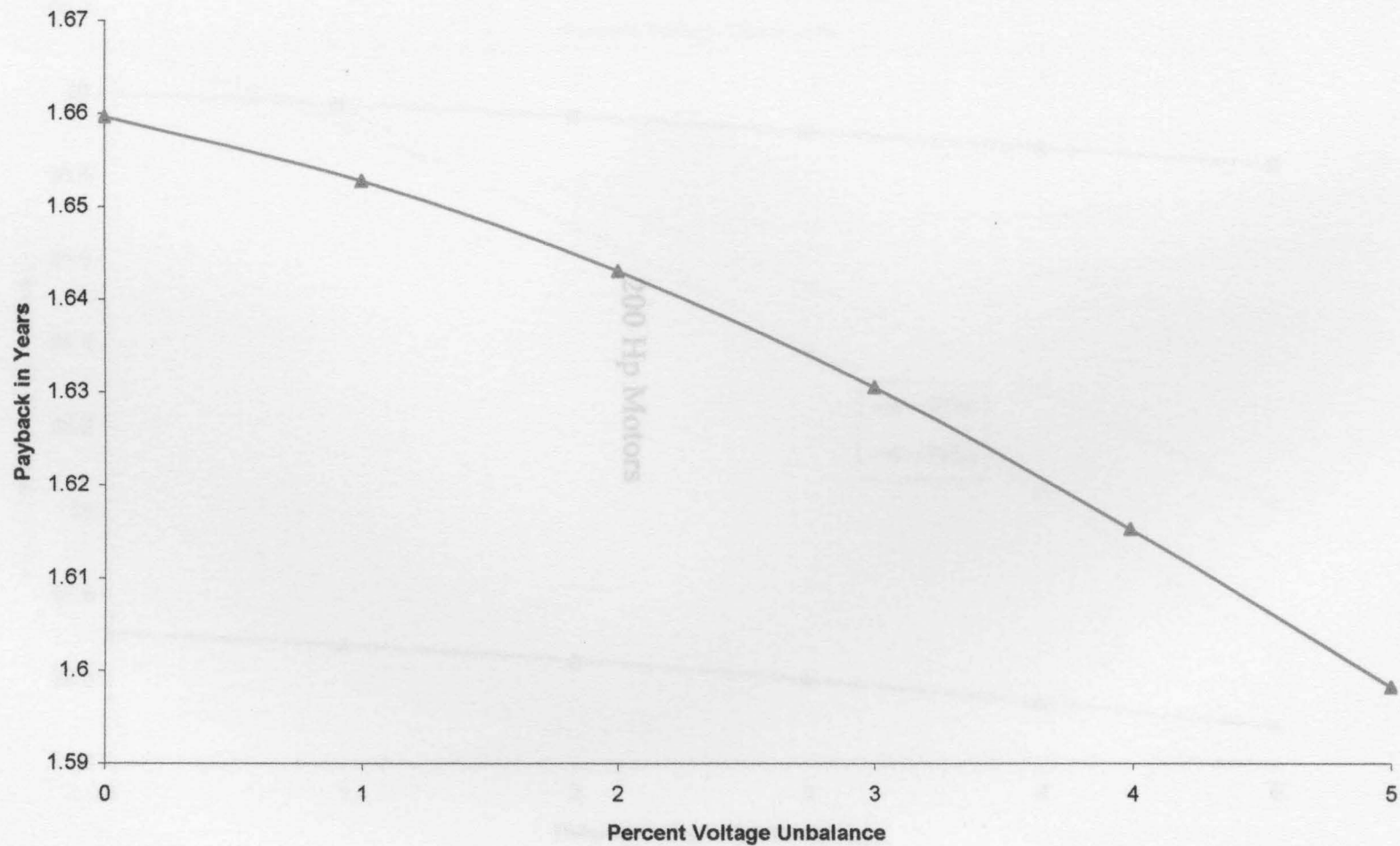
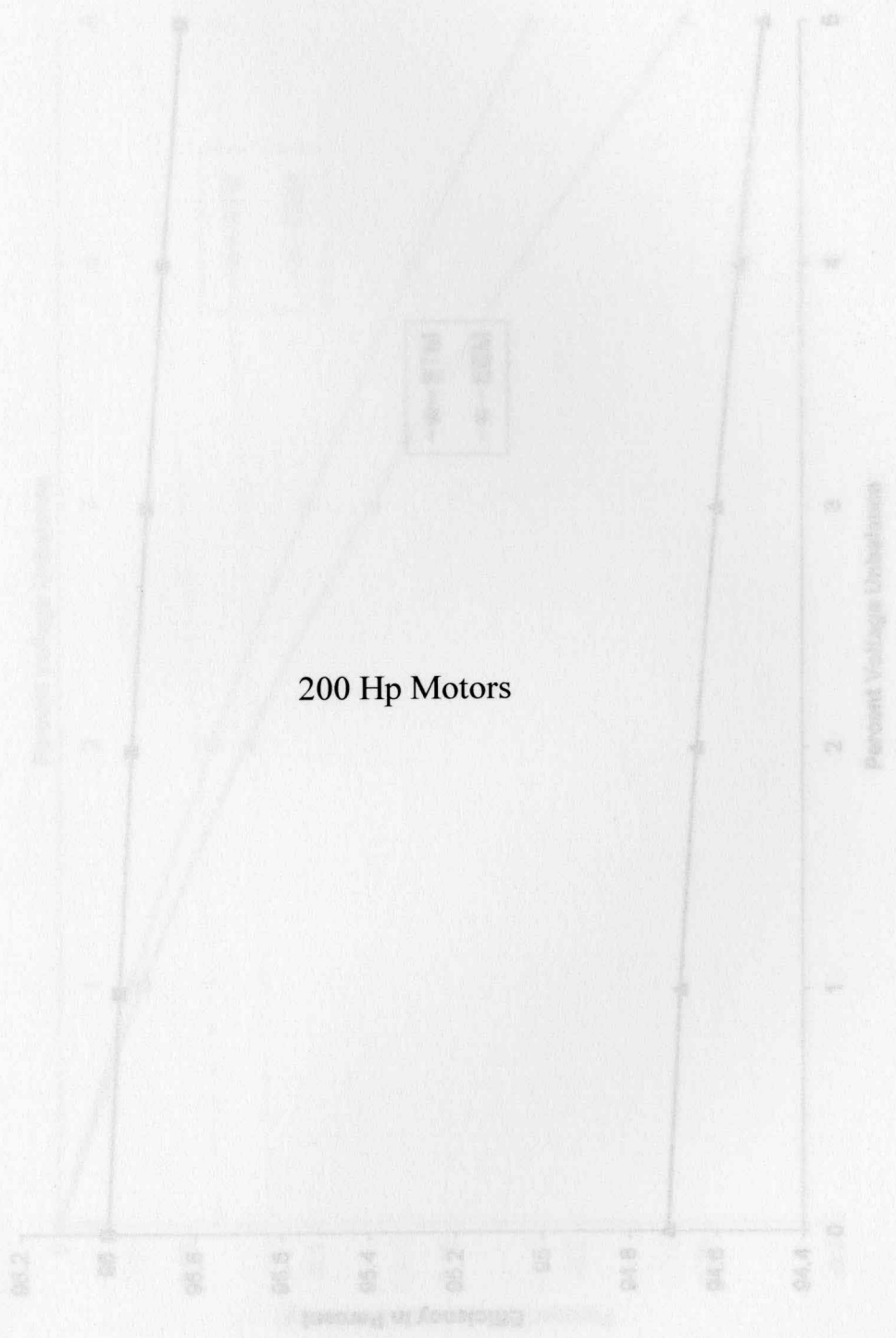


Figure 4.29: Efficiencies for 200 hp STM and EEM vs. Percent Voltage Unbalance



200 Hp Motors

Figure 4.29: Efficiencies for 200 hp STM and EEM vs. Percent Voltage Unbalance

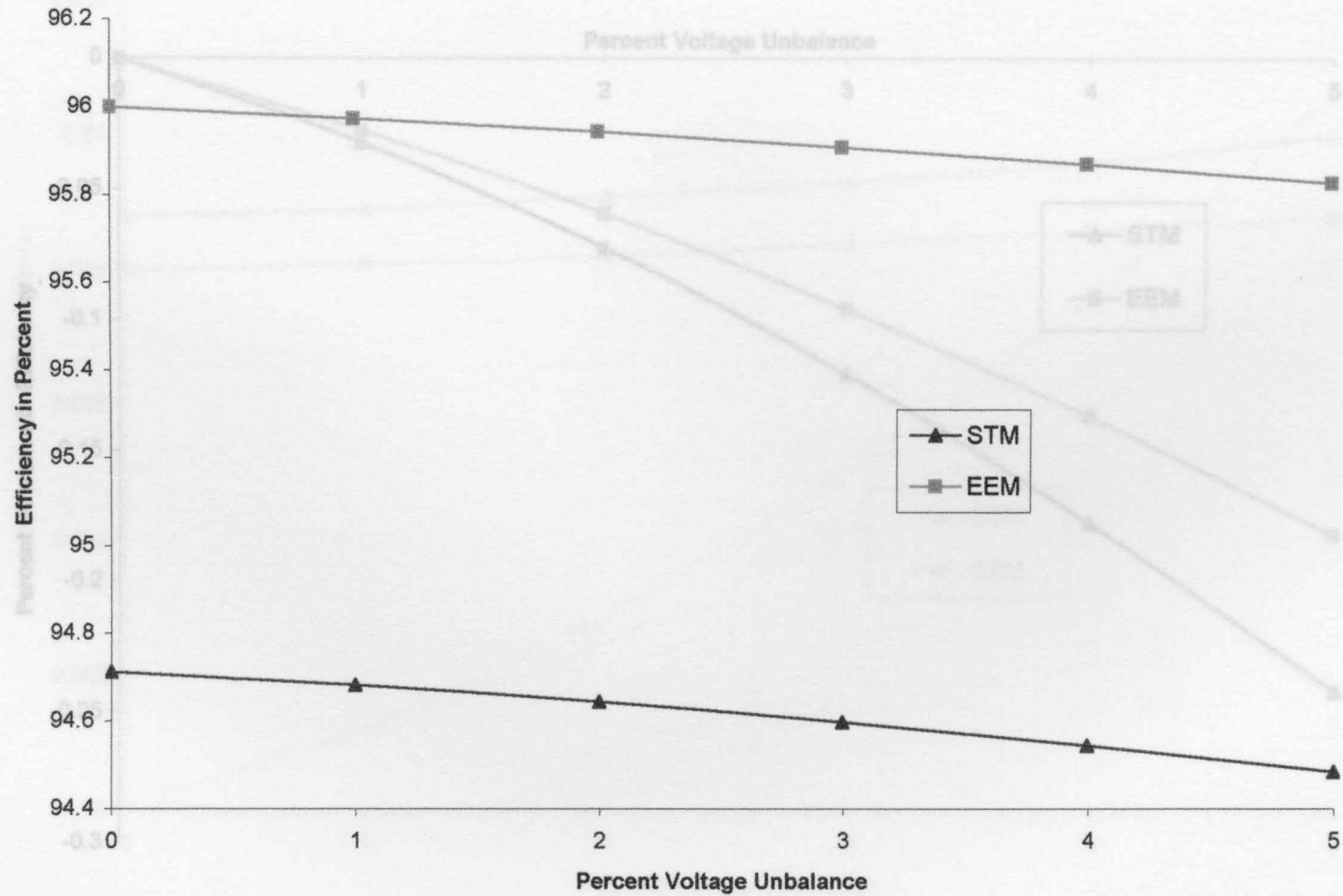


Figure 4.30: Percent Decrease in Efficiencies for 200 hp STM and EEM vs. Percent Voltage Unbalance

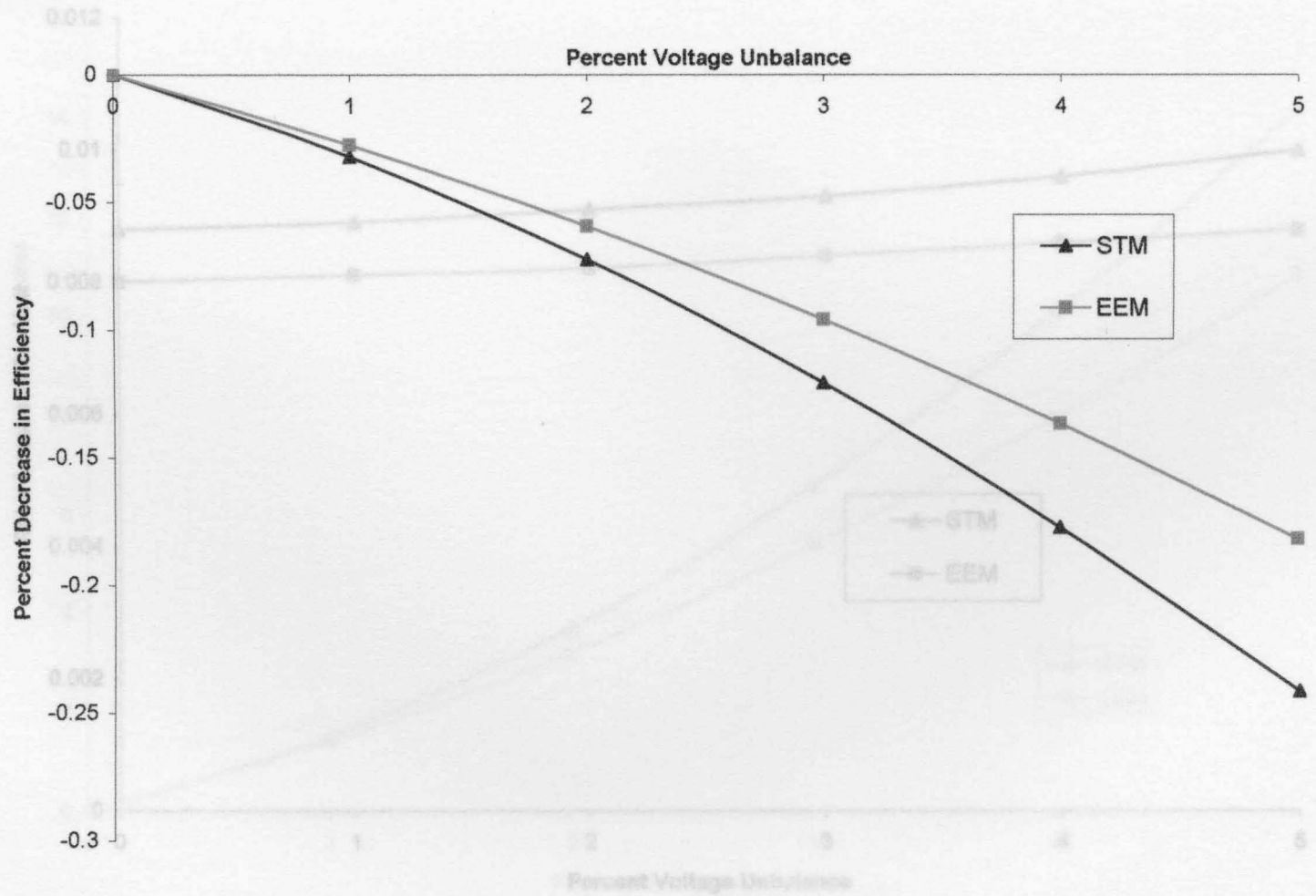


Figure 4.31: Rotor Losses for 200 hp STM and EEM vs. Percent Voltage Unbalance

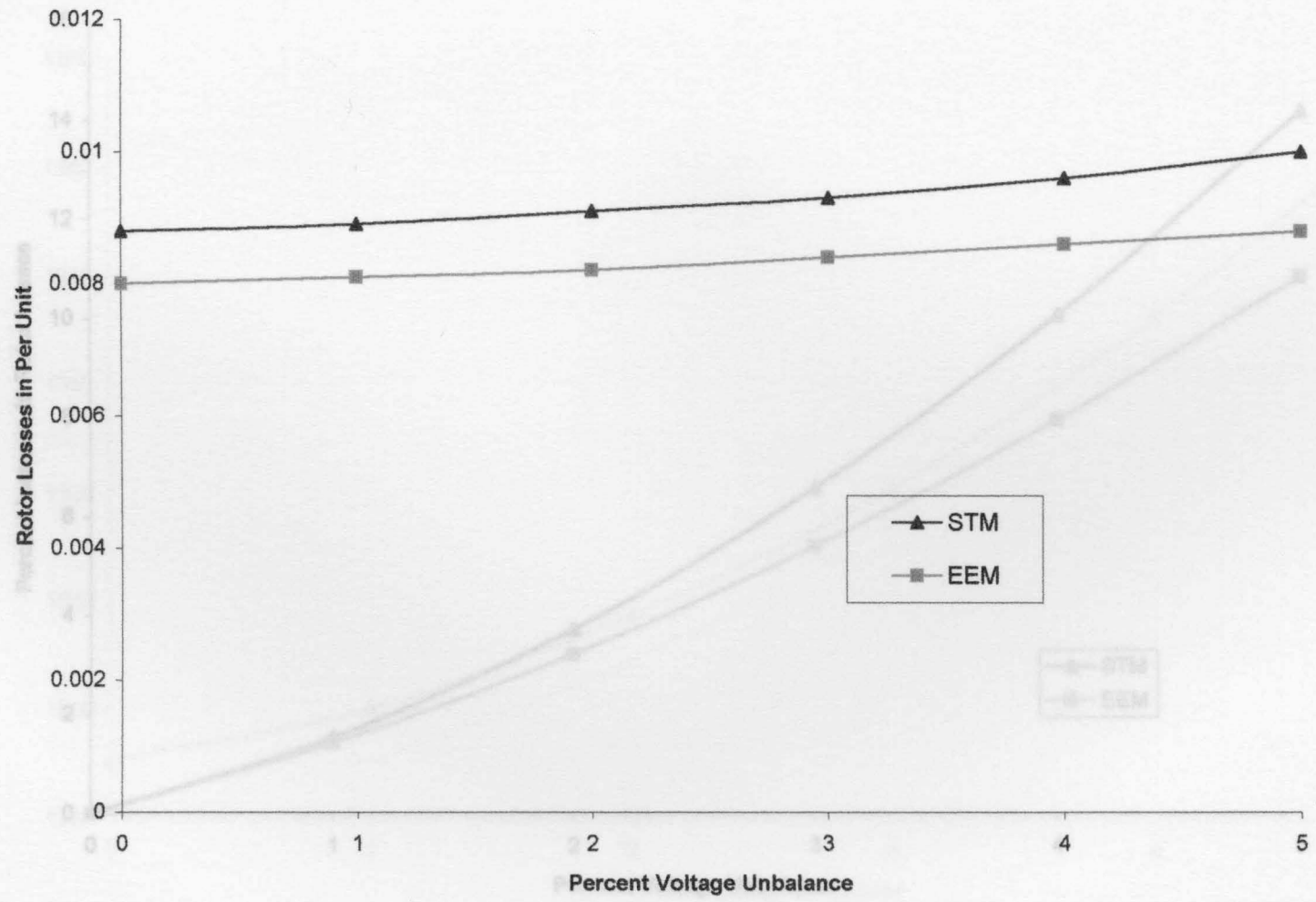


Figure 4.32: Percent Increase in Rotor Losses for 200 hp STM and EEM vs. Percent Voltage Unbalance

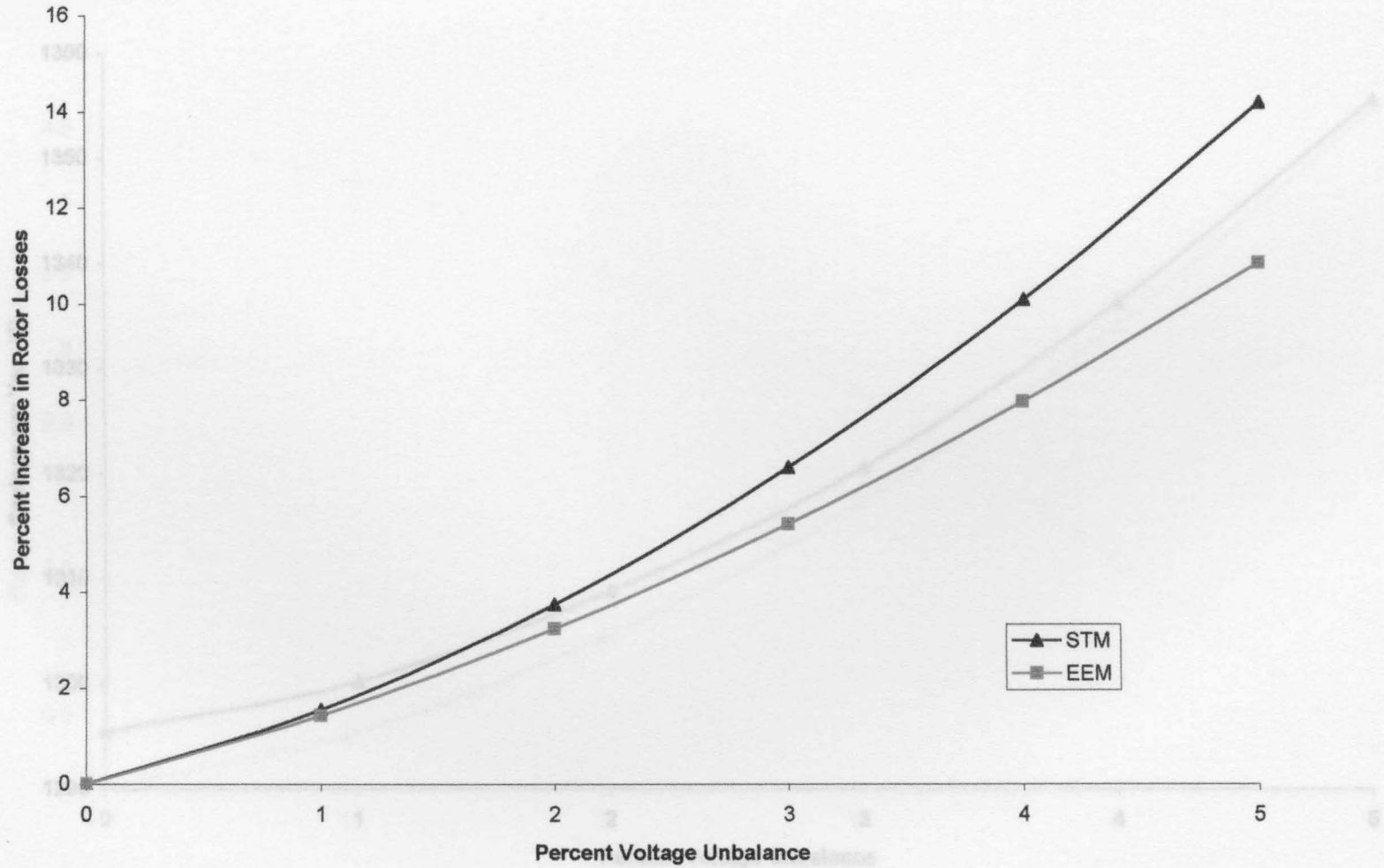


Figure 4.33: Yearly Savings for 200 hp by Using EEM over STM vs. Percent Voltage

Percent Unbalance

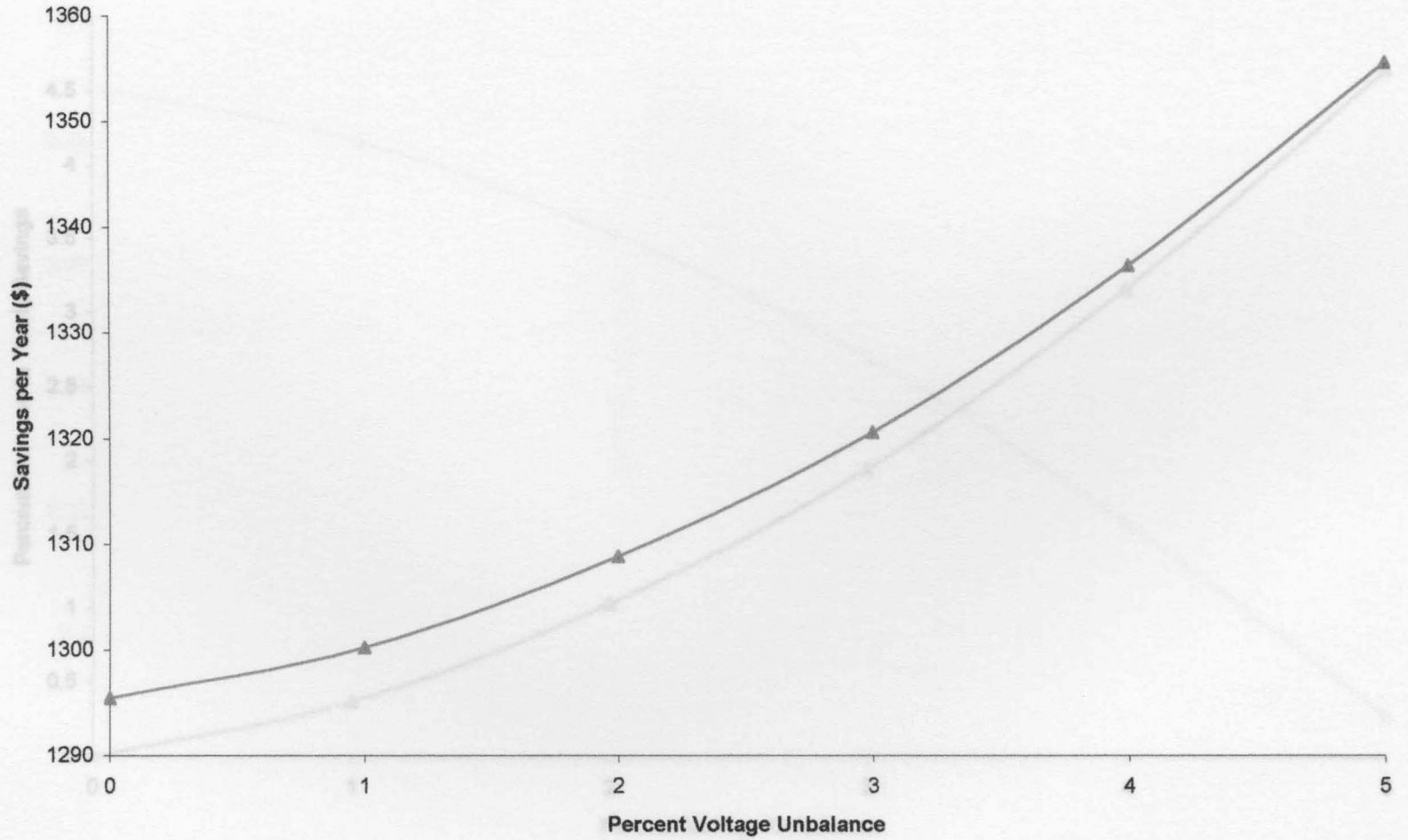


Figure 4.34: Percent Increase in Yearly Savings for 200 hp by Using EEM over STM vs. Percent Voltage Unbalance

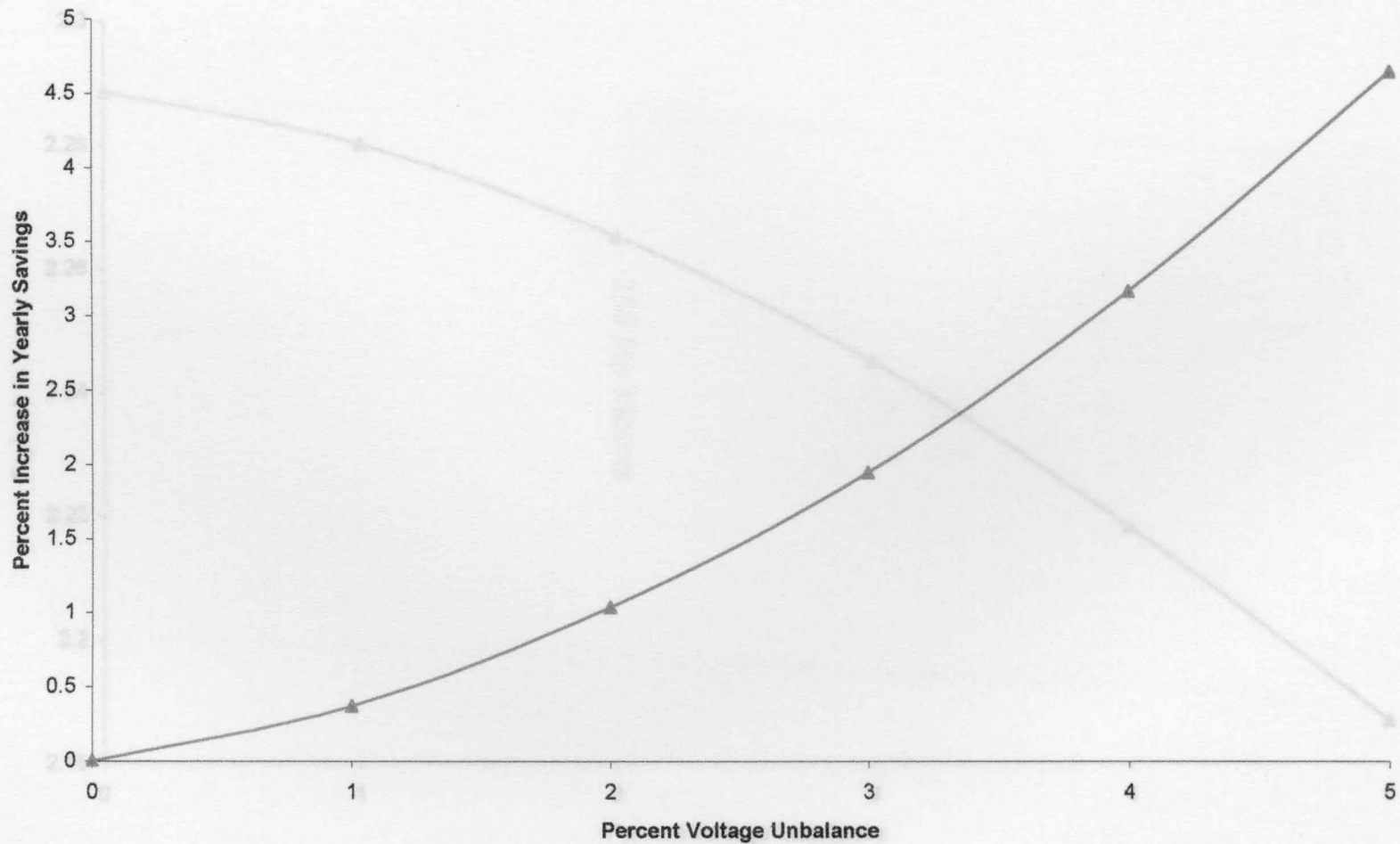


Figure 4.35: Payback Time for 200 hp STM and EEM vs. Percent Voltage Unbalance

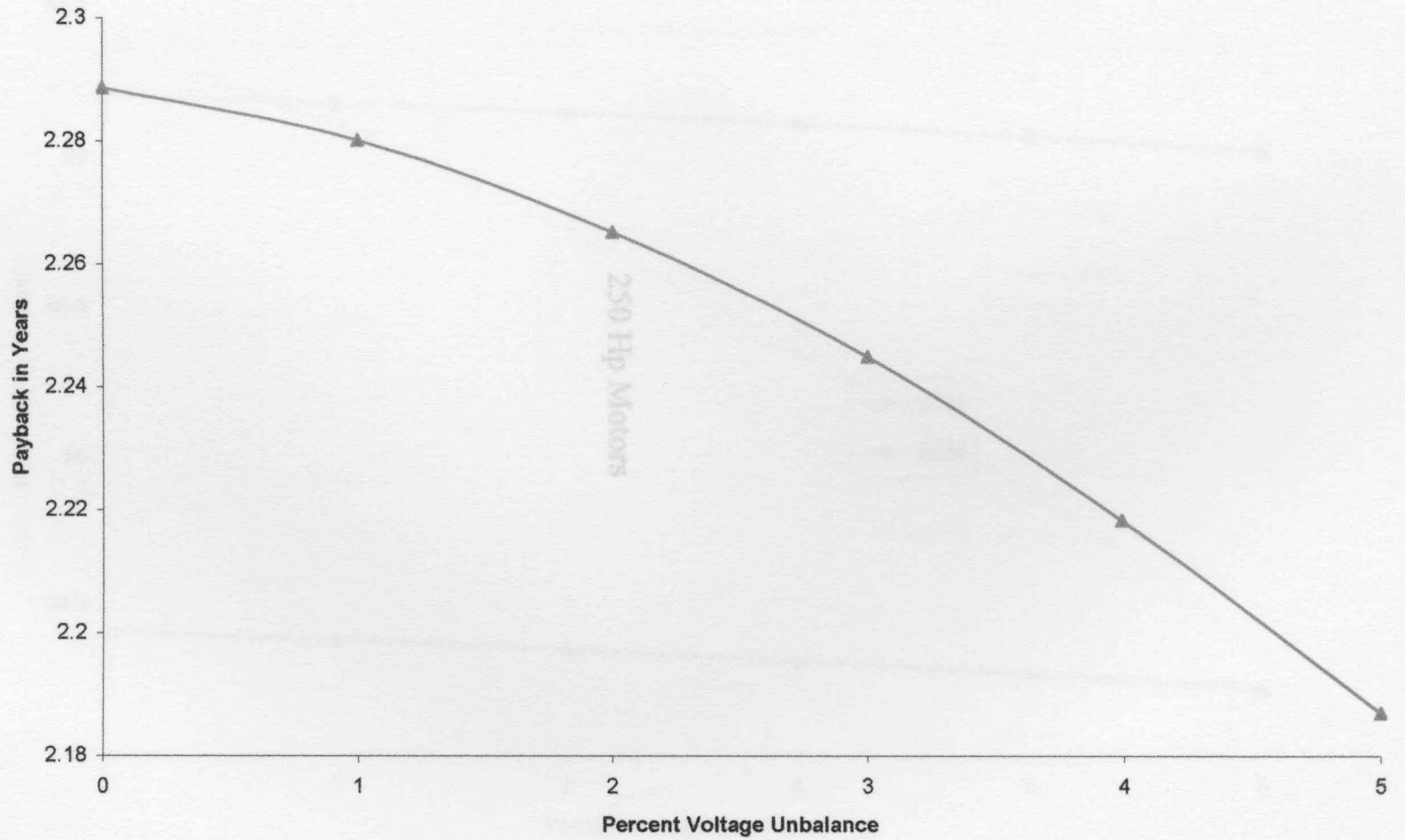
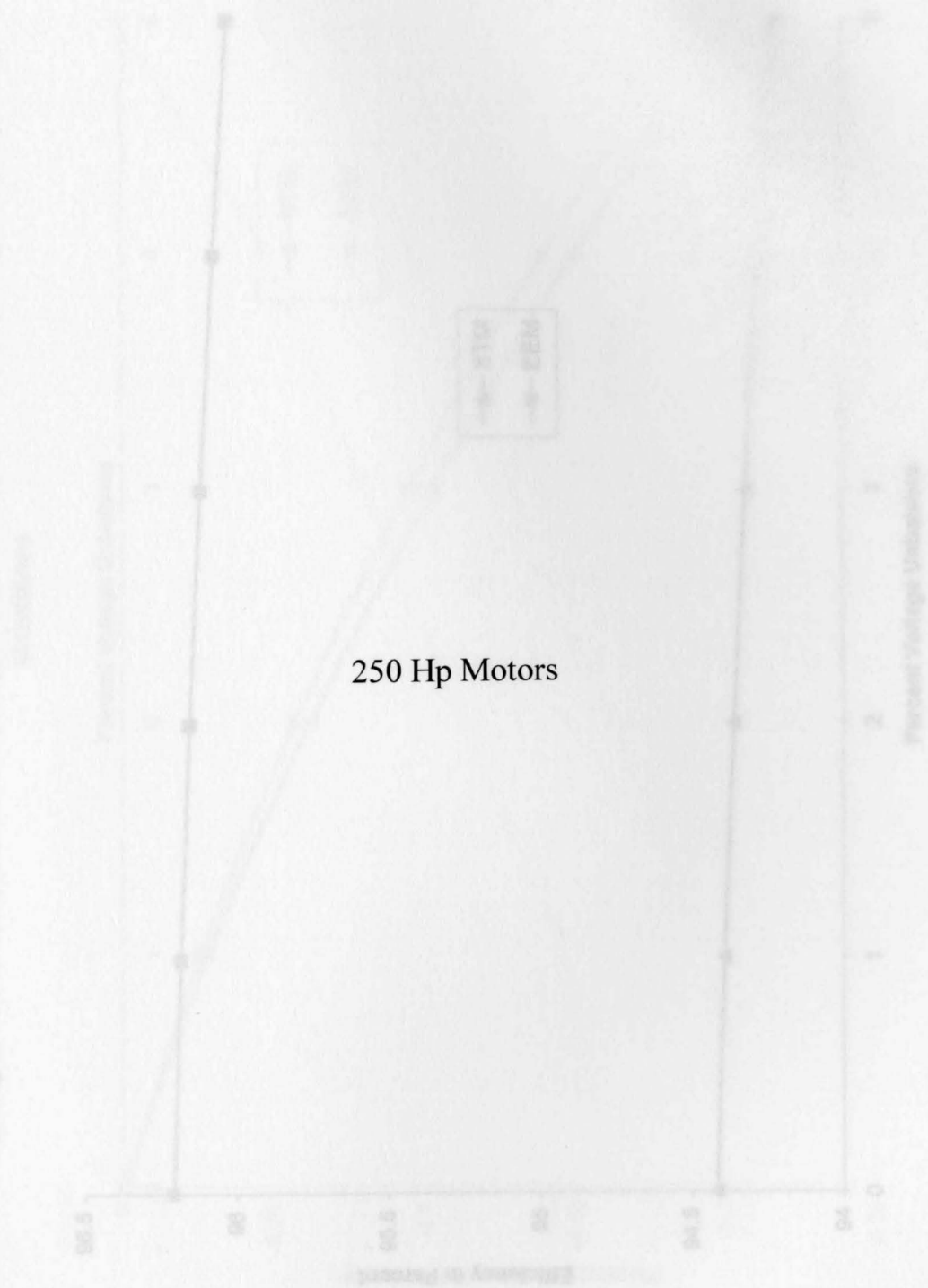


Figure 4.36: Efficiencies for 250 hp STM and CEM vs. Percent Voltage Unbalance



250 Hp Motors

Figure 4.36: Efficiencies for 250 hp STM and EEM vs. Percent Voltage Unbalance

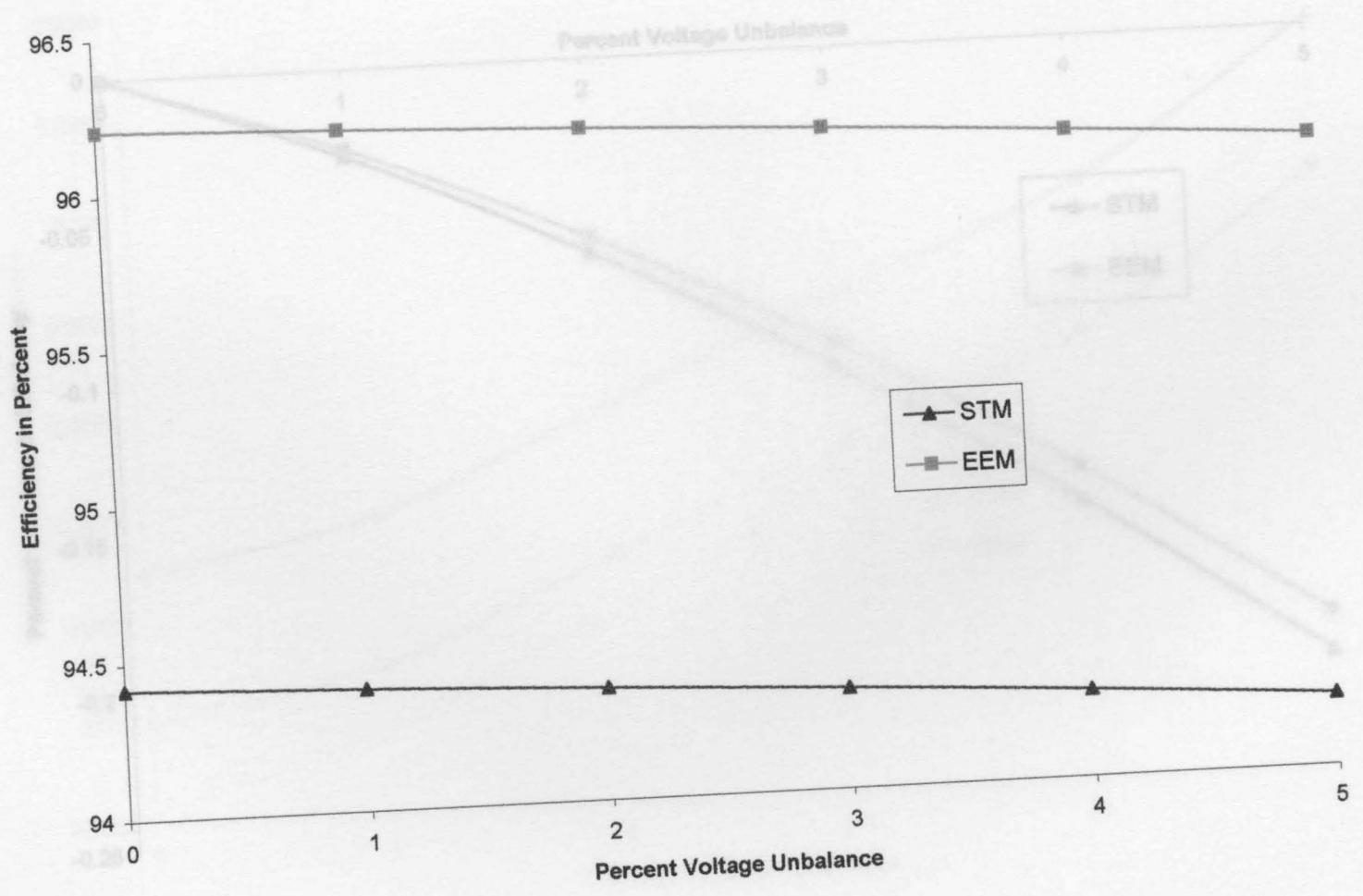


Figure 4.37: Percent Decrease in Efficiencies for 250 hp STM and EEM vs. Percent Voltage Unbalance

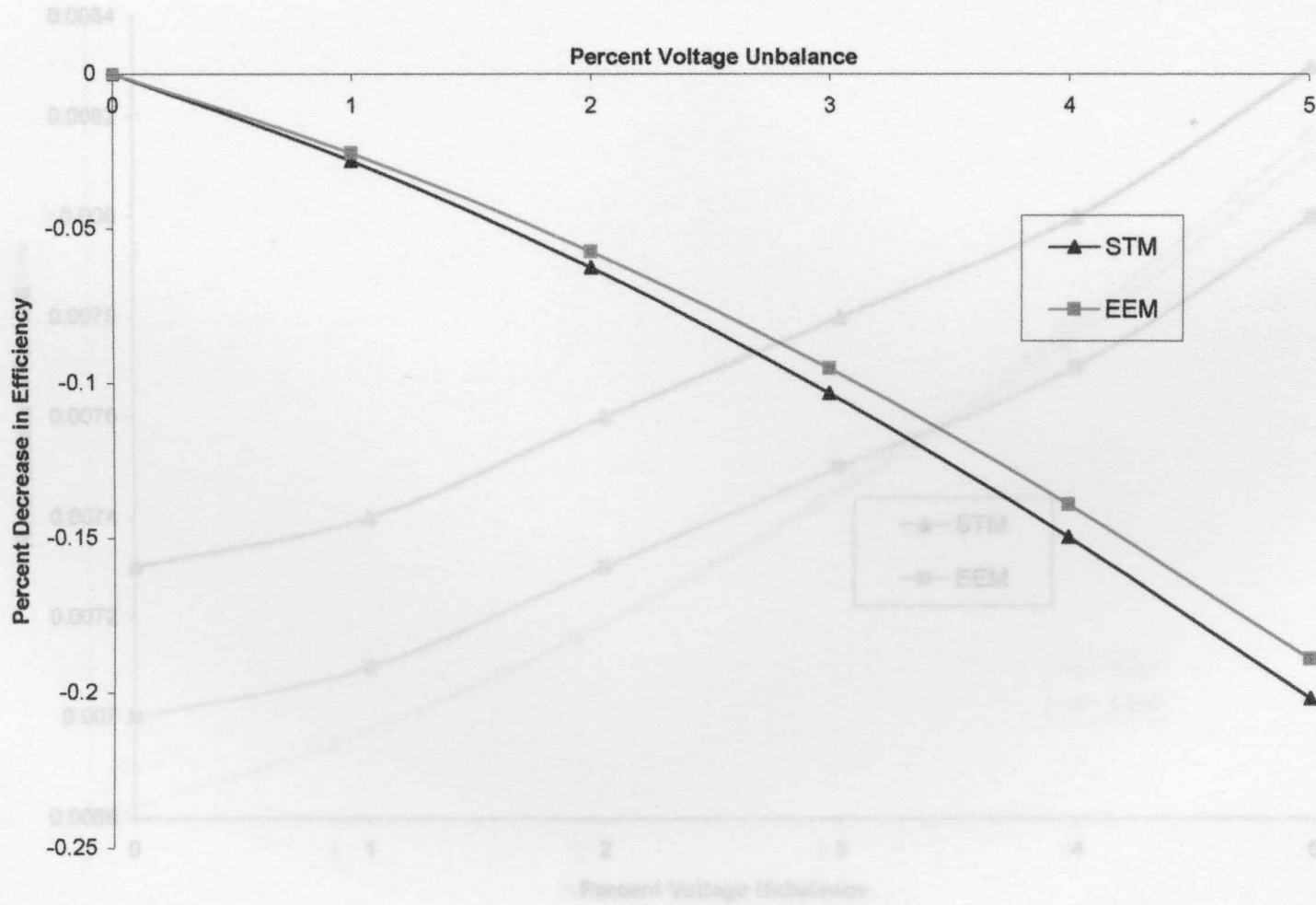


Figure 4.38: Rotor Losses for 250 hp STM and EEM vs. Percent Voltage Unbalance

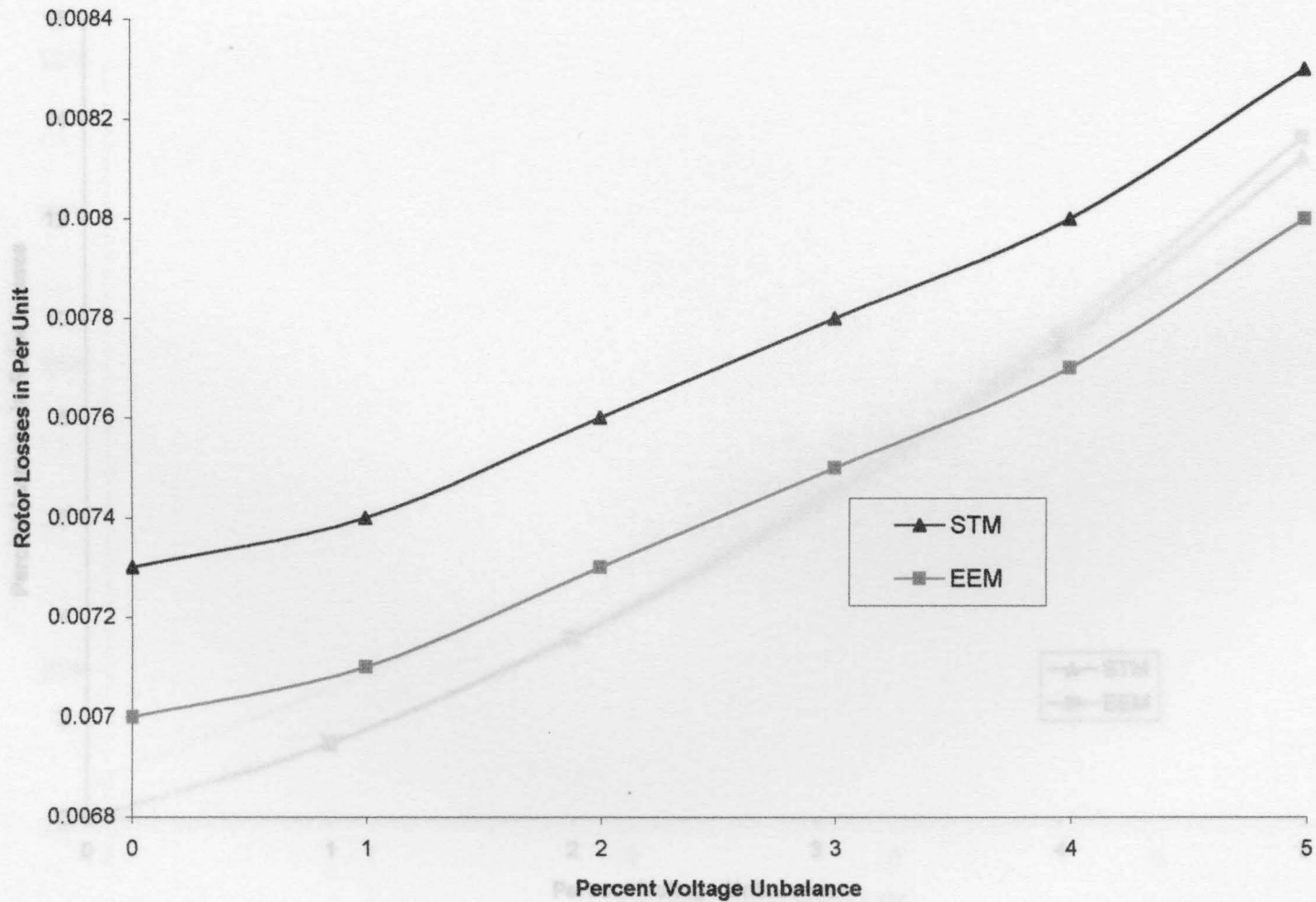


Figure 4.39: Percent Increase in Rotor Losses for 250 hp STM and EEM vs. Percent Voltage Unbalance

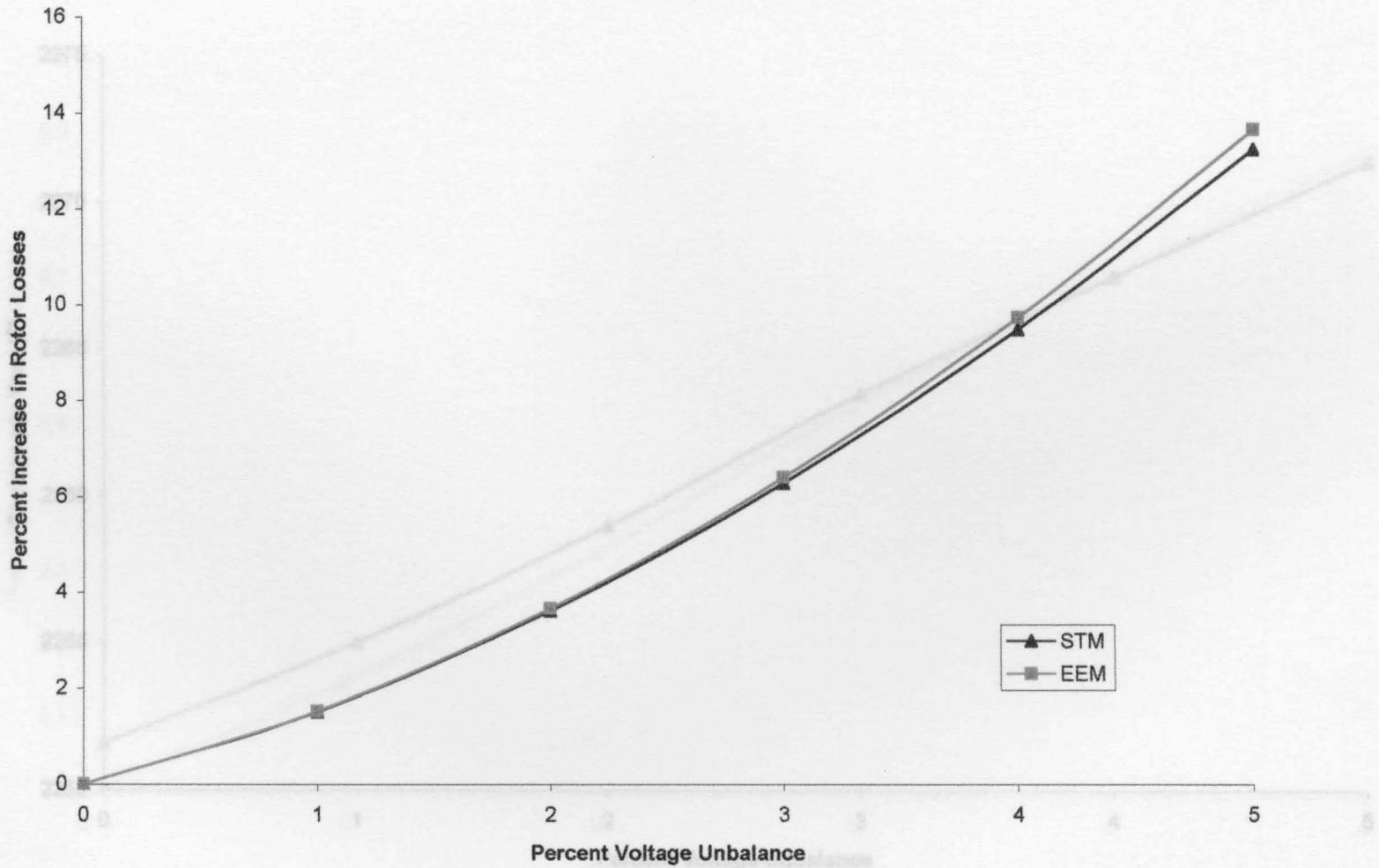


Figure 4.40: Yearly Savings for 250 hp by Using EEM over STM vs. Percent Voltage Unbalance

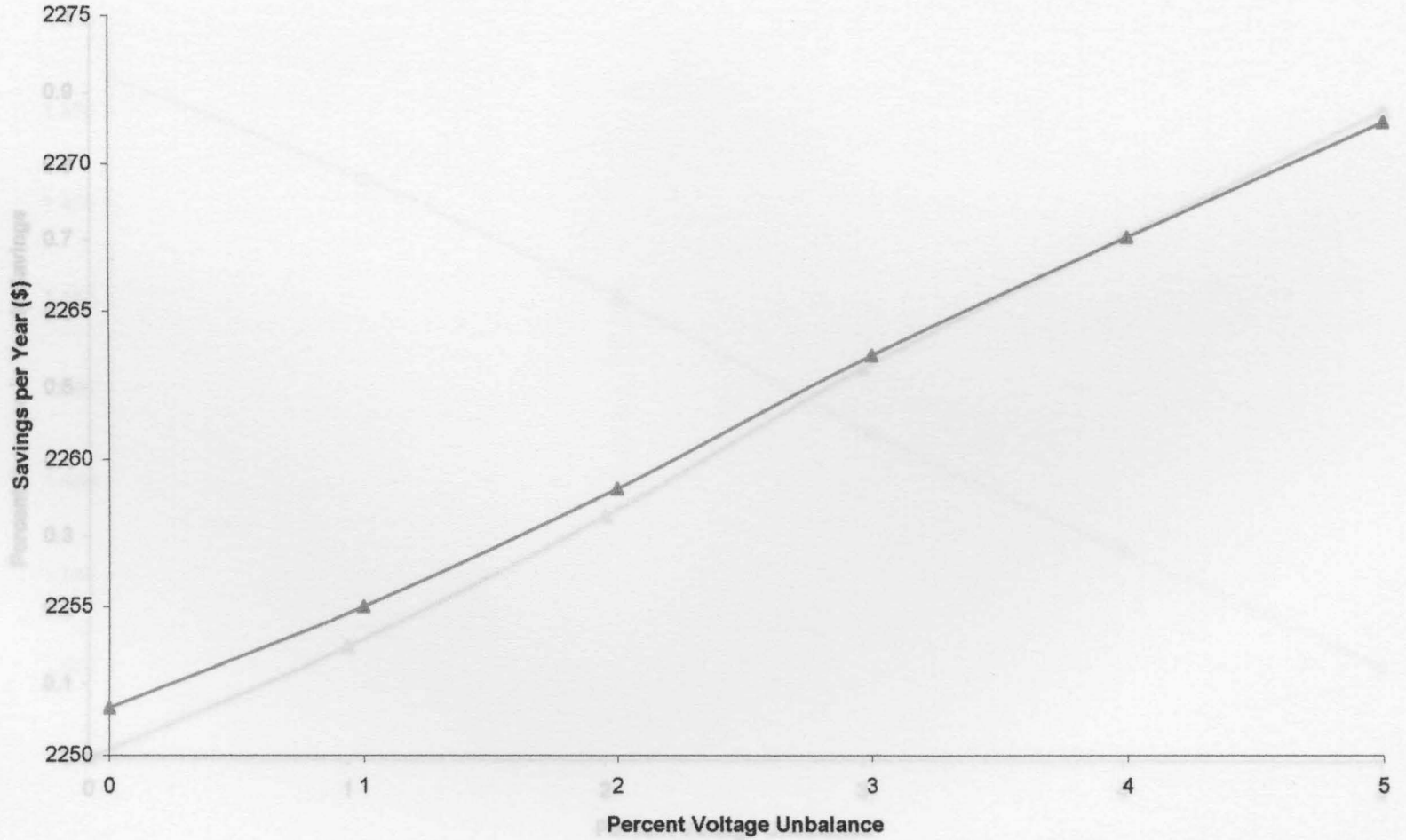


Figure 4.41: Percent Increase in Yearly Savings for 250 hp by Using EEM over STM vs. Percent Voltage Unbalance

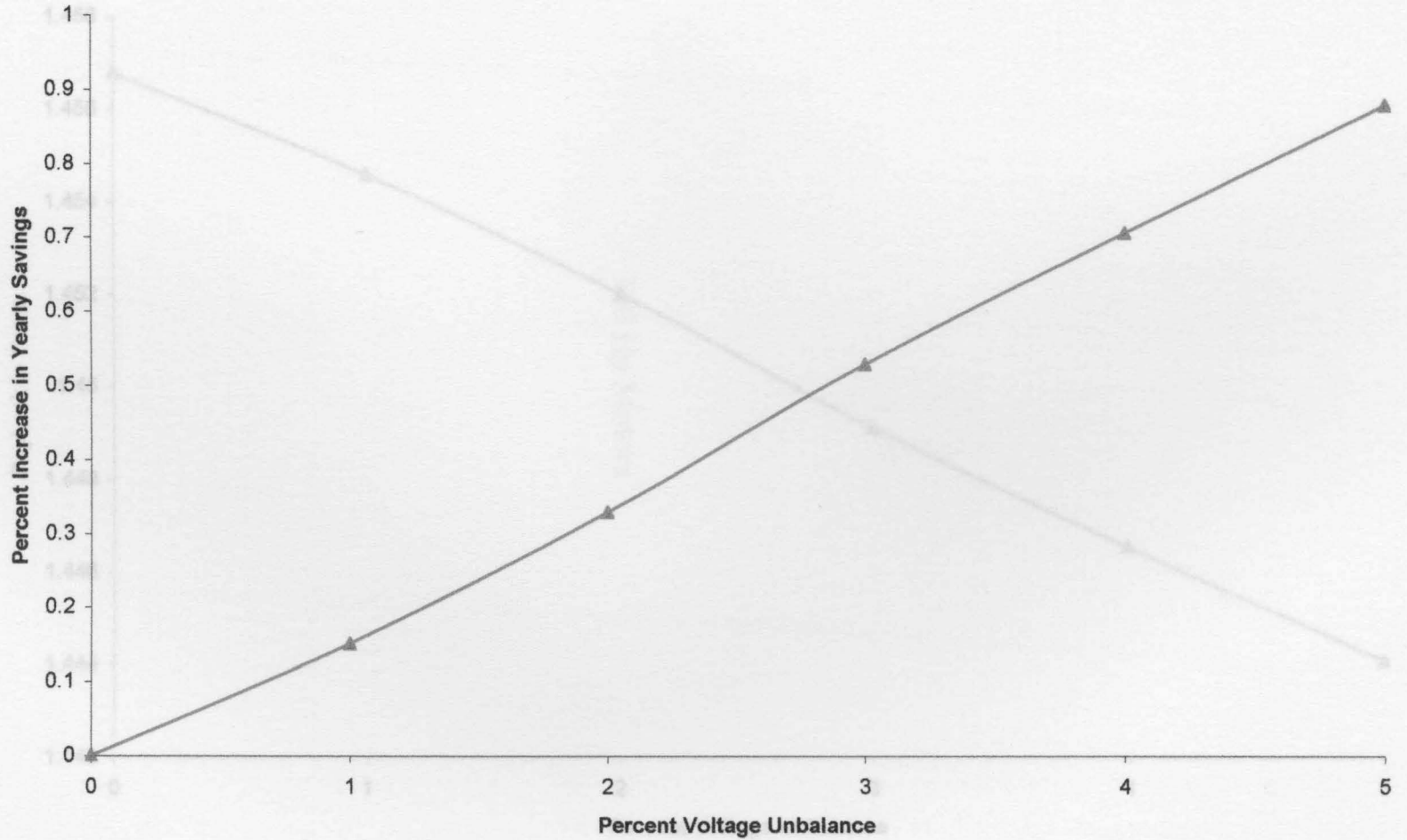


Figure 4.42: Payback Time for 250 hp STM and EEM vs. Percent Voltage Unbalance

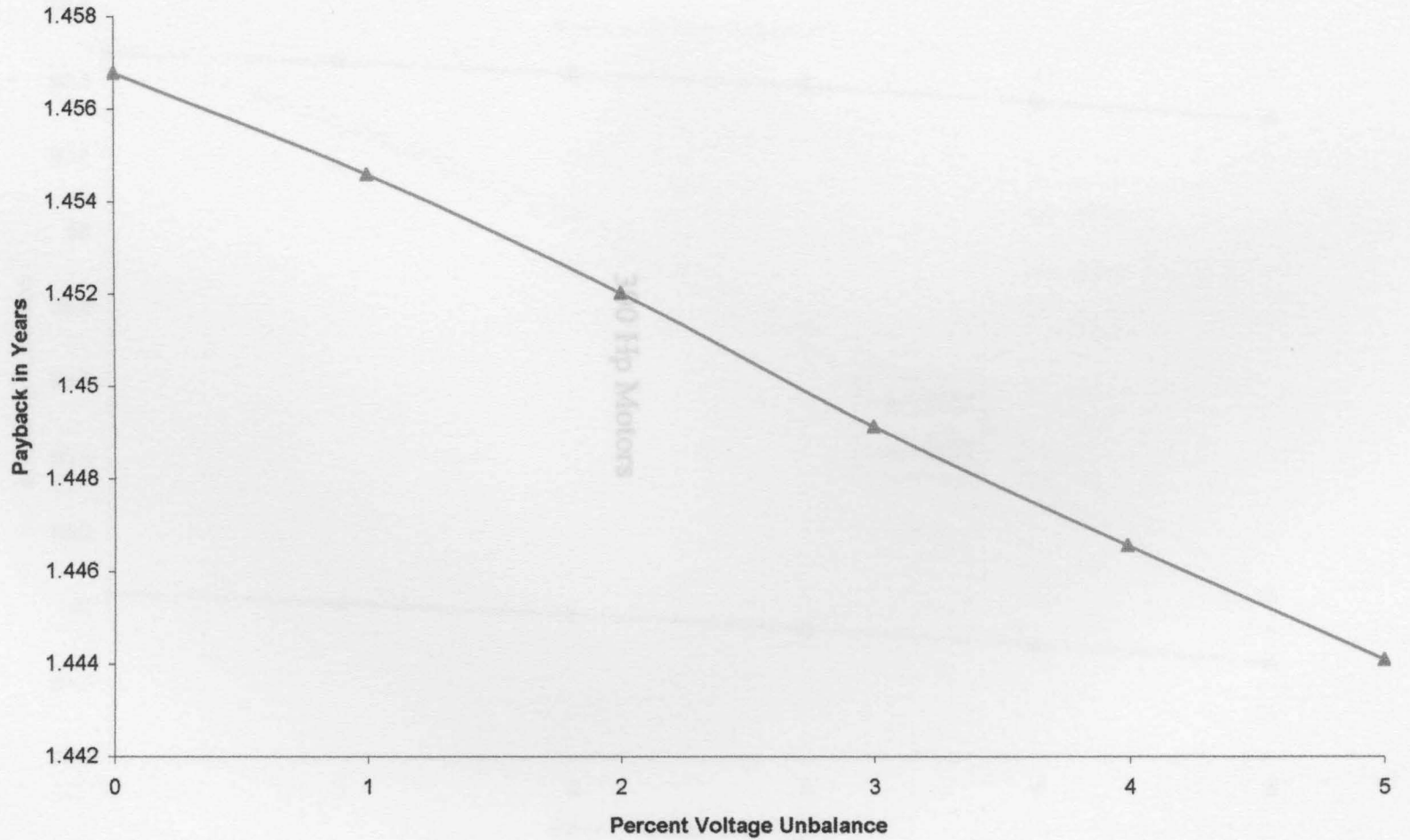
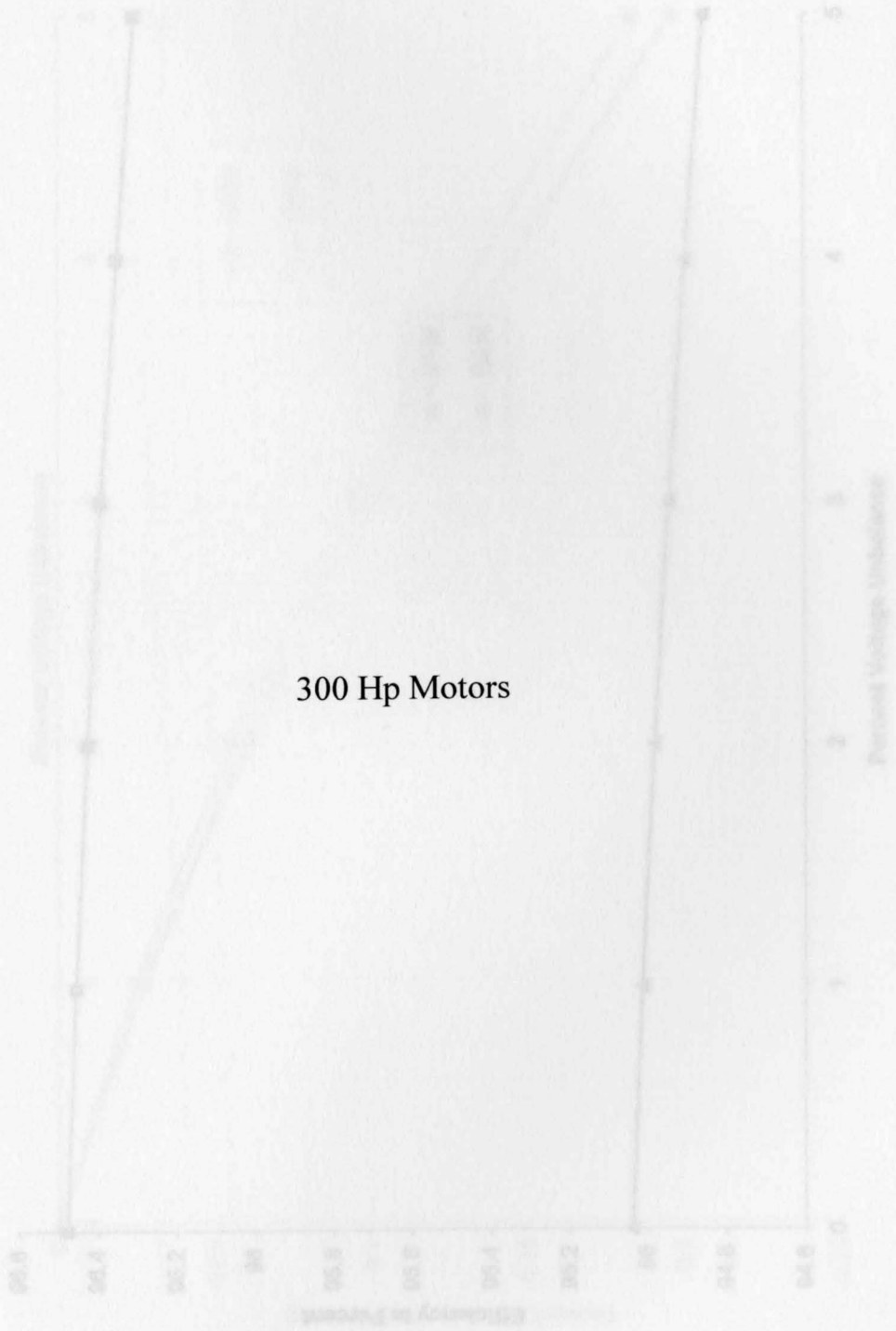


Figure 4.43: Efficiencies for 300 hp STM and EEM vs. Percent Voltage Unbalance



300 Hp Motors

Figure 4.43: Efficiencies for 300 hp STM and EEM vs. Percent Voltage Unbalance

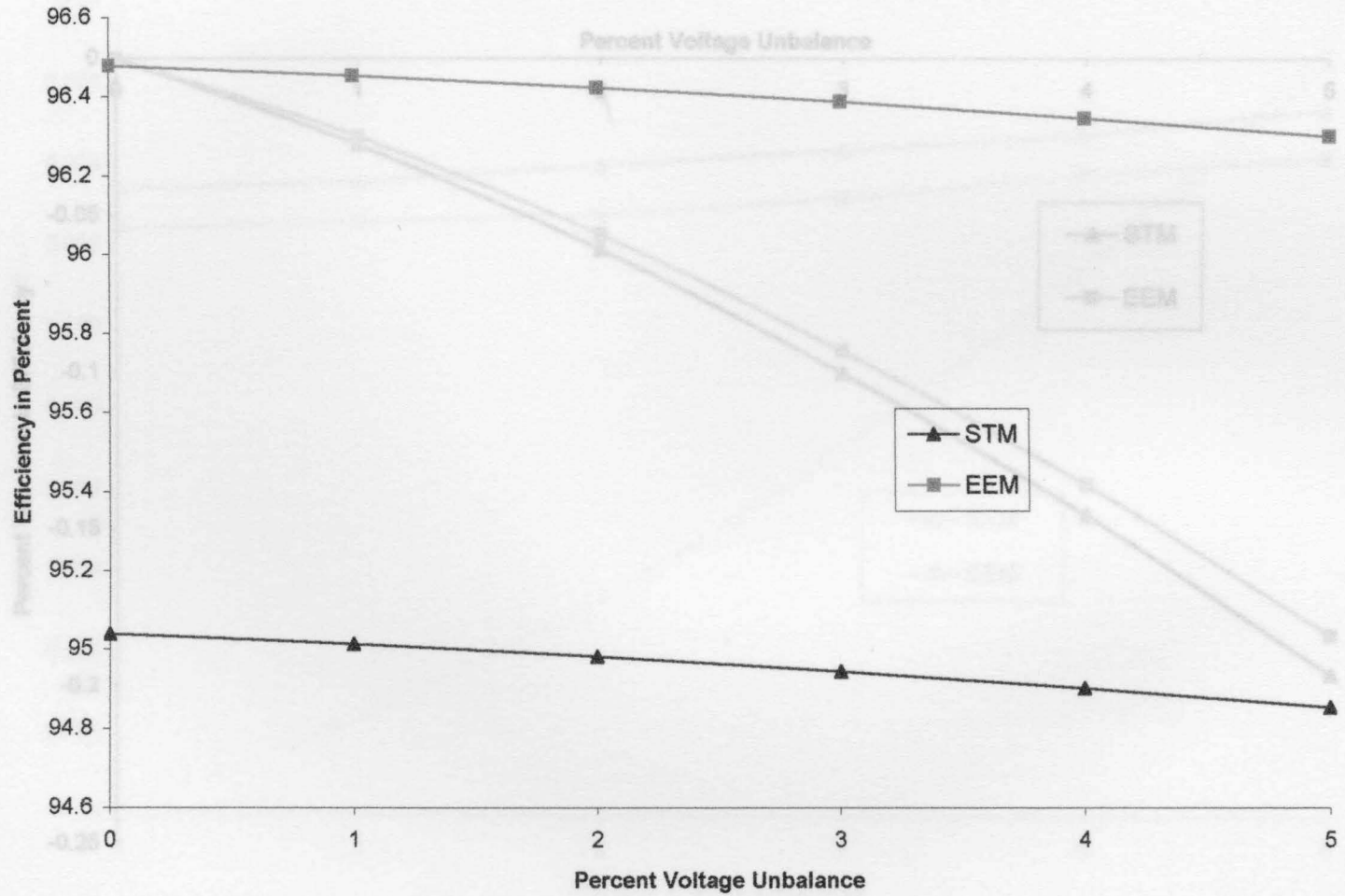


Figure 4.44: Percent Decrease in Efficiencies for 300 hp STM and EEM vs. Percent Voltage Unbalance

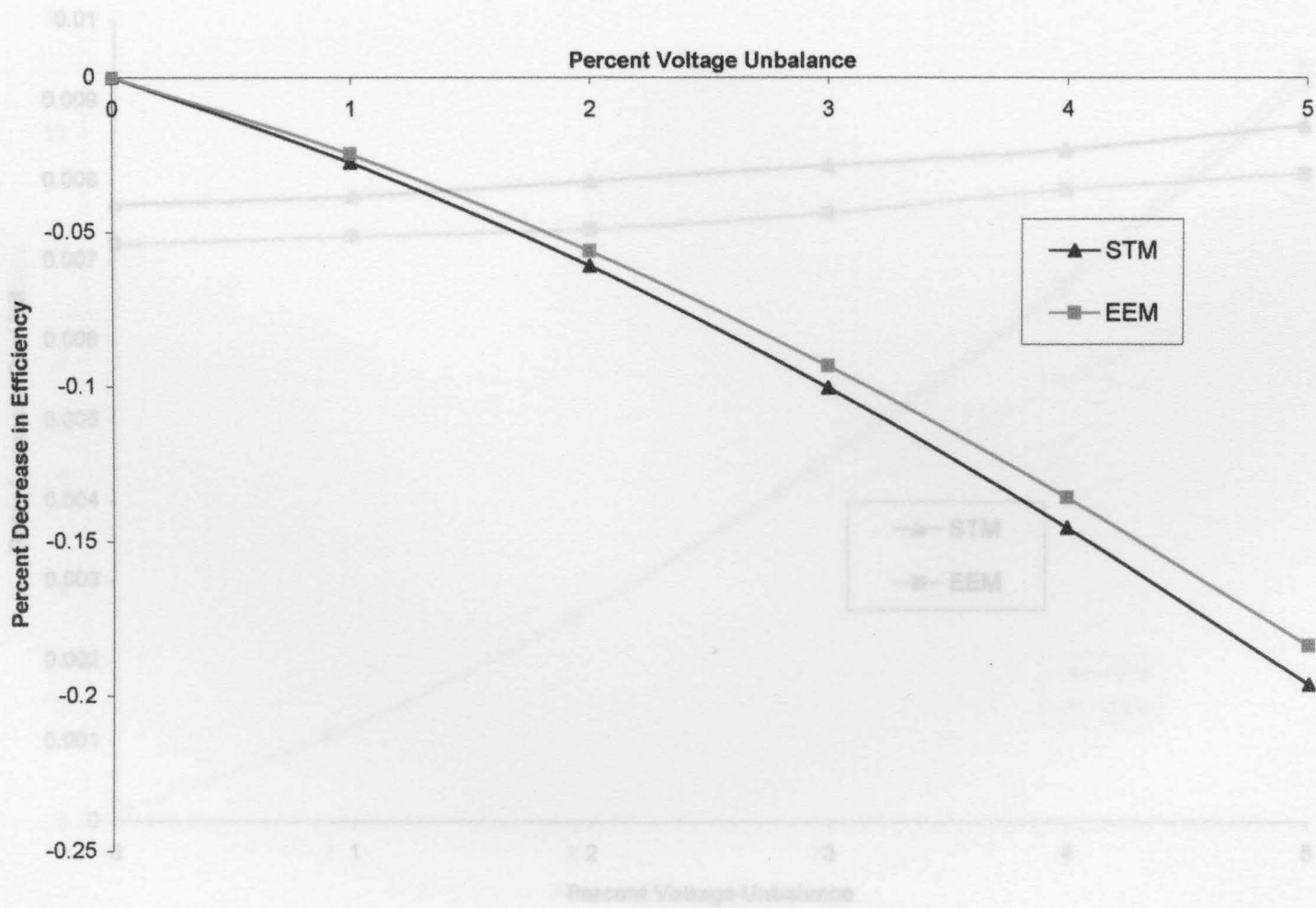


Figure 4.45: Rotor Losses for 300 hp STM and EEM vs. Percent Voltage Unbalance

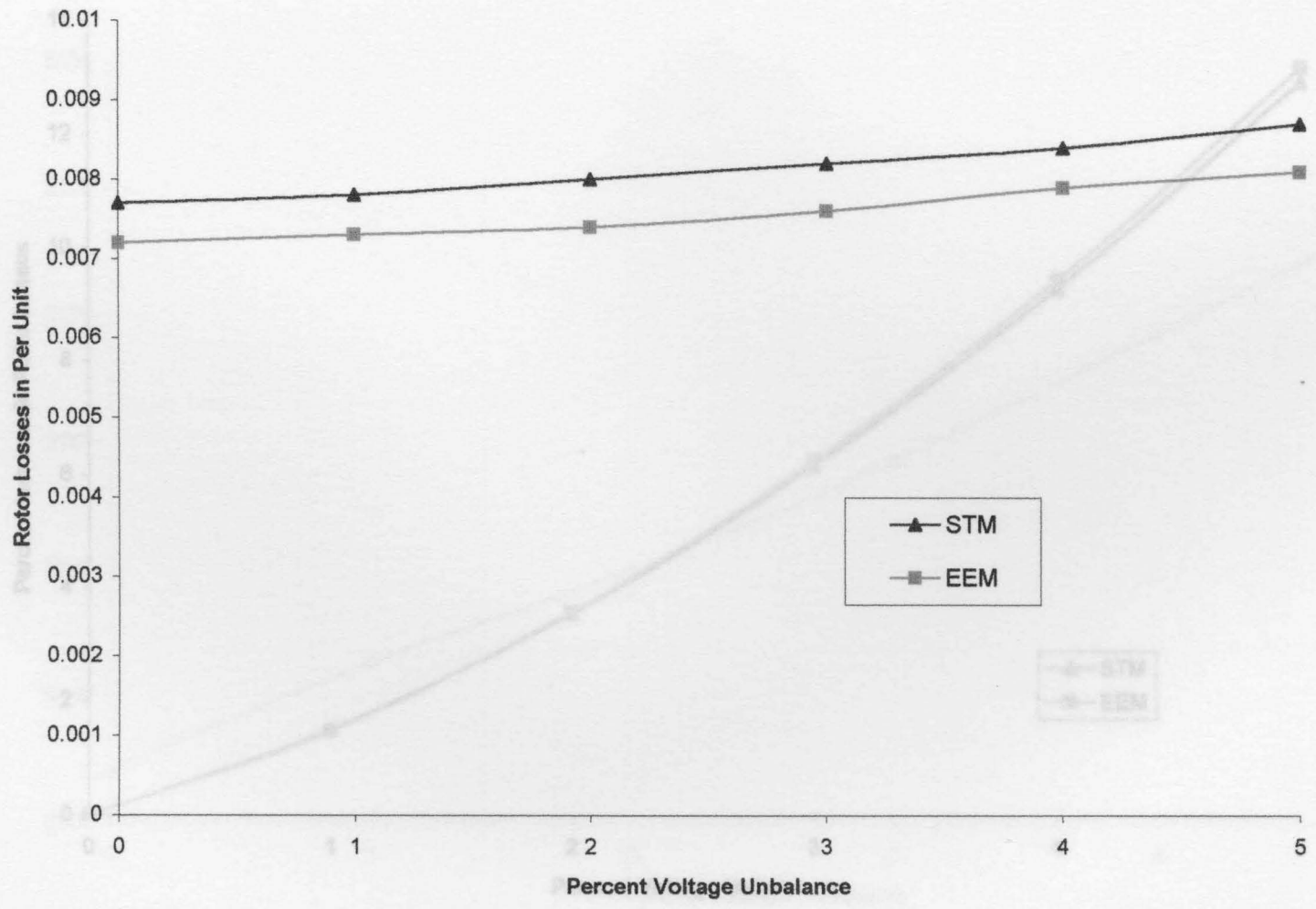


Figure 4.46: Percent Increase in Rotor Losses for 300 hp STM and EEM vs. Percent Voltage Unbalance

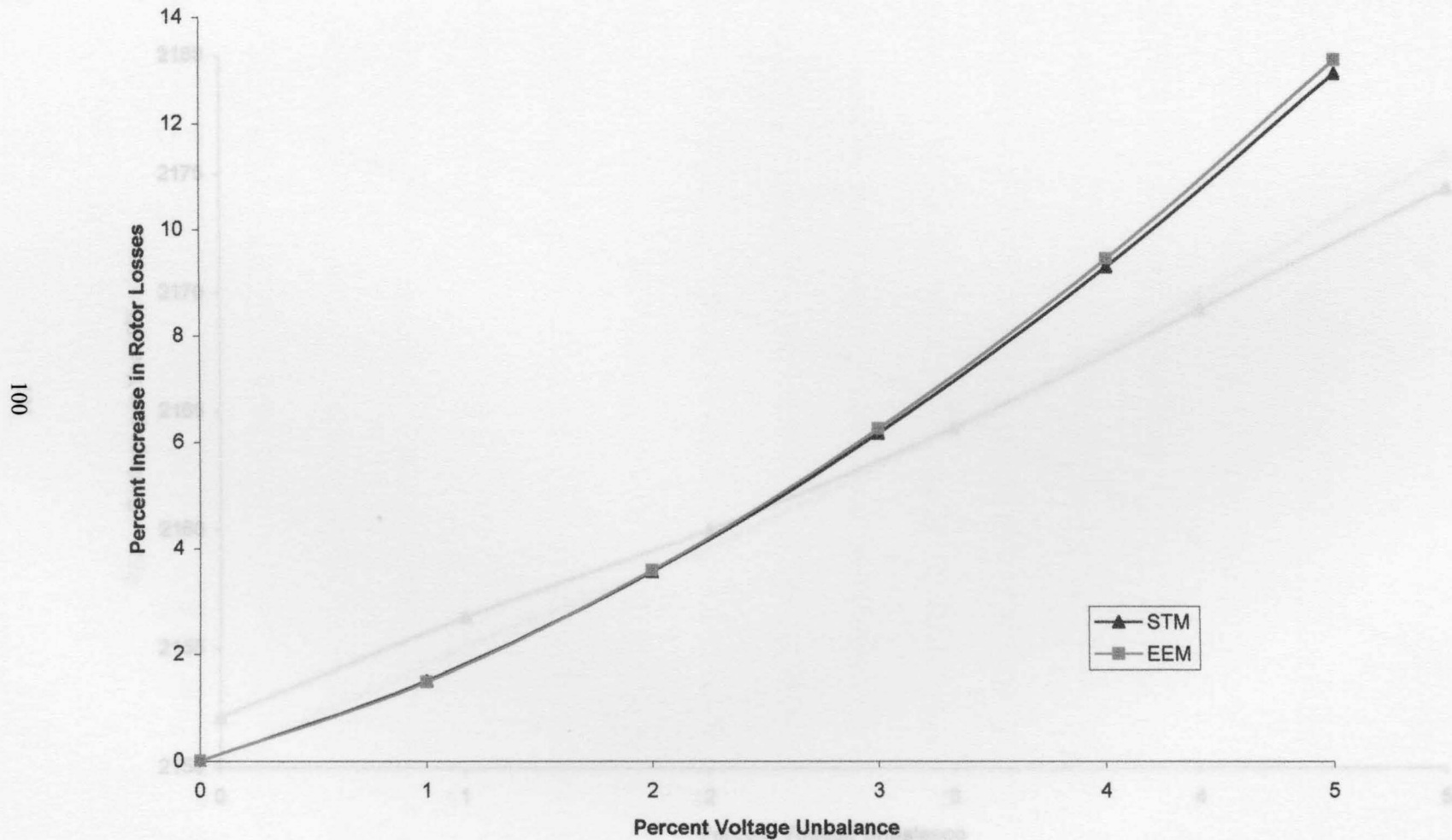


Figure 4.47: Yearly Savings for 300 hp by Using EEM over STM vs. Percent Voltage Unbalance

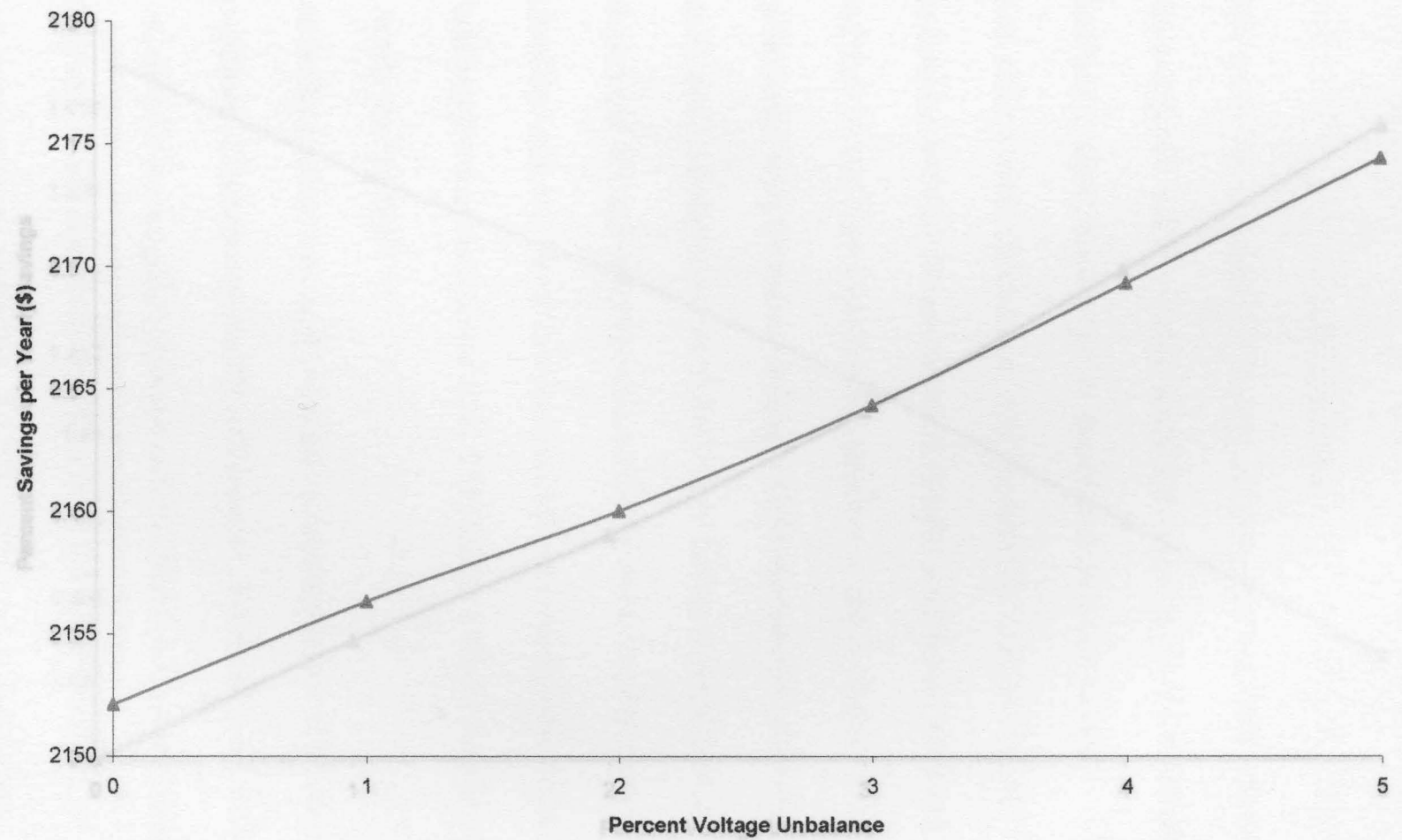


Figure 4.48: Percent Increase in Yearly Savings for 300 hp by Using EEM over STM vs. Percent Voltage Unbalance

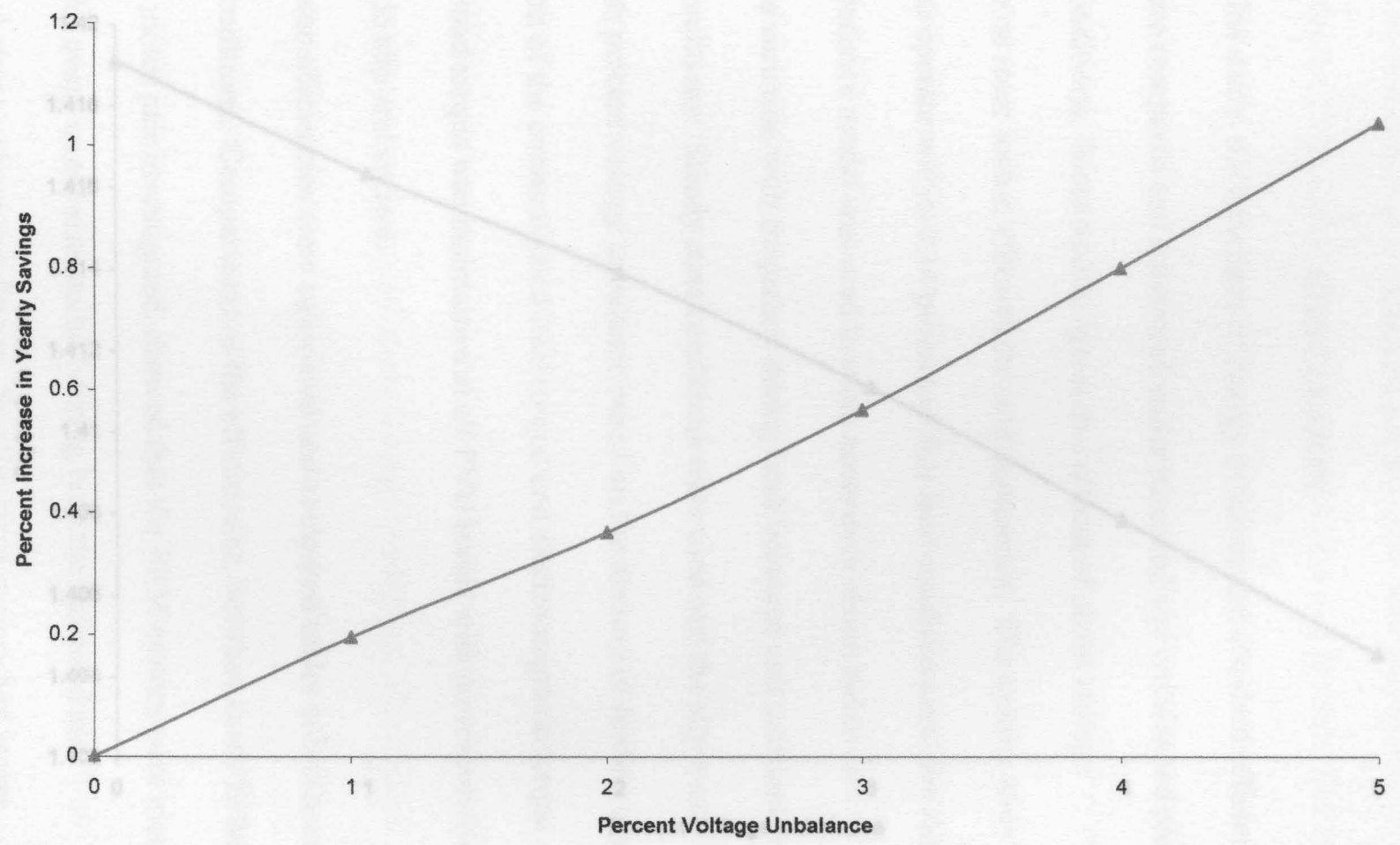
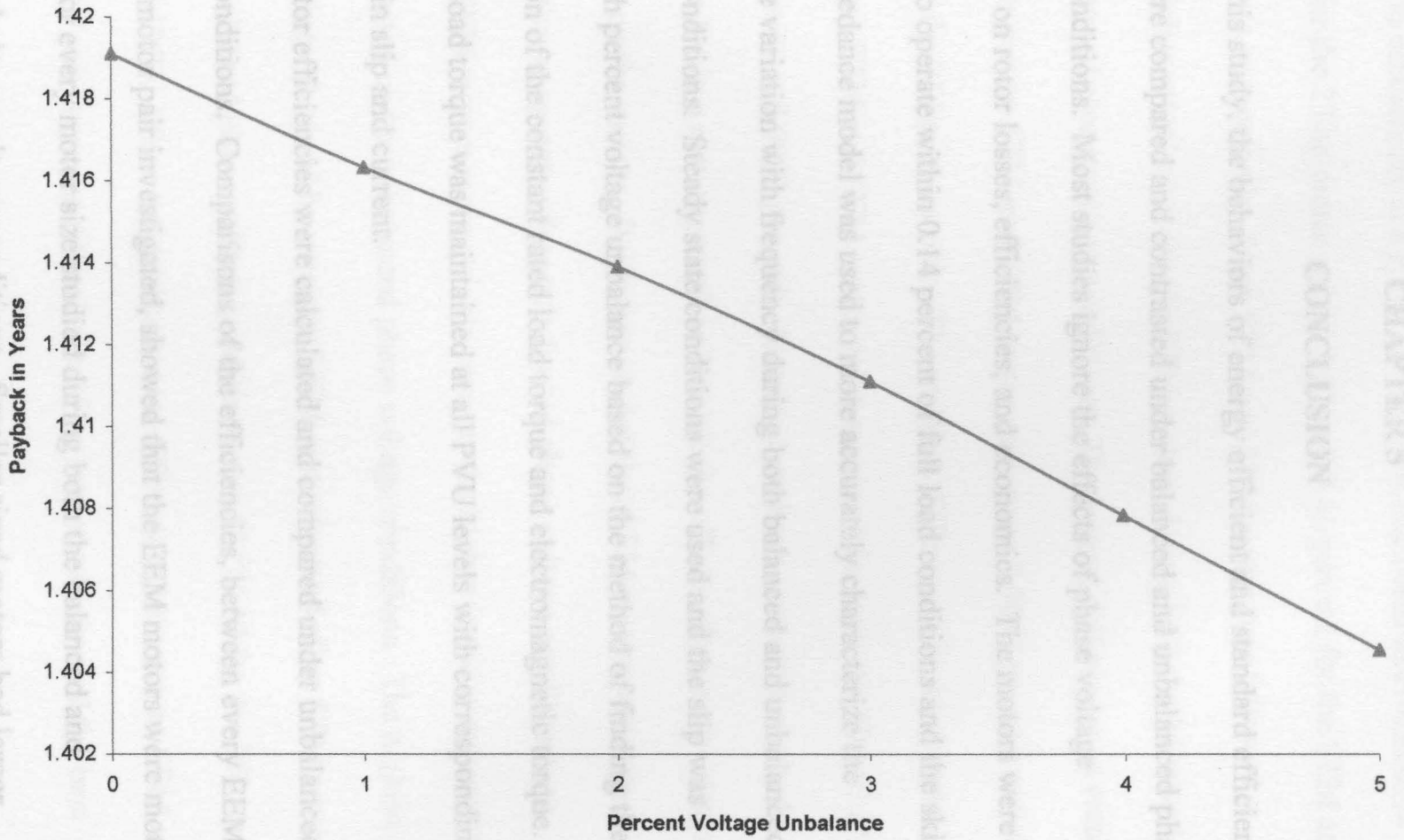


Figure 4.49: Payback Time for 300 hp STM and EEM vs. Percent Voltage Unbalance



CHAPTER 5

CONCLUSION

In this study, the behaviors of energy efficient and standard efficiency motors were compared and contrasted under balanced and unbalanced phase voltage conditions. Most studies ignore the effects of phase voltage unbalance on rotor losses, efficiencies, and economics. The motors were assumed to operate within 0.14 percent of full load conditions and the skin effect impedance model was used to more accurately characterize the impedance variation with frequency during both balanced and unbalanced voltage conditions. Steady state conditions were used and the slip was varied with percent voltage unbalance based on the method of finding the intersection of the constant rated load torque and electromagnetic torque. Constant load torque was maintained at all PVU levels with corresponding increases in slip and current.

Motor efficiencies were calculated and compared under unbalanced voltage conditions. Comparisons of the efficiencies, between every EEM and STM motor pair investigated, showed that the EEM motors were more efficient for every motor size studied during both the balanced and unbalanced phase voltage conditions. Smaller sized motors had larger

decreases in efficiencies at 5 PVU. The largest decreases in efficiencies occurred for the 25 hp motor pair at 0.53 and 0.41 percent for the STM and EEM motors, respectively. Each STM and EEM motor pair followed a trend of higher rotor losses for the STM motors during both the balanced and unbalanced phase voltage conditions. The largest differences in rotor losses, between an STM and EEM motor pair, were 0.0047 per unit at 0 and 5 PVU for the 25 hp motor pair. The smallest differences in rotor losses, between any STM and EEM motor pairs, occurred for both the 50 and 250 hp motor pairs at 0.0003 per unit. Standard payback economic methods were extended in a new approach to include the effects of percent voltage unbalance on the motors. It was concluded that EEM motors are even more cost effective to operate when unbalanced phase voltage conditions are present. EEM motors more quickly recover the higher initial purchase costs when operated under unbalanced phase voltage conditions. The highest yearly savings obtained by using an EEM motor instead of an STM motor under unbalanced phase voltage conditions was \$2271.40 for the 250 hp motor at 5 PVU. When the purchase cost differences between an EEM and STM motor pair were considered, the 25 hp motor pair showed the best

incentive for using an EEM motor because it had the shortest payback recovery times of only 1.21 and 1.15 years at 0 and 5 PVU, respectively.

1. ...
2. ...
3. ...
4. ...
5. ...

WORKS CITED

1. ...
2. ...
3. ...
4. ...
5. ...
6. ...
7. ...
8. ...

1. Eltom, Ahmed H. Induction Motor behavior During Single Phase To Ground Fault. M.S. Thesis, Potsdam, NY: Clarkson College of Technology, March 1982.
 2. Brown, D. and Hamilton, E. P. Electromechanical Energy Conversion. NY: Macmillan Publishing Company, 1984.
 3. Fitzgerald, A. E., Kingsley, C. and Umans, S. D. Electric Machinery 4th Edition, NY: McGraw-Hill, Inc., 1983.
 4. Jordan, E. Howard. Energy Efficient Electric Motors and Their Applications. 2nd Edition, NY: Plenum Press, 1994.
 5. Ormeyer, T.H. Analysis of Induction Machine Dynamics During Power System Unbalance. M.S. Thesis, Ames, IA: Iowa State University, 1980.
- WORKS CITED**
6. Moharari, Nader S. Microprocessor Based Protection Of Induction Motors, Using Thermal, Mechanical, And Skin Effect Electrical Models To Predict Motor Temperature Rise. M.S. Thesis, TN: University of Tennessee at Chattanooga, 1989.
 7. Abazid, Ziad Y. Effect of Voltage Unbalance on the Performance and on the Economic Evaluation of Energy Efficient Motors. M.S. Thesis, TN: University of Tennessee at Chattanooga, 1994.

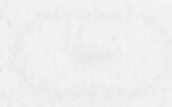
1. Eltom, Ahmed H. Induction Motor behavior During Single Phase To Ground Fault. M.S. Thesis, Potsdam, NY: Clarkson College of Technology, March 1982.
2. Brown, D. and Hamilton, E. P. Electromechanical Energy Conversion. NY: Macmillan Publishing Company, 1984.
3. Fitzgerald, A. E., Kingsley, C. and Umans, S. D. Electric Machinery. 4th Edition, NY: McGraw-Hill, Inc., 1983.
4. Jordan, E. Howard. Energy Efficient Electric Motors and Their Applications. 2nd Edition, NY: Plenum Press, 1994.
5. Ortmeyer, T. H. Analysis of Induction Machine Dynamics During Power System Unbalance. Ph.D Dissertation, Ames, IA: Iowa State University, 1980.
6. Moharari, Nader S. Microprocessor Based Protection Of Induction Motors, Using Thermal, Mechanical, And Skin Effect Electrical Models To Predict Motor Temperature Rise. M.S. Thesis, TN: University of Tennessee at Chattanooga, 1989.
7. Abazid, Ziad Y. Effect of Voltage Unbalance on the Performance and on the Economic Evaluation of Energy Efficient Motors. M.S. Thesis, TN: University of Tennessee at Chattanooga, 1994.

8. Alibakhshi, Aliashraf. Rotor Bar Design, A New Approach To Improve Motor Efficiency. M.S. Thesis, TN: University of Tennessee at Chattanooga, 1989.
9. Eltom, Ahmed. H. and Sadanandan, N. D. Energy Efficient Motors Reference Guide. TN: Tennessee Valley Authority, 1992.
10. Andreas, John C. Energy Efficient Electric Motors Selection and Application. NY: Marcel Dekker, Inc., 1992.
11. Nasar, S. A. and Unnewehr, L. E. Electromechanics and Electric Machines. NY: John Wiley and Sons, 1979.
12. Babb, D. S. and Williams, J. E. Circuit Analysis Method for Determination of A-C Impedances of Machine Conductors. Transactions AIEE Vol. 70, 1951, pp. 661-666.
13. Kueck, John D., Casada, D. A., and Otaduy A Comparison of Two Energy Efficient Motors. IEEE Transactions on Energy Conversion, Vol. 13, No. 2, June 1998, pp. 140-147.
14. Zocholl, Stanley E., Schweitzer III, Edmund O. and Aliaga-Zegarra, Antenor. Thermal Protection of Induction Motors Enhanced by Interactive Electrical and Thermal Models. IEEE Transactions on Power Apparatus and Systems, Vol. PAS-103, No. 7, July 1984, pp. 1749-1755.

15. Bonnet, Austin H. Reliability Comparison Between Standard and Energy Efficient Motors. 1995 IEEE Petroleum and Chemical Industry Technical Conference, pp. 83-90.
16. Montgomery, David C. The Motor Rewind Issue--A New Look. IEEE Transactions on Industry Applications, Vol. 1A-20, No. 5, September/October 1984, pp. 1330-1336.
17. Cummings, Paul B., Dunki-Jacobs, John R. and Kerr, Robert H. Protection of Induction Motors Against Unbalanced Voltage Operation. IEEE Transactions on Industry Applications, Vol. 1A-21, No. 4, May/June 1985, pp. 778-792.
18. Gafford, B. N., Duesterhoeft Jr., W. C. and Mosher III, C. C. Heating of Induction Motors on Unbalanced Voltages. AIEE Transactions, June 1959, pp. 282-287.
19. Woll, R. F. Effect of Unbalanced Voltage on the Operation of Polyphase Induction Motors. IEEE Transactions on Industry Applications, Vol. 1A-11, No. 1, January/February 1975, pp. 39-42.
20. Gleason, Lyle L. and Elmore, W. A. Protection of 3-Phase Motors Against Single-Phase Operation. Transactions AIEE, Part III, Vol. 77, December 1958, pp. 1112-1119.

21. Westinghouse. Electrical Transmission and Distribution Reference Book. Westinghouse, 1964, pp. 12-31.
22. McCoy, Gilbert A., Litman, Todd, and Douglass, John G. Energy Efficient Electric Motor Selection Handbook. U. S. Department of Energy, January 1993.
23. Scheihing, Paul E. Office of Industrial Technologies. U. S. Department of Energy, 1996.

APPENDICES
APPENDICES



Step 1

Step 2

Step 3

Step 4

Step 5

Step 6

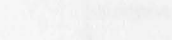
Step 7

Step 8

Step 9

APPENDIX A APPENDICES

Program Flow Chart and Program Listing



Step 1

Step 2

Step 3

Step 4

Step 5

Step 6

Step 7

Step 8

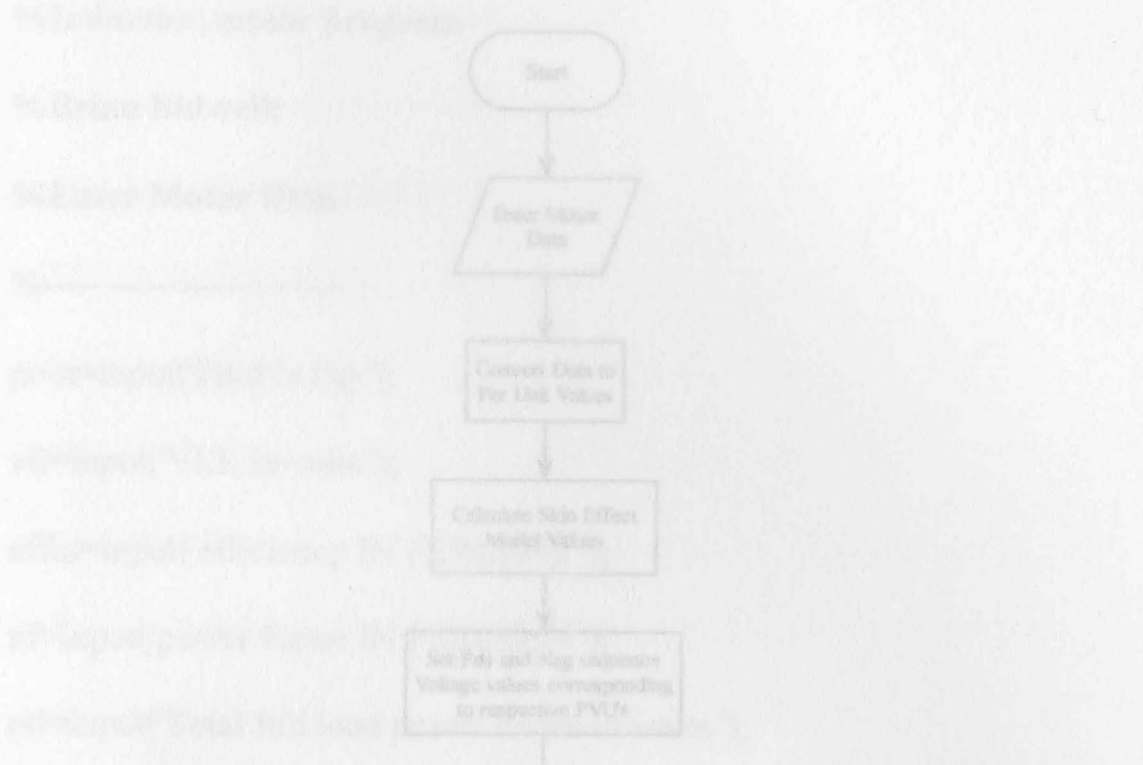
Step 9

Appendix A
Program Listing

Appendix B
Program Listing

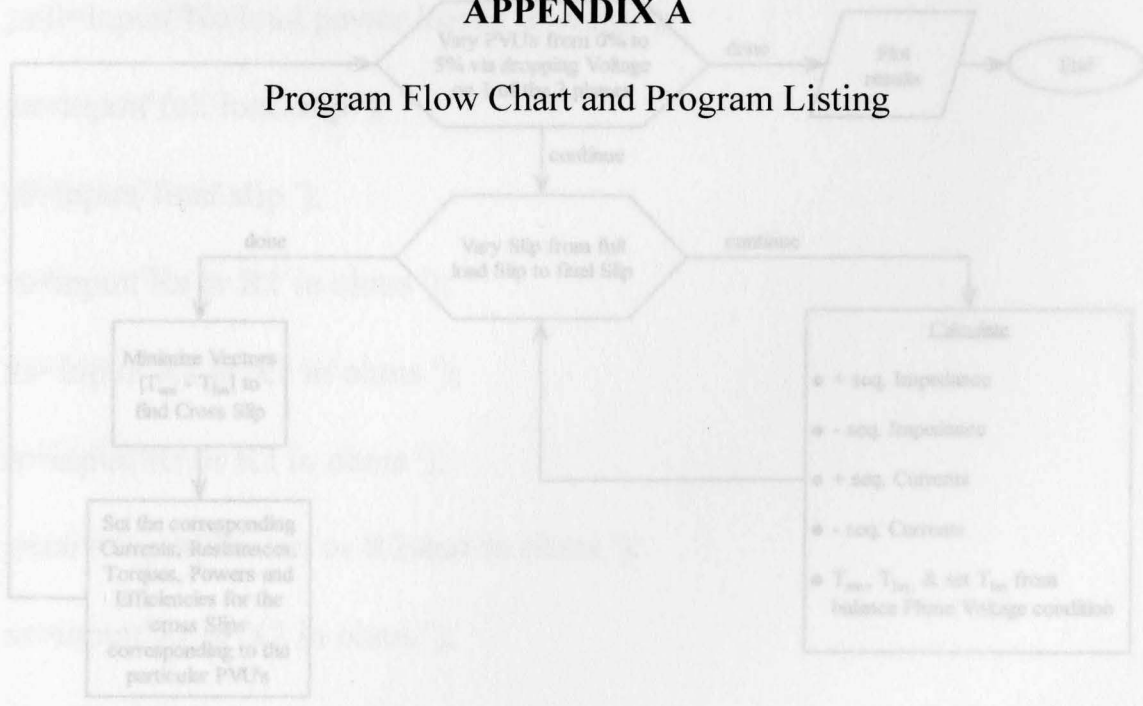
Appendix C
Program Listing

Manfaat M-File Motor Flow Chart

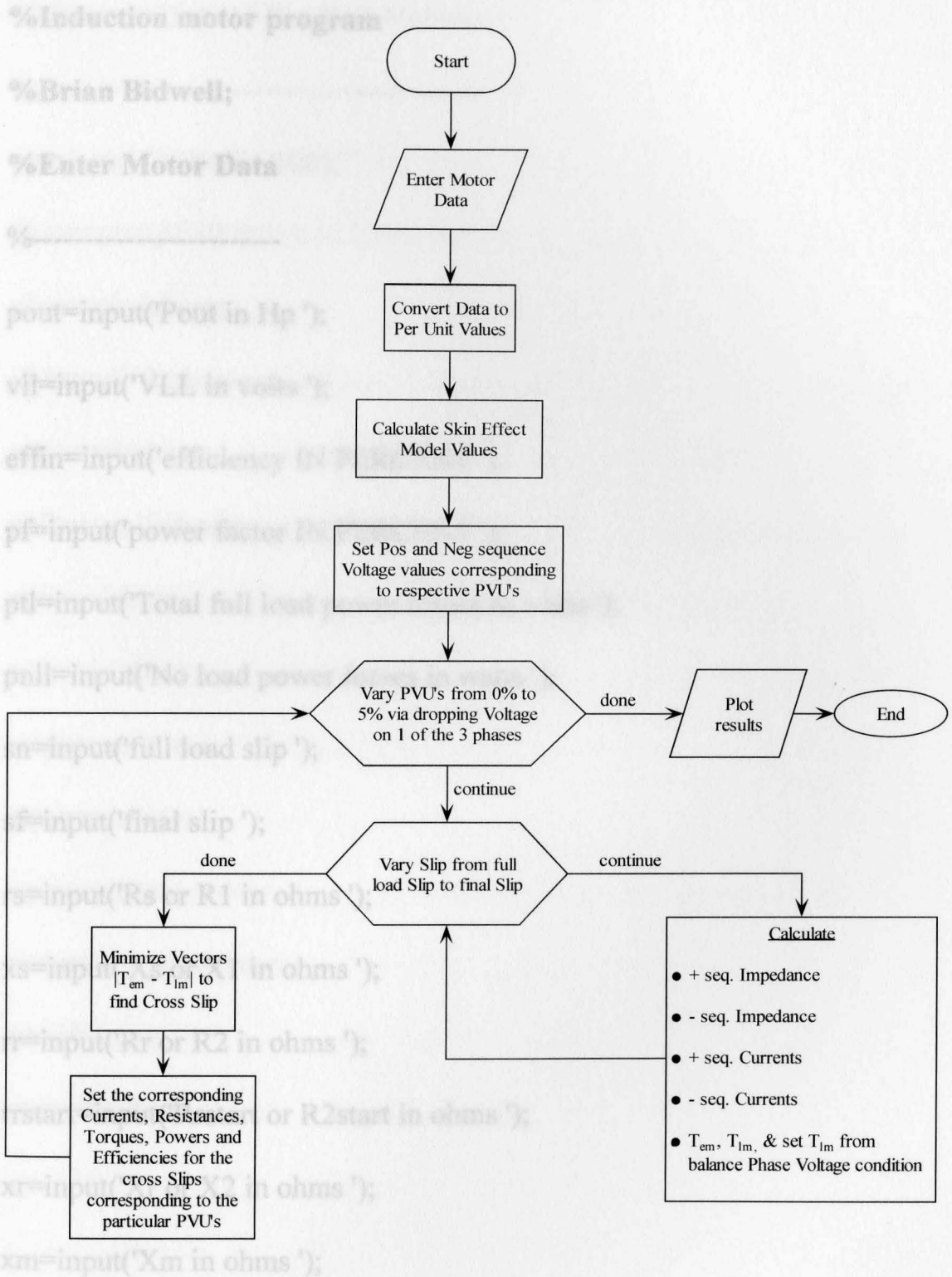


APPENDIX A

Program Flow Chart and Program Listing



Matlab M-file Motor Flow Chart



PROGRAM LISTING

%Induction motor program

%Brian Bidwell;

%Enter Motor Data

%-----

pout=input('Pout in Hp ');

vll=input('VLL in volts ');

effin=input('efficiency IN PERCENT ');

pf=input('power factor IN PERCENT ');

ptl=input('Total full load power losses in watts ');

pnll=input('No load power losses in watts ');

sn=input('full load slip ');

sf=input('final slip ');

rs=input('Rs or R1 in ohms ');

xs=input('Xs or X1 in ohms ');

rr=input('Rr or R2 in ohms ');

rrstart=input('Rrstart or R2start in ohms ');

xr=input('Xr or X2 in ohms ');

xm=input('Xm in ohms ');

PROGRAM LISTING

%Convert Data to Per Unit Values

%-----

pin=pout*746/(effin/100);

pbase=pin/(pf/100);

pinpu=pin/pbase;

zbase=vll^2/pbase;

ptlpu=ptl/pbase;

pnllpu=pnll/pbase;

rspu=rs/zbase;

xspu=xs/zbase;

xmpu=xm/zbase;

xrpu=xr/zbase;

rrpu=rr/zbase;

rrstartpu=rrstart/zbase;

zm=j*xmpu;

zs=rspu+j*xspu;

l4=lll*0.4;

x(1)=xg+l1/2;

PROGRAM LISTING

%Calculate Skin Effect Model Values

%-----

$rrnegpu = (rrstartpu - rrupu) * (2 - sn) + rrupu;$

%Internal Inductance of Rotor bar lli corresponding to respective

$lli = rrnegpu^2 / rrupu;$

%External Inductance(Gap) of Rotor bar xg -----

$xg = xrpu - lli / 3;$

%Rotor resitances

$r(1) = rrupu / 0.1;$

$r(2) = rrupu / 0.2;$

$r(3) = rrupu / 0.3;$

$r(4) = rrupu / 0.4;$

%Rotor Inductances % to 5% via dropping Voltage on 1 of the 3

$l1 = lli * 0.1;$

$l2 = lli * 0.2;$

$l3 = lli * 0.3;$

$l4 = lli * 0.4;$

$x(1) = xg + l1 / 2;$

PROGRAM LISTING

```
x(2)=11/2+12/2;
x(3)=12/2+13/2;
x(4)=13/2+14/2;

%Set + and - sequence Voltage values corresponding to respective
%PVU's
%-----
%vvar=[1 .9850746 .9702970 .9556650 .9411765 .9268293 ]
vpos=[1.000000000000000 0.995024866666667 0.990099000000000
0.985221666666667 0.980392166666667 0.975609766666667];
vneg=[0 -0.004975133333333 -0.009901000000000 -0.014778333333333 -
0.019607833333333 -0.024390233333333 ];
pvu=[0 1 2 3 4 5];
%Vary PVU's from 0% to 5% via dropping Voltage on 1 of the 3
%phases
%-----
for m=1:6;
ru=1;
end
```

PROGRAM LISTING

% Vary Slip from full load Slip to final Slip

%-----

for s=sn:0.000001:sf;

% Calculate--positive sequence Impedance

%-----

zp(4)=r(4)/s+j*x(4);

for k=3:-1:1;

zp(k)=(zp(k+1)*r(k)/s)/(zp(k+1)+r(k)/s)+j*x(k);

end

zrpeq=zp(1);

rrpeqt(ru)=real(zp(1))*s;

zpt=zs+zm*zrpeq/(zm+zrpeq);

% Calculate--negative sequence Impedance

%-----

zn(4)=r(4)/(2-s)+j*x(4);

for k=3:-1:1;

zn(k)=(zn(k+1)*r(k)/(2-s))/(zn(k+1)+r(k)/(2-s))+j*x(k);

end

PROGRAM LISTING

```
zrneq=zn(1);
```

```
rrneqt(ru)=real(zn(1))*(2-s);
```

```
znt=zs+zm*zrneq/(zm+zrneq);
```

```
%Calculate--positive sequence Current
```

```
%-----
```

```
ispt(ru)=abs(vpos(m)/zpt);
```

```
irpt(ru)=ispt(ru)*abs(zm/(zrpeq+zm));
```

```
%Calculate--negative sequence Current
```

```
%-----
```

```
isnt(ru)=abs(vneg(m)/znt);
```

```
irnt(ru)=isnt(ru)*abs(zm/(zrneq+zm));
```

```
%Calculate-Torques
```

```
%-----
```

```
%Electromagnetic Torque--Tem
```

```
tempt(ru)=(rrpeqt(ru)/s)*irpt(ru)^2;
```

```
temnt(ru)=(rrneqt(ru)/(2-s))*irnt(ru)^2;
```

```
temt(ru)=tempt(ru)-temnt(ru);
```

```
slip(ru)=s;
```

PROGRAM LISTING

```
if m==1,
tout=temt(1);
end
%Constant Torque Tlm
tlmt(ru)=tout;
ru=ru+1;
end
%Minimize Vectors |Tem-Tlm| to find cross Slip
%-----
[yu, ju]=min(abs(temt-tlmt));
%Set the corresponding values for cross Slips corresponding with
%PVU's:
%-----
%Currents
irp(m)=irpt(ju);
irn(m)=irnt(ju);
isp(m)=ispt(ju);
isn(m)=isnt(ju);
```


PROGRAM LISTING

%Resistances

```
rrpeq(m)=rrpeqt(ju);
```

```
rrneq(m)=rrneqt(ju);
```

%Torques

```
temp(m)=tempt(ju);
```

```
temn(m)=temnt(ju);
```

```
tem(m)=temt(ju);
```

```
tlm(m)=tlmt(ju);
```

%Slip

```
sit(m)=slip(ju);
```

%Powers

```
psp(m)=rspu*isp(m)^2;
```

```
psn(m)=rspu*isn(m)^2;
```

```
prp(m)=rrpeq(m)*irp(m)^2;
```

```
prn(m)=rrneq(m)*irn(m)^2;
```

```
ps(m)=psp(m)+psn(m);
```

```
pr(m)=prp(m)+prn(m);
```

```
pstraypu=ptlpu-ps(1)-pr(1)-pnllpu;
```

PROGRAM LISTING

```
ploss(m)=ps(m)+pr(m)+pstraypu+pnllpu;
```

```
princ(m)=(pr(m)-pr(1))*100/pr(1);
```

%Efficiencies

```
eff(m)=tout*(1-sit(1))*100/((tout*(1-sit(1)))+ploss(m));
```

```
deceff(m)=((eff(m)-eff(1))/eff(1))*100;
```

```
end
```

%Plot results

```
%-----
```

```
plot(pvu, eff),title('eff'), xlabel('PVU'),ylabel('%');
```

```
figure;
```

```
plot(pvu, deceff),title('deceff'),xlabel('PVU'),ylabel('%');
```

```
figure;
```

```
plot(pvu, pr), title('pr'),xlabel('PVU'),ylabel('P.U.');
```

```
figure;
```

```
plot(pvu, princ),title('princ'),xlabel('PVU'),ylabel('%');
```

25 hp EEM and STM parameters

GENERAL DATA

Horse power	25
SPEED	1800 RPM Synchronous
Voltage	480 v, 3 phase, 60 Hz
Motor Purchase Cost	\$207.35(STM), \$1308.31(EEM)

Electrical Model Data for STM and EEM

	STM(P.U.)	EEM(P.U.)
Stator:		
R_s	0.0342	0.0246
X_s	0.1063	0.1122
Rotor:		
R_r	0.0189	0.0139
X_r	0.1498	0.1787
Mutual:		
X_m	4.0682	3.4275
Slip:	0.0194	0.014
R_l	0.1889	0.1391

APPENDIX B

Motor Data

R2: 0.094 TABLE B.1 0.0695

R3: 25 hp EEM and STM parameters 0.0164

GENERAL DATA

Horse power

0.0115 :25

0.03144

SPEED

0.0345 :1800 RPM Synchronous

Voltage

0.0574 :460 v, 3 phase, 60 Hz

Motor Purchase Cost

0.0804 :\$887.35(STM), \$1308.31(EEM)

Electrical Model Data for STM and EEM

STM(P.U.)

EEM(P.U.)

Stator:

R_s

0.0342

0.0246

X_s

0.1063

0.1122

Rotor:

R_r

0.0189

0.0139

X_r

0.1498

0.1787

Mutual:

X_m

4.0682

3.4275

Slip:

0.0194

0.014

R1:

0.1889

0.1391

R2:	0.0945	0.0695
R3:	0.063	0.0464
R4:	0.0472	0.0348
X1:	0.0115	0.02144
X2:	0.0345	0.0643
X3:	0.0574	0.1072
X4:	0.0804	0.1501

Electrical Model Data for STM and EEM

	STM(P.U.)	EEM(P.U.)
Stator:		
R_s	0.027	0.0239
X_s	0.1152	0.1097
Rotor:		
R_r	0.014	0.0138
X_r	0.1723	0.1665
Mutual:		
X_m	4.3753	4.0697
Slip:	0.0144	0.014
R1:	0.1398	0.1375

TABLE B.2**50hp EEM and STM parameters****GENERAL DATA**

Horse power	:50
SPEED	:1800 RPM Synchronous
Voltage	:460 v, 3 phase, 60 Hz
Motor Purchase Cost	:\$1680.50(STM), \$3889.40(EEM)

Electrical Model Data for STM and EEM

	STM(P.U.)	EEM(P.U.)
Stator:		
R_s	0.027	0.0239
X_s	0.1152	0.1097
Rotor:		
R_r	0.014	0.0138
X_r	0.1723	0.1665
Mutual:		
X_m	4.3753	4.0697
Slip:	0.0144	0.014
R_1	0.1398	0.1375

R2:	0.0699	0.0688
R3:	0.0466	0.0458
R4:	0.0349	0.0344
X1:	0.0218	0.0203
X2:	0.0654	0.0608
X3:	0.109	0.1014
X4:	0.1526	0.1419

Electrical Model Data for STM and EEM

	STM(P.U.)	EEM(P.U.)
Stator:		
R_s	0.0148	0.0137
X_s	0.1249	0.113
Rotor:		
R_r	0.0094	0.0087
X_r	0.1482	0.1392
Mutual:		
X_m	3.3892	3.3585
Slip:	0.0094	0.0087
R1:	0.0938	0.0875

TABLE B.3**100 hp EEM and STM parameters****GENERAL DATA**

Horse power	:100
SPEED	:1800 RPM Synchronous
Voltage	:460 v, 3 phase, 60 Hz
Motor Purchase Cost	:\$3889.40(STM), \$5575.41(EEM)

Electrical Model Data for STM and EEM

	STM(P.U.)	EEM(P.U.)
Stator:		
R_s	0.0148	0.0137
X_s	0.1249	0.113
Rotor:		
R_r	0.0094	0.0087
X_r	0.1482	0.1392
Mutual:		
X_m	3.3892	3.3585
Slip:	0.0094	0.0087
R_1	0.0938	0.0875

R2:	0.0469	0.0437
R3:	0.0313	0.0292
R4:	0.0234	0.0219
X1:	0.0184	0.0190
X2:	0.0553	0.0570
X3:	0.0921	0.0949
X4:	0.1289	0.1329

Electrical Model Data for STM and EEM

	STM(P.U.)	EEM(P.U.)
Stator:		
R_s	0.0159	0.0123
X_s	0.1349	0.1187
Rotor:		
R_r	0.0106	0.0092
X_r	0.1511	0.1851
Mutual:		
X_m	4.1832	3.5436
Slip:	0.0309	0.0092
R1:	0.1064	0.0919

TABLE B.4

150 hp EEM and STM parameters

GENERAL DATA

Horse power	:150
SPEED	:1800 RPM Synchronous
Voltage	:460 v, 3 phase, 60 Hz
Motor Purchase Cost	:\$6102.37(STM), \$8532.74(EEM)

Electrical Model Data for STM and EEM

	STM(P.U.)	EEM(P.U.)
Stator:		
R_s	0.0159	0.0123
X_s	0.1349	0.1187
Rotor:		
R_r	0.0106	0.0092
X_r	0.1511	0.1851
Mutual:		
X_m	4.1032	3.5436
Slip:	0.0109	0.0092
R_1	0.1064	0.0919

R2:	0.0532	ABLE B.5	0.046
R3:	0.0355	and STM param	0.0306
R4:	0.0266	GENERAL DATA	0.023
X1:	0.0152	se power	0.0202
X2:	0.0608	ED	0.0404
X3:	0.0912	age	0.0606
X4:	0.1216	or Purchase Cost	0.0808

Electrical Model Data for STM and EEM

	STM(P.U.)	EEM(P.U.)
Stator:		
R_s	0.0137	0.0111
X_s	0.1193	0.1171
Rotor:		
R_r	0.01	0.0093
X_r	0.1504	0.1899
Mutual:		
X_m	4.25	3.8878
Slip:	0.0101	0.0094
R1:	0.0999	0.0933

TABLE B.5**200 hp EEM and STM parameters****GENERAL DATA**

Horse power	:200
SPEED	:1800 RPM Synchronous
Voltage	:460 v, 3 phase, 60 Hz
Motor Purchase Cost	:\$7413.92(STM), \$10,378.57(EEM)

Electrical Model Data for STM and EEM

	STM(P.U.)	EEM(P.U.)
Stator:		
R_s	0.0137	0.0111
X_s	0.1193	0.1171
Rotor:		
R_r	0.01	0.0093
X_r	0.1504	0.1899
Mutual:		
X_m	4.25	3.8878
Slip:	0.0101	0.0094
R_1	0.0999	0.0933

R2:	0.0499	0.0467
R3:	0.0333	0.0311
R4:	0.025	0.0233
X1:	0.0143	0.0103
X2:	0.0429	0.0309
X3:	0.0714	0.0515
X4:	0.1	0.0721

Electrical Model Data for STM and EEM

	STM(P.U.)	EEM(P.U.)
Stator:		
R_s	0.0126	0.0108
X_s	0.1462	0.1331
Rotor:		
R_r	0.0083	0.0079
X_r	0.1425	0.1441
Mutual:		
X_m	4.1623	4.3604
Slip:	0.0085	0.0081
R1:	0.0826	0.0792

R2: 0.041 **TABLE B.6** 0.0396

R3: **250 hp EEM and STM parameters** 0.04

GENERAL DATA

Horse power	0.0134	:250	0.0138
SPEED	0.0401	:1800 RPM Synchronous	
Voltage	0.0667	:460 v, 3 phase, 60 Hz	
Motor Purchase Cost	0.0934	:\$9740.18(STM), \$13,020.27(EEM)	

Electrical Model Data for STM and EEM

	STM(P.U.)	EEM(P.U.)
Stator:		
R_s	0.0126	0.0108
X_s	0.1462	0.1331
Rotor:		
R_r	0.0083	0.0079
X_r	0.1425	0.1441
Mutual:		
X_m	4.1623	4.3604
Slip:	0.0085	0.0081
R1:	0.0826	0.0792

R2:	0.0413	TABLE B.7	0.0396
R3:	0.0275	and STM param	0.0264
R4:	0.0206	GENERAL DATA	0.0198
X1:	0.0134	300	0.0128
X2:	0.0401	1800 RPM	0.0383
X3:	0.0667	460 v, 3 ph	0.0637
X4:	0.0934	\$10,955.54	0.0892
X5:	0.0799	\$14,029.57(EEM)	

Electrical Model Data for STM and EEM

	STM(P.U.)	EEM(P.U.)
Stator:		
R_s	0.0115	0.0104
X_s	0.1396	0.1251
Rotor:		
R_r	0.0086	0.008
X_r	0.1452	0.1466
Mutual:		
X_m	4.5359	4.7147
Slip:	0.0088	0.0082

R1: 0.085 **TABLE B.7** 0.0802

R2: **300 hp EEM and STM parameters** 0.0191

GENERAL DATA 0.0285 0.0267

Horse power 0.0214 :300 0.0201

SPEED 0.0128 :1800 RPM Synchronous

Voltage 0.0383 :460 v, 3 phase, 60 Hz

Motor Purchase Cost 0.0639 :\$10,955.54(STM),

X4: 0.0894 \$14,009.57(EEM) 4

Electrical Model Data for STM and EEM

	STM(P.U.)	EEM(P.U.)
Stator:		
R_s	0.0115	0.0104
X_s	0.1396	0.1251
Rotor:		
R_r :	0.0086	0.008
X_r :	0.1452	0.1466
Mutual:		
X_m :	4.5359	4.7147
Slip:	0.0088	0.0082

R1:	0.0855	0.0802
R2:	0.0428	0.0401
R3:	0.0285	0.0267
R4:	0.0214	0.0201
X1:	0.0128	0.0118
X2:	0.0383	0.0353
X3:	0.0639	0.0588
X4:	0.0894	0.0824

APPENDIX C

Example skin effect parameters calculation using the 25 Hp EEM motor

From Table 1.1.4, the parameters of the 25 Hp motor are listed in the table below. The skin effect parameters are calculated using the following equations. The values are given in the table below. The negative values are given in the table below.

$$R_{1s} = R_1 \left(1 + \frac{1}{2} \left(\frac{f}{f_c} \right)^2 \right)$$

$$R_{2s} = R_2 \left(1 + \frac{1}{2} \left(\frac{f}{f_c} \right)^2 \right)$$

The internal inductance L_{1s} is a function of the diameter of the conductor. The value of L_{1s} is given in the table below.

Motor data for the 25 Hp EEM motor from the manufacturer's data sheet that has been converted to per unit values to provide an illustrative example of the skin effect calculations as conducted in the computer program.

Given motor data for 25 Hp EEM:

$$r_r = 0.0246 \text{ pu,}$$

$$x_s = 0.1122 \text{ pu,}$$

$$x_m = 3.4275 \text{ pu,}$$

$$r_r = 0.0139 \text{ pu,}$$

$$r_{r \text{ start}} = 0.0458 \text{ pu,}$$

$$x_r = 0.1787 \text{ pu,}$$

$$s_0 = 0.014.$$

APPENDIX C

Example skin effect parameters calculation using the 25 Hp EEM motor

From Zocholl's (14) equations of the linear approximation to the rotor bar skin effect, the following equation can be adapted for use here to find the negative rotor resistance value.

$$r_{neg} = (r_{start} - r_r) * (2 - s_0) + r_r \quad (3.1)$$

$$r_{neg} = (0.0458 - 0.0139) * (2 - 0.014) + 0.0139 = 0.0773 \text{ pu.}$$

The internal inductance L_{ii} , that is a function of the current distribution in the rotor bar conductor, is calculated (5).

Motor data for the 25 Hp EEM motor from the manufacturer's data sheet that has been converted to per unit values to provide an illustrative example of the skin effect calculations as conducted in the computer program. (3.3)

Given motor data for 25 Hp EEM:

$$r_s = 0.0246 \text{ pu,}$$

$$x_s = 0.1122 \text{ pu,}$$

$$x_m = 3.4275 \text{ pu,}$$

$$r_r = 0.0139 \text{ pu,}$$

$$r_{r \text{ start}} = 0.0458 \text{ pu,}$$

$$x_r = 0.1787 \text{ pu,}$$

$$s_{fl} = 0.014.$$

From Zocholl's (14) equations of the linear approximation to the rotor bar skin effect, the following equation can be adapted for use here to find the negative rotor resistance value.

$$r_{\text{neg}} = (r_{\text{rstart}} - r_r) * (2 - s_{fl}) + r_r, \quad (3.1)$$

$$r_{\text{neg}} = (0.0458 - 0.0139) * (2 - 0.014) + 0.0139 = 0.0773 \text{ pu.}$$

The internal inductance L_{ii} , that is a function of the current distribution in the rotor bar conductor, is calculated (5).

$$L_{ii} = r_{\text{meg}}^2 / r_r = 0.0773^2 / 0.0139 = 0.4298 \text{ pu.} \quad (3.2)$$

The rotor bar equivalent circuit parameters L_1 , L_2 , L_3 and L_4 that are shown in figure 2.2 can now be calculated.

$$L_1 = L_{ii} * 0.1 = 0.0430 \text{ pu,} \quad (3.3)$$

$$L_2 = L_{ii} * 0.2 = 0.086 \text{ pu,}$$

$$L_3 = L_{ii} * 0.3 = 0.1289 \text{ pu,}$$

$$L_4 = L_{ii} * 0.4 = 0.1719 \text{ pu.}$$

The external inductance x_{gap} is a function of the geometry of the circuit and the materials involved and is not a function of the currents flowing in the rotor bar conductor (5).

$$x_{\text{gap}} = x_r - L_{ii} / 3 = 0.1787 - 0.4298 / 3 = 0.0354 \text{ pu.} \quad (3.4)$$

The parameters of figures 2.3 and 2.4 showing the impedance models for the positive and negative sequences, respectively, can be found. Summing the inductances based on the methods of Babb and Willams (12) and others (1, 5) yields the following.

$$x_1 = x_{\text{gap}} + L_1 / 2 = 0.0354 + 0.0430 / 2 = 0.0569 \text{ pu,} \quad (3.5)$$

$$x_2 = L_1 / 2 + L_2 / 2 = 0.0430 / 2 + 0.086 / 2 = 0.0645 \text{ pu,}$$

$$x_3 = L_2 / 2 + L_3 / 2 = 0.086 / 2 + 0.1289 / 2 = 0.1075 \text{ pu,}$$

$$x_4 = L_3 / 2 + L_4 / 2 = 0.1289 / 2 + 0.1719 / 2 = 0.1504 \text{ pu.}$$

The constant resistance values that apply to figures 2.2, 2.3 and 2.4 are calculated.

$$R_1 = r_r / 0.1 = 0.0139 / 0.1 = 0.1390, \quad (3.6)$$

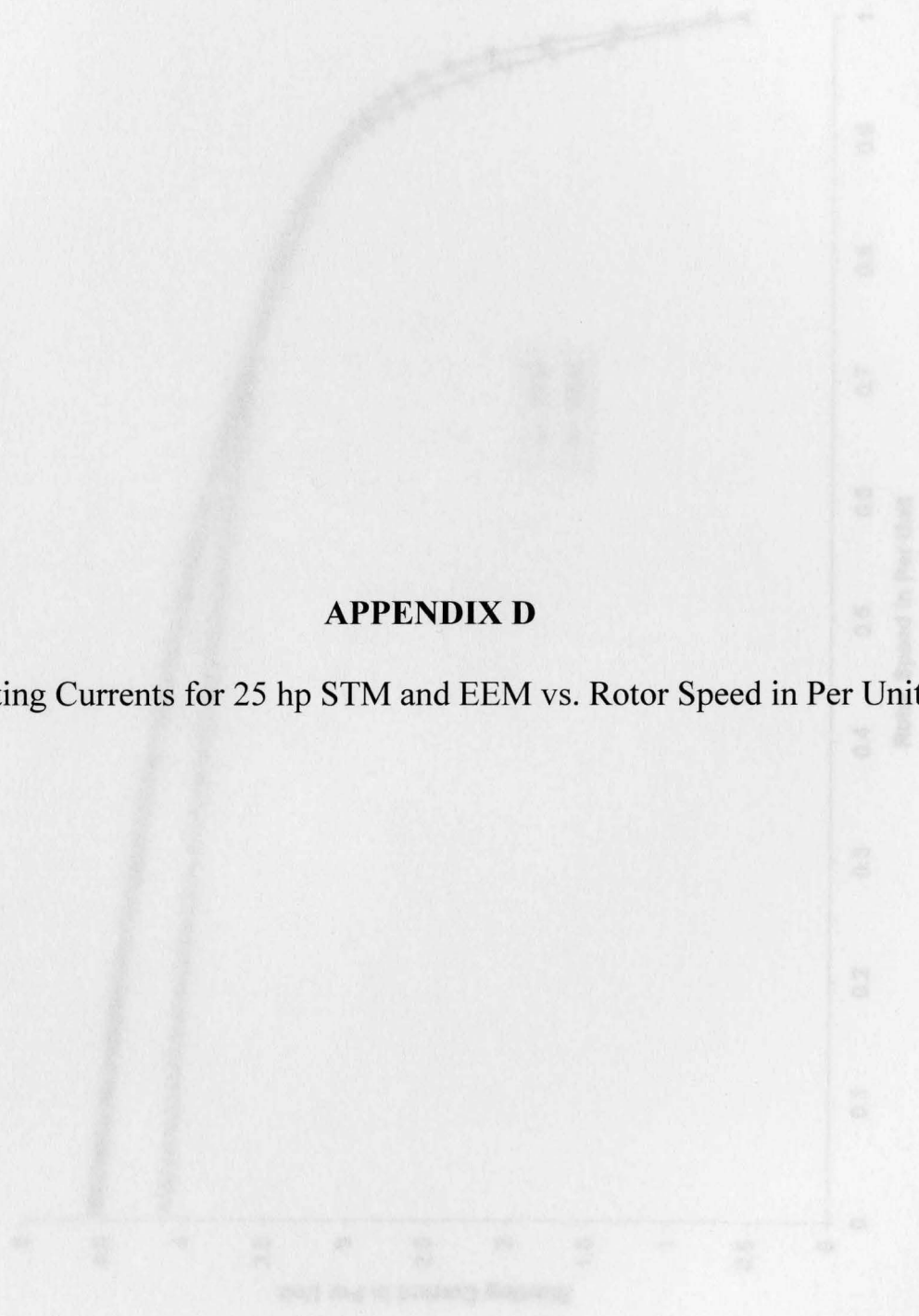
$$R_2 = r_r / 0.2 = 0.0139 / 0.2 = 0.0695,$$

$$R_3 = r_r / 0.3 = 0.0139 / 0.3 = 0.0463,$$

$$R_4 = r_r / 0.4 = 0.0139 / 0.4 = 0.0348.$$

These constant resistances are converted to variable resistances that vary with frequency when they are divided by the slip, as presented in figures 2.3 and 2.4, as R_n/s and $R_n/(2-s)$ for positive and negative sequences, respectively.

Figure D.1: Starting Currents for 25 hp STM and EEM vs. Rotor Speed in Per Unit



APPENDIX D

Starting Currents for 25 hp STM and EEM vs. Rotor Speed in Per Unit

Figure D.1: Starting Currents for 25 hp STM and EEM vs. Rotor Speed in Per Unit

